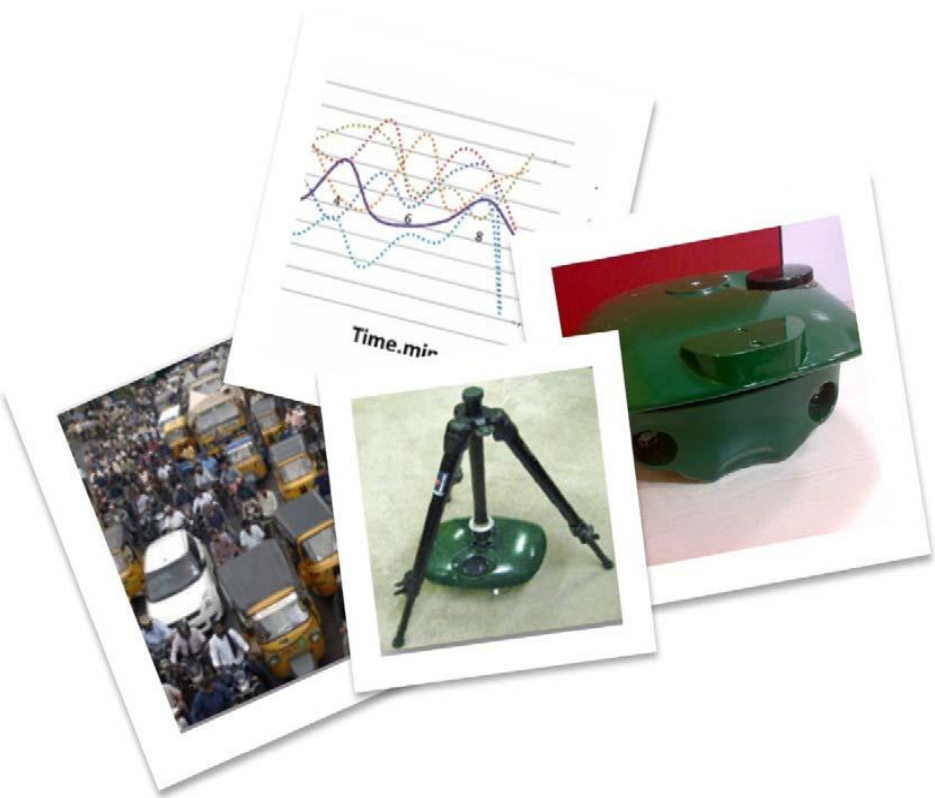**DEVELOPMENT AND EVALUATION OF TRAFFIC SENSORS UNDER INDIAN TRAFFIC CONDITIONS**

June 2016

Final Report on

DEVELOPMENT AND EVALUATION OF TRAFFIC SENSORS UNDER INDIAN TRAFFIC CONDITIONS

A sub-project from the "Center of Excellence in Urban Transport"
Sponsored by
The Ministry of urban Development, Government of India.

IIT Madras
June 2016

Final Report on

DEVELOPMENT AND EVALUATION OF TRAFFIC SENSORS UNDER INDIAN TRAFFIC CONDITIONS

Dr. Lelitha Vanajakshi
Associate Professor
Department of Civil Engineering
Indian Institute of Technology Madras
Chennai 600 036
INDIA
Ph: 91 44 2257 4291, Fax: 91 44 2257 4252
E-mail: lelitha@iitm.ac.in

Dr. Boby George
Assistant Professor
Department of Electrical Engineering
Indian Institute of Technology Madras
Chennai 600 036
INDIA

Mr. Arul Stephen, Mr. Sivasubramaniam, Mr. Ramesh, Mr. Shashi, Mr. Sheik Mohammedali, Mr. Mohamed Badhrudeen and Ms. Ameena Salim
Project staff, CoEUT,
Dept. of Civil Engg.
IIT Madras
Chennai 600 036

The rapidly increasing use of vehicles in India, spurred by the population boom and economic upturn has resulted in acute traffic congestion in its urban roads. The principal reason for traffic congestion and related inconveniences in India is that the road space and infrastructure have not improved in par with the traffic. According to road transport ministry, road space in India has only increased at an annual rate of 2.5%, compared to an over 10% annual rate of increase in vehicular population in the last year. Possible solutions to these problems include easing congestion by staggering office hours, carpooling, tele-work, and the more recent Intelligent Transportation Systems (ITS).

ITS technologies such as state-of-art data acquisition technology, communication networks, digital mapping, video monitoring, sensors and variable message signs are creating new trends in traffic management throughout the world. Data acquisition is the first step towards planning and implementing ITS. Although there are several data collection techniques all over the world, they may not work as such in India due to the unique nature of the Indian traffic condition - heterogeneity and lack of lane discipline. Until now, there are no proven data-acquisition technologies suited specifically to Indian traffic conditions. The present study attempts to evaluate and compare the performance of some of the most successful ITS data collection technologies under Indian traffic conditions. The comparative evaluations described can serve as guidelines for user agencies in choosing the best data collection technology suited to their specific application. Comparison of various technologies in terms of performance, initial cost, installation difficulty, maintenance issues, and technical support is provided, which will help the user agencies to choose the appropriate technology for their requirement. This report also details the developmental work carried out for sensors specifically suited for Indian conditions as part of this project.

Based on the comprehensive review and commercial availability, the following technologies were identified as potential sensors that can be used under Indian conditions with appropriate calibration/modification/redevelopment.

- Video based sensors
- Radar based sensors
- Infrared based sensors
- Inductive loop detector

Of the above, the presently available inductive loop detectors are better suited for lane-based organized traffic and hence cannot be used under traffic conditions will poor lane discipline. Hence, a new inductive loop detector that can identify different classes of vehicles as well as with poor lane discipline is developed as part of this project.

Video based sensors have the potential to work under varying traffic conditions and are

evaluated in this study. Collect-R, a commercially available integrated system that processes videos at site, was evaluated. Trazer, a real-time video processing systems suited for heterogeneous traffic conditions have been analyzed for mid-block locations. Gridsmart is another video based sensor specifically designed for an intersection was also evaluated. Attempts are also underway for in-house development of an image processing solution. The TIRTL (Transportable Infra-Red Traffic logger), an IR detector manufactured by CEOS Pvt. Ltd., Australia, was tested for its capacity to classify vehicles, detect the lane in which the vehicle is passing, speed and volume. Smartsensor, a commercially available radar based sensor of Wavetronix, was also evaluated.

This report summarizes results that have been obtained during preliminary testing of the selected data acquisition devices. These results pave the way for more extensive testing that will aid in the development of indigenous data acquisition technologies for future intelligent transport systems in India.

Acknowledgements

CHAPTER 1
INTRODUCTION

A recent report titled "India Automotive 2020: The Next Giant from Asia," by J.D. Power and Associates, states that India surpassed France, the United Kingdom and Italy to become the sixth-largest automotive market in the world in 2010. According to the study, more than 2.7 million light motor vehicles, of which 80 percent were either mini cars or subcompact passenger cars [Figure 1] were sold in India in 2010, up from just 700,000 light vehicles sold in 2000.
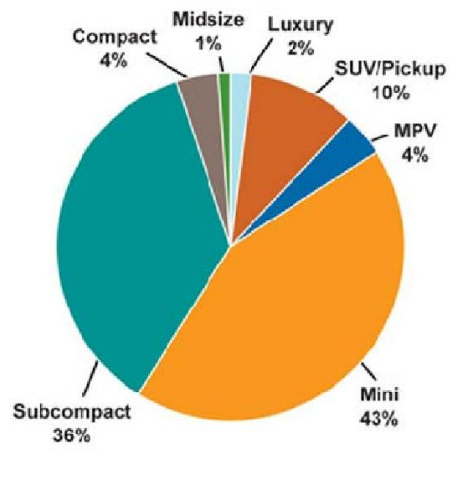
Figure 1: Passenger-Vehicle Sales Segment Share of the 2.7 million light vehicles sold in India in 2010 [1]

Reasons for burgeoning vehicle ownership use are two-fold.

1. The growing population of the country and the need to travel. In particular, the urban population has increased tremendously. According to the 2001 census data, 108 million Indians, or 10.5 per cent of the national population, lived in the country's 35 largest cities [2]. Preliminary information from the 2011 census data indicates that the urban population further increased by 3.34 % since 2001 [3].

2. Economic upturn has resulted in greater vehicle ownership. According to analysts at Morgan Stanley, India's economy will continue to grow at a GDP growth rate of 9-10% till 2013 [4]. The economic progress, coupled with a consumer-driven culture promises further increase in vehicle usage as shown in the prediction by J.D. Power and Associates [1] [Figure 2].

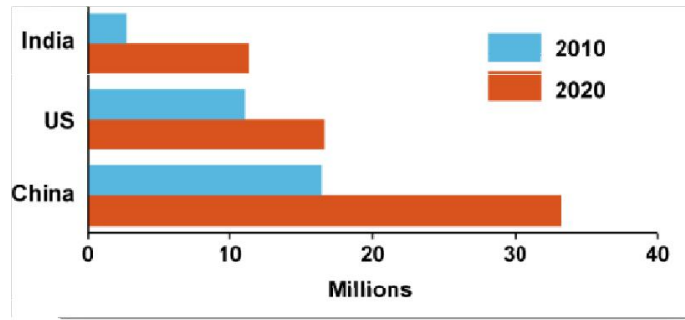**Figure 2:** India is stated to become the third-largest light-vehicle market in the world in2020 [1]

The direct outcome of vehicle ownership is acute traffic congestion in its urban roads. The variety of vehicles in India – two, three and four wheelers, in addition to a large pedestrian population, complicates the situation [Figure 3]. The Chennai metropolitan area alone faces an overload of two wheelers; the Master Plan II of the Chennai Metropolitan Development Authority [5] reports that two wheelers constitute 76% of the total vehicles on Chennai roads. This percentage is significantly higher than that in the other three major cities of India – Delhi (67%), Mumbai (41.5%) and Calcutta (43%).

Figure 3: Heterogeneity of urban traffic in India

The principal reason for traffic congestion and related inconveniences in India is that the road space and infrastructure have not improved in par with the traffic. According to road transport ministry, road space in India has only increased at an annual rate of 2.5%, compared to an over 10% annual rate of increase in vehicular population in the last year [6]. The seriousness of the problem is reflected in the report of World Bank that the economic losses incurred on account of congestion and poor roads alone run as high as $6 billion a year in India [7]. Improvements in infrastructure are constrained by space availability and other logistic problems.

Possible solutions to these problems include easing congestion by staggering office hours, carpooling, tele-work, and the more recent Intelligent Transportation Systems (ITS). ITS is aimed to evaluate, develop, analyze and integrate new technologies and

concepts to achieve traffic efficiency, improve environmental quality, save energy, conserve time and enhance safety and comfort for drivers, pedestrians, and other traffic groups [8]. ITS technologies such as state-of-art data acquisition technology, communication networks, digital mapping, video monitoring, sensors and variable message signs are creating new trends in traffic management throughout the world.
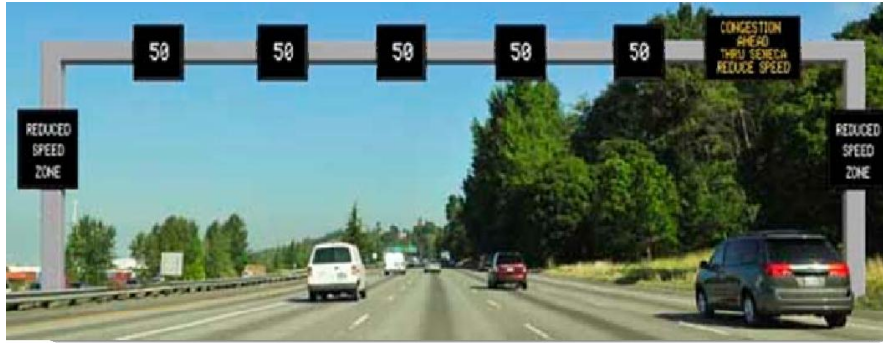

Figure 4: An example of ITS implementation – Dynamic message boards [9]

The efficiency and reliability of ITS depend critically on the following components:

Automated Data acquisition
Fast data communication to traffic management centers
Accurate analysis of data at the management centers
Reliable information to public

Automated and reliable data collection is the first step that sets the stage for the other components. Rapid, exhaustive and accurate data acquisition is critical for real-time monitoring and strategic planning. Various tools commonly used all over the world for automated traffic data collection include sensors such as magnetic, radar, infrared, laser, inductive, video etc., automatic vehicle identifiers (AVI), and GPS based Automatic Vehicle Location (AVL). Although these are proven data collection technologies for traffic conditions elsewhere, they may not work for Indian traffic condition, with its heterogeneity and lack of lane discipline. Most of the existing data collection technologies are limited by the need for lane based traffic and cannot classify different types of vehicles. Until now, there are no proven technologies suited specifically to Indian traffic conditions. The present study attempts to evaluate the performance of some of the most successful ITS data collection technologies for Indian traffic conditions. The comparative evaluations described can serve as guidelines for user agencies in choosing the best data collection technology suited to their specific application. Comparison of various technologies in terms of performance, initial cost, installation difficulty, maintenance issues, and technical support is provided, which will help the user agencies to choose the appropriate technology for their requirement. This report also details the developmental work carried out for sensors specifically suited for Indian conditions as part of this

project. This includes Inductive loop detector and a video image processing sensor.

The various tasks involved in the project are listed below.

1. Review on state-of-art of ITS data collection technologies to identify the ones that can work and be developed for Indian traffic conditions.
2. Procurement of the identified systems or development of the identified sensor - Technologies that have potential to work under Indian scenario by calibration or modification were procured and those that can be developed were identified and attempted.
3. Permissions and field installations
4. Calibration
5. Data communication
6. Evaluation - a comparison of performance of selected specific sensors developed/modified/evaluated under Indian traffic conditions will be carried out.
7. Modification of the system for better performance, wherever possible
8. Developmental work - Development of an Inductive loop detector and an image processing solution
9. Final field implementation

This report will discuss each of the above tasks in detail. The sensors identified for direct evaluation are (a) Smartsensor from Wavetronix - a radar based system, and (b) Collect R from Trafficon - a virtual loop based video sensor namely. The manufacturers worked closely with the project team to improve the performance of three sensors, viz. Trazer from Kritikal solutions - a video image processing software for mid-blocks, TIRTL from CEOS - an infrared based sensor and Gridsmart from Gridsmart technologies - a video image tracking software developed especially for intersections. Developmental work is being performed for an inductive loop detector suitable for heterogeneous traffic conditions with little lane discipline and for a cost effective image processing solution for automated extraction of traffic parameters from videos. A comprehensive review of state-of-art developments that led to the selection of the above specific technologies is given below.

CHAPTER 2
DATA COLLECTION TECHNOLOGIES

2.0. Introduction

Traffic detectors can be classified as vehicle detector/identifier and vehicle tracking devices. The vehicle detector/identifiers are mostly location-based and collect data from the entire vehicle population that crosses the location. They cannot collect spatial parameters such as travel time or density. Vehicle tracking devices are usually fixed inside vehicles and can collect spatial parameters such as travel time from that individual vehicle. However, data can be obtained only from vehicles that voluntarily participate by housing the tracking device. This limits the sample size. A brief discussion on each of these groups is provided below.

2.1. Spatial based Vehicle Trackers (Individual or selective vehicle detection)

Individual vehicles in a stream are tracked using technologies such as Automatic vehicle identification (AVI), Automatic Vehicle Locators (AVL), Global Positioning System (GPS) and mobile phone/Bluetooth tracking.

AVI systems use RFID (Radio Frequency Identification). RFIDs are used in US electronic toll collection. The RFID system uses a combination of radio frequency antennae, tags or transponders in the vehicles, and a central computer system. The antennae are located on roadside or overhead structures or as a part of an electronic toll collection booth [Figure 5] [10]. The antennae emit radio frequency signals within a capture range across one or more freeway lanes. When a probe vehicle, with transponders fitted in them, enters the antenna's capture range, the transponders respond to the radio signal and its unique ID is assigned a time and date stamp by the reader. This data is then transmitted to a central computer facility, where it is processed and stored.

Figure 5: Overhead RFID Antennae

Another possible vehicle tracking technique is license plate matching using image processing. This technique uses video cameras to record the characters of the license plate of vehicles along with a time frame, at different locations of a mid-block section so that the same characters can be matched to find out the travel time of vehicle. This technology, if available, can be used for large sampling. A vehicle can be tracked for a

longer distance if used throughout the path of the vehicle.

Automatic Vehicle Location techniques are commonly used for commercial and heavy vehicles. Beacon Signpost detection and Long Range Navigation (*Loran) C* technology using Radio emissions are some of the tools of automatic vehicle location.
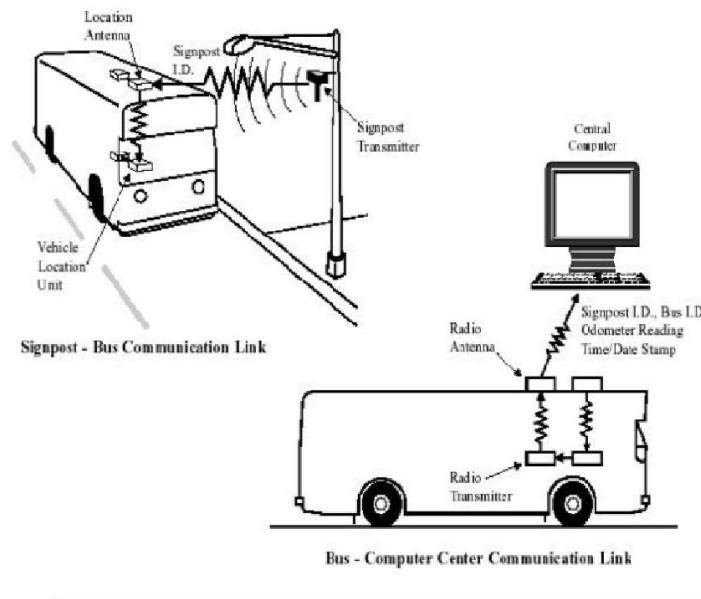

Figure 6: Beacon Signpost Detection [11]

Electronic beacons located at the bus stops or in other bus routes, emit a low powered signal which can be detected by a receiver in the vehicle. This signal gives the location of vehicle at any point and the information is transferred to the traffic management system where decisions on various routes and priorities are taken. The accuracy of tracking is within 500 meters using this tool and is best suited for fixed route vehicles and not demand-responsive vehicles. This technology is expensive, involves installing signposts at various locations, and involves coordinated signal processing from a large number of vehicles in the network.

In LORAN C, a radio transmission land station emits timed pulses that are detected by a receiver in the vehicle. The distance traveled by the signal is calculated by comparing the time at which pulses are received from different origins. The radio pulses are emitted from the different stations at an interval of milliseconds and hyperbolic curves of reception helps to pin-point the position of the receiver. This technique can track any

vehicle having the receiver, but the signals may be affected by electromagnetic radiations from other applications such as power lines, fluorescent light within vehicles, etc. and are expensive. The GPS has largely replaced the use of the Loran C technology for tracking.

The GPS is a worldwide radio navigation system that provides a fast, flexible, and relatively inexpensive method to collect data on a vehicle's position and velocity in real time. GPS is a US owned space-based system of twenty four satellites providing 24x7 monitoring of the earth. The 24 satellites are distributed uniformly in six orbital planes, at an altitude of approximately 20,200 km such that at least four satellites are visible at any time and from any point on the earth's surface [12]. GPS positioning is based loosely on three-dimensional positioning of manmade landmarks/"stars" using trilateration related techniques. Based on spatial and temporal data, traffic engineers can determine the most useful traffic information, including travel time, travel speed, travel distance and delay. One disadvantage of GPS is the performance getting affected where signal reception is poor such as, inside tunnels and near tall buildings and trees.
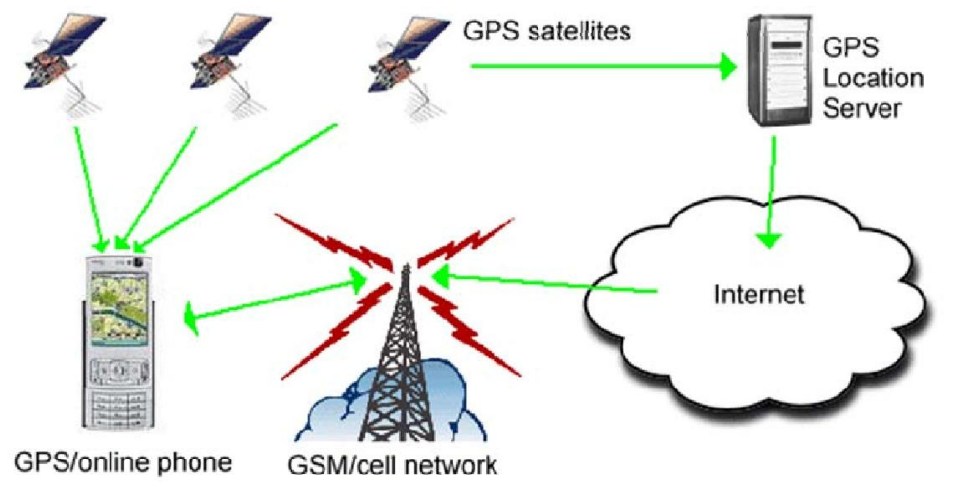
Figure 7: GPS [13]

Mobile Phones are another recent source for traffic data that is being explored world all over. Mobile tracking is performed by monitoring cell phone/SIM number of volunteers by the mobile phone tower in the area. Cell phone tracking is not as accurate as GPS and accuracy vary based on availability of cell towers.

Many modern cell phones are equipped with Bluetooth devices that can interact within a certain range. Thus, an activated Bluetooth device can connect to Bluetooth receivers thus enabling tracking. The accuracy of detection is not good enough to predict the speed of the vehicle with respect to spatial points. However, this method is cheap and can be easily executed.

The main disadvantage of these systems is the need for voluntary participation by the public to implement the technique. Hence, only a small number of vehicles can be tracked with this system. The only exception to this will be license plate matching systems, which are difficult to implement due to the difficulties in automated image processing which will be discussed in the next section.

2.2. Location based Vehicle detection and identification (Traffic stream detectors)

These location based traffic stream detectors are classified into intrusive and non-intrusive types.

2.2.1 Intrusive Detectors

Intrusive detectors include piezo/road tube detectors, inductive loop detectors, and magnetic sensors. Non intrusive detectors are many and some of the popular ones include microwave Radar sensors, Laser Radars, passive Infrared sensors, ultrasonic sensors, passive acoustic array sensors, and traffic camera sensors & image processing unit. Some of these are discussed below.

Inductive loops consist of a coiled wire that is installed under the surface of the roadway. Inductive loops work like a metal detector as they measure the change in the magnetic field when objects pass over them. A single loop can calculate vehicle count and dual loops can calculate count, speed and occupancy. Inductive loop sensors are reliable and can maintain accuracy under all weather and lighting conditions. A primary disadvantage of inductive loop detectors is the cost and effort involved in installing and repairing loops. They suffer from cross-talk errors and can cause stress to pavement.

Piezo Sensors are also embedded in the lane of travel and provide data on count, classification, and also Weigh-In-Motion. Piezo sensors work by producing a signal (voltage and current) when an axle/tire comes on top of them in the roadway. Piezo sensors are costly, require significant road construction to install, require regular maintenance, and their accuracy is sensitive to temperature and weather conditions and time, thus leading to larger uncertainty in data collection.
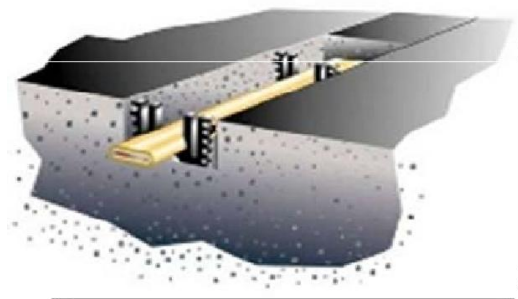
Figure 8: Piezo sensors [14]

Road tubes are used to detect vehicle axles by sensing air pluses that are created when each axle (tire) of the vehicle crosses the tube in the roadway. This air pulse is sensed by the unit and is recorded or processed to create volume, speed, or axle classification data. While one road tube is used to collect volume, two road tubes can be used to collect speed and class data. The life span of road tube varies depending on the location, installation and volume of traffic. The counts are performed between two intersections to give a total for each direction of the street. The main problems with the tube systems are difficulty in installation, low levels of accuracy, poor durability, and need for maintenance.

Figure 9: Road tube

Frequent wear and tear due to the traffic and weather is the biggest disadvantage of these sensors. This warrants frequent maintenance involving cutting of the pavement. Thus, the in-ground loops involve both short-term and long-term costs. The immediate costs include labour charges to saw-cut pavement while shutting down that lane of traffic and material cost (wire, conduit, loop processors). In the long run, additional costs like maintenance are incurred. Saw cutting of the pavement weakens its strength, resulting in shorter service life and more maintenance costs for pavement repair. When in-ground loops fail, the entire loop must be re-cut into the pavement, so the labor and traffic disruption costs are repeated.

Also, most of these are lane based and hence may not be suitable for traffic conditions with poor lane discipline. Furthermore, the vehicle classification capability of these sensors is very limited making them less suitable in heterogeneous traffic conditions such as the one in India.

Magnetic sensors detect changes in earth magnetic field caused by ferrous metal objects, such as a vehicle. There are two types of magnetic sensors - two axis fluxgate magnetometer and magnetic detectors. The former is used to identify both stationary and moving vehicles by increments in the magnetic flux above and below the vehicle. Magnetic detectors detect only moving vehicles by amplifying the voltage created by the
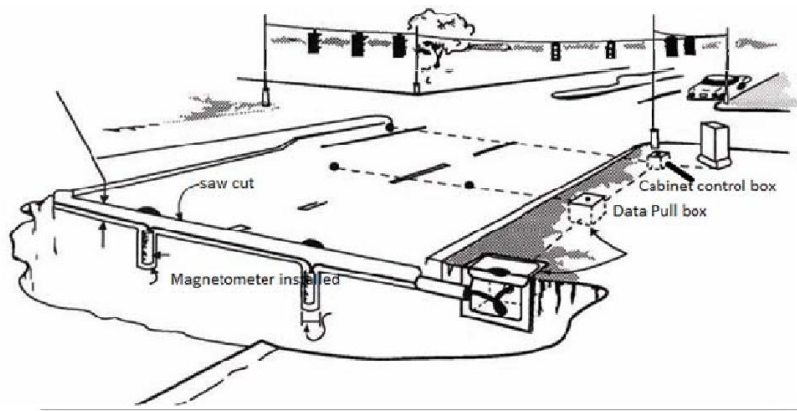
change in flux.

Figure 10: Magnetic Sensor installation [15]

Magnetic sensors have the following advantages:

Magnetometers have lead in their wires and they survive more with heavy traffic.

> An array of magnetometers having a common signal processor can locate, track and classify vehicles.
> In bridge decks, inductive loop installation is difficult due to steel inclusion whereas magnetometers can be installed.
> Magnetometers can differentiate vehicles separated by as little as one feet.

The disadvantages of magnetometers are that they require saw cut in the pavement and maintenance requires the road to be closed. Further, a single magnetometer cannot detect speed and occupancy and multiple units have to be installed. An additional drawback is that magnetic detectors require at least 6 to 15 Kmph vehicle speed to be detected, which limits its use in urban areas. Also, performance depends on the geographic location, in terms of distance from the equator.

The main advantage of these sensors is that there is no need for participation of vehicles for data collection and can collect the data from the entire vehicle population. These are mature technologies and hence have a historic knowledgebase for installation and calibration. Among these Inductive loop detectors are the most popular and proven technology available.

2.2.2 Non-Intrusive Detectors:

Non-intrusive techniques are based on remote observations. Usually, these detectors emit waves and sense vehicle based on Doppler Effect or by sensing the interruption to the emitted wave. Microwave radar, ultrasonic, infrared, optical and laser radar are some examples.

Radar detectors emit radar waves in a particular region and detect vehicles by sensing radar interruption. Microwave radar and laser radar are used for vehicle detection and counting. Radars can be continuous wave Doppler radar or Frequency modulated continuous wave Radar. Continuous wave Doppler radar produces constant frequency signals with respect to time. When a vehicle crosses the radar field, the frequency in which the signal is received from the vehicle increases if the vehicle is approaching and decreases as the vehicle recedes from the location. This frequency shift allows vehicle counting. Stationary vehicles cannot be identified due to absence of change in frequency of the received signal.

In frequency modulated continuous wave radar, the frequency of waves produced constantly changes with respect to time. This type is used to detect stationary vehicles due to the changing frequency technique. This type of detection can be used to monitor up to eight lanes.

Laser radars split emitted laser into multiple beams with wide degrees of separation. Receivers receive the reflected laser with respect to time. This enables the sensor to measure the speed of the vehicle.

Infrared sensors are also used to non-intrusively detect vehicles. There are two types of infrared sensors, namely Passive, and active. Passive infrared (PIR) devices [Figure 11] sense temperature changes and are more commonly called motion detectors. They detect heat emitted or reflected by the vehicle. This is converted into electric signal which provides information on occupancy, speed, length of vehicle, etc. The sensitivity of the detection is poor during fog or rain in the field of view.

Figure 11: Passive IR Detector [16]

Active infrared devices detect disruption in a beam of IR as a vehicle crosses it to count it. Transmitters emit infrared pulses which are received by a receiver on the opposite side of the road. When a vehicle passes between the transmitter and receiver, it breaks the beam and this interruption is counted.

Ultrasonic Sensors emit 25-50 kHz sound pulses that are inaudible to human beings. They measure the distance between the road surface and vehicle by detecting the reflected waveforms from the defined background. A distance higher than the defined space indicates the presence of the vehicle. They can provide information on volume count, occupancy, speed, vehicle presence etc. by producing two sound pulses at a known distance.
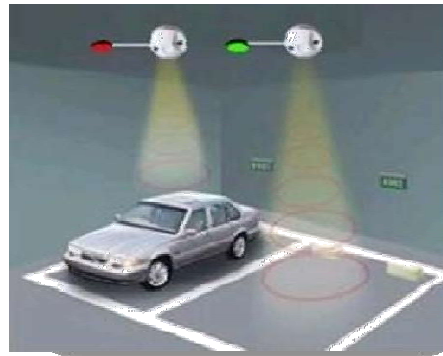
Figure 12 : Ultrasonic detector principle [17]

Acoustic Sensors detect vehicles by sensing the sound produced by the interaction of the vehicle tire with road surfaces as the vehicle approaches. The sound detected is converted into an electronic signal with an intelligent sound pulse algorithm to generate data of vehicle passage, vehicle presence, and speed.

Figure 13: Acoustic sensors

Video surveillance is another non-invasive form of vehicle tracking. Video cameras

capture visual images of the road and a video image processing software analyzes the images and extracts data such as volume, speed, gap, headway, occupancy, classification and even lateral gap which indicates the lateral placement of vehicles in the mixed traffic condition. For vehicle detection, the image processing concentrates on a unique and similar pattern of image detections for a particular type of vehicle. The large number of detections improves accuracy.

Video surveillance may be carried out in two ways. The video sensor (camera) may be built with integrated software that processes the visual information and transmits the processed data. Alternately, the video camera is not associated with processing software and merely transmits the videos to a management center where the image is processed.
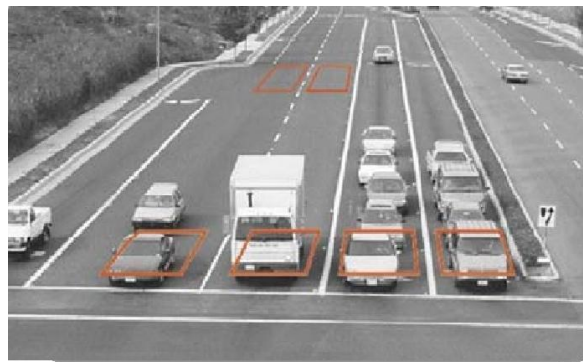

Figure 14: Image processing

The main advantages of video tracking are that cameras are cheap and installation is easy because the cameras are fixed over the surface, obviating digging activities. Thus, when cameras or processors fail, they are economically and quickly replaced without a great disturbance to traffic flow.

The use of automated traffic stream sensors under Indian traffic conditions has been very limited until now. Automated traffic sensing is very challenging due to the heterogeneous nature of the Indian traffic and lack of lane discipline. Area Traffic Control programmes in Pune [18] and Mumbai [19] have reported use of loop based and video based vehicle presence/absence sensors. Use of detectors for real-time traffic data collection is very limited. An example is the use of piezo loop sensors installed at NH-8 between Delhi and Jaipur to collect data such as volume count and classified volume count [20]. This project failed due to the following problems:

1) Being an intrusive sensor, it required roads to be grooved and sealed after installation. This involved labour and traffic interruptions.
2) Indian roads are tar topped and need frequent overlays. Induction sensors were damaged during overlays.
3) Due to low sensitivity and minimum time headway required for the loop to

reactivate to sense the next vehicle, it could not detect fast moving and light vehicles which form a large fraction of the vehicles plying on Indian roads. Thus, only 42% of total traffic was detected.

4) Any loop-to-loop disconnections or other malfunctions required more digging and blocking of traffic for repair.

Though video cameras are being installed for surveillance in many cities, most of them do not carry out automated processing of videos and are mainly used for manually identifying violations.

CHAPTER 3
SELECTED SENSORS

3.0. Detector selection for present work

Based on the comprehensive review and commercial availability, the following technologies were identified as potential sensors that can be used under Indian conditions with appropriate calibration/modification/redevelopment.

- Video based sensors
- Radar based sensors
- Infrared based sensors
- Inductive loop detector

Of the above, the inductive loop detectors are better suited for lane based traffic and hence cannot be used under Indian traffic conditions because of the poor lane discipline characteristic of traffic. Hence, inductive loop detectors were considered developmental work as detailed in section 7.

Video based sensors have the potential to work under varying traffic conditions and are also evaluated in this study. Collect-R, a commercially available integrated system that processes videos at site, was procured from Trafficon. Details of Collect-R and experimental protocols are discussed in section 6.1. Trazer, a real-time video processing system, which has been developed for heterogeneous traffic conditions was also analyzed for mid block locations. Trazer has been explained in section 6.4.For intersection data collection, GRIDSMART from GRIDSMART technologies was also selected and discussed in section 6.5. Attempts are also underway for in-house development of an image processing solution.
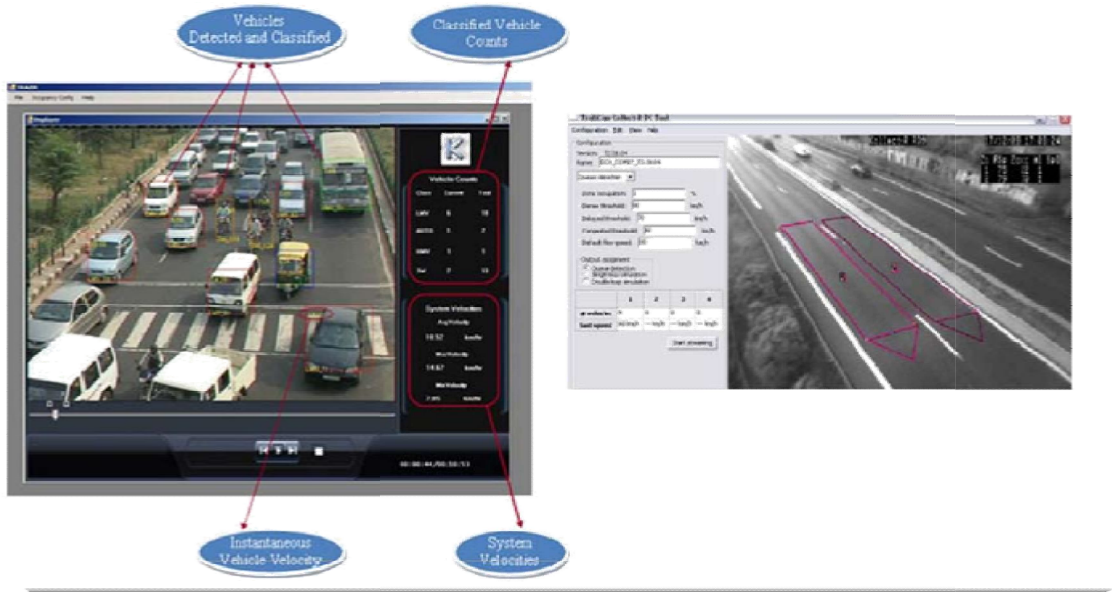
Figure 15: Screen shots of image processing software used for video-based tracking

The TIRTL (Transportable Infra-Red Traffic logger), from CEOS Pty Ltd, Australia, is the identified infrared detector. Using the beam breaking and making technology it can classify vehicles, detect the lane in which the vehicle is passing, speed and volume. The product is customized for various traffic scenarios and an India specific classification table is available. Its procurement, installation and evaluation are detailed in section 6.2.

Figure 16: TIRTL

Smartsensor, a commercially available radar based sensor of Wavetronix, was also chosen for the present study. It is a multi-zone presence detecting radar. It produces two high definition radar beams with which volume, speed, occupancy, gap, Headway, and classification of the vehicles can be identified. Its procurement, installation and evaluation are detailed in section 6.3.

Figure 17: Smartsensor-Multi-zone presence detecting sensor [21]

3.1. Procurement of devices

All equipments were procured according to the procurement rules of IIT Madras, which follows the rules of Government of India. Tenders were published at web site and the quotations were received. Tenders were received in two bid system with technical and commercial bids received separately. Those that meet the technical specifications only will be opened in the commercial level and the lowest bidder in that will be selected. Items which are proprietary were procured after justifying the case and with due permission from the purchase committee/authority in charge.

Traficam Collect-R was procured directly from the manufacturers M/S Trafficon, Belgium, Europe (http://www.traficon.com) through single quotation since it is a single-source item. TIRTL, Gridsmart, and Wavetronix Smartsensor were procured through web-based tendering from the lowest bidder - CMS India, the local agent for these two products. Trazer was purchased as per software purchase rules, directly from the manufacturers.

CHAPTER 4
STUDY SITE

The test bed for this project was in the initial stretches of Rajiv Gandhi salai (IT Corridor) between Madhyakailash junction and Perungudi Toll Plaza. It is a 6 lane roadway with 3 lanes in each direction and approximately 12 km in length. This corridor houses many IT companies and hence carries heavy traffic volume during peak hours. The roadway comes under the Tamil Nadu Road Development Corporation (TNRDC) and permissions for the installation of the identified items are obtained from them. The study site details are shown in picture below marking the locations of each of the equipments.
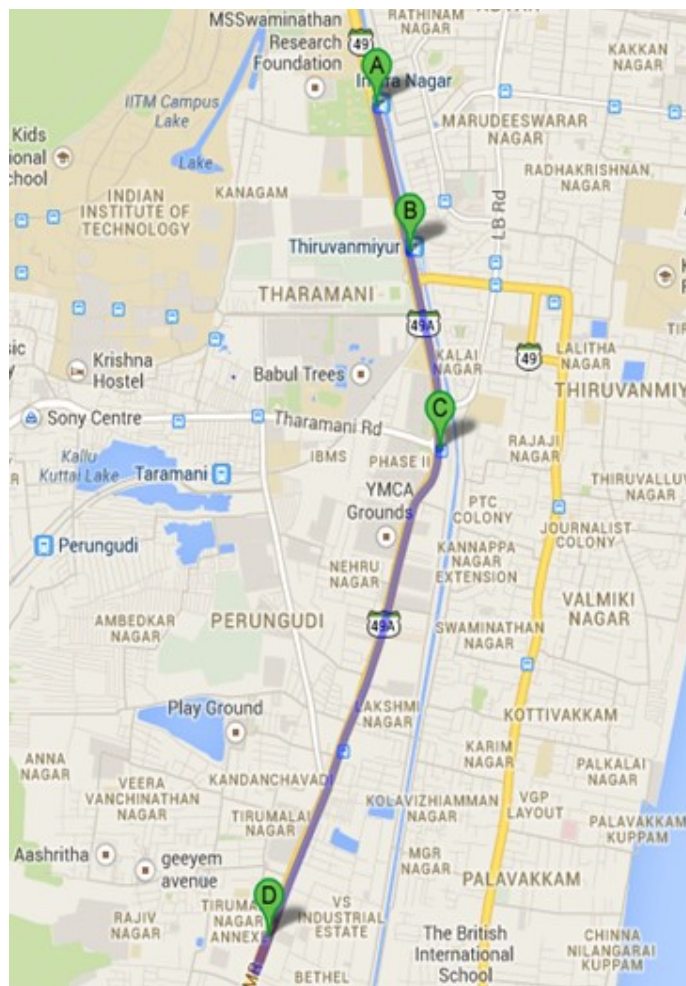
Figure 18: Test sites for the study (Source: http://maps.google.co.in)

Collect-R is fixed on the second foot over-bridge facing northbound traffic near to Indiranagar railway station (A) in the IT corridor. This site was deemed suitable since the collect-R has to be mounted at 6m height overhead facing the traffic.

The smart sensor unit is also fixed near the second foot over-bridge near to the southbound traffic near to Women's Polytechnic (A) in the IT corridor. It is fixed on a pole at the roadside.

Figure 19: Details of test site 1 showing approximate sensor locations
(Source: http://maps.google.co.in/)

Cameras for the Trazer feed are fixed on the second and third foot over-bridge facing northbound traffic. The camera is mounted on the foot over-bridge at the middle of the lanes, as shown in Figures 19 and 20.

The camera for the GRIDSMART sensor is fixed at SRP Tools intersection (C in Figure18) in the IT corridor. The camera is mounted on a pole in the traffic island, in the middle of the intersection.

Figure 20: Details of test site 2 showing approximate sensor locations
(Source: http://maps.google.co.in/)

The TIRTL unit procured is a portable one and hence was tested at various locations as detailed in the section 6.2.3, and finally installed permanently at Perungudi near toll plaza (D in Figure18).

The Inductive Loop Detector developed in-house was tested in IIT Madras campus roads as part of the developmental work and has not yet been fixed permanently in a roadway.
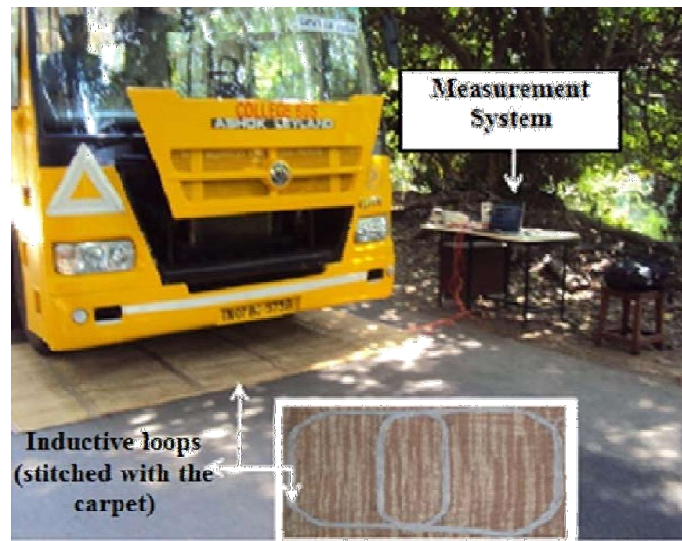

Figure 21: Inductive loop sensor developed at IIT M.

CHAPTER 5

DATA TRANSFER AND STORAGE

5.0 Introduction

Data from the deployed equipment are transferred in real time. Video feeds are transferred using wireless technology. Data generated by systems such as Smart sensor and Traficam Collect-R are transferred using GPRS using two modems at both ends or using one modem at the site and a fixed IP server as the receiver in the other end. Data from TIRTL is transferred using GPRS enable static IP SIMcard to the server in the other end, and data from Gridsmart sensor is accessed and downloaded at the traffic monitor center at IIT Madras using an established VNC connection. Data management is through SQL database in the storage servers placed in the traffic monitoring center at IIT Madras.

5.1 Data backup and archiving

The process of data backing up refers to copying data so it may be used to restore the original data after a data loss event. So data backups are a secondary copy of current data, kept on hand to replace the primary copy of that data, while data archives are the primary copy of historical data that is no longer actively used, usually retained for the long -term. Making copies of files is the simplest and most common way to perform a data backup.

Data from different devices (Traficon, Wavetronics, Tirtl, and GRIDSMART) are stored as CSV(comma- separated values) files in a pre defined folder in the storage servers placed in the traffic monitoring center at IIT Madras (Refer 5.0 Data transfer and storage). Data from these stored files are segregated based on date and saved as a separate CSV file on a daily basis. Java and Python programming languages are used for backing up of data.

The different Traficon data stored in the CSV files for are Time, Lane, Headway (m), Concentration (vehicles/km), Occupancy (%), Confidence, Class, No of vehicles, Gap(s/10), Speed (km/h).

The different Wavetronics data stored are Name, Volume, Occupancy, Speed, 85% speed, Class of the vehicle, Headway, Gap, YYYY-MM-DD, HH:MM:SS, Interval sec, and Direction.

TIRTL data is processed before storing in CSV mode. The different data stored are Date, Time, Average Speed, Class, Flow (Veh/Hour), Name, Occupancy, Density (Veh/Km). These data are processed from the following data: Date, Time, Lane, Velocity, Average Speed, Direction, Class, Axles, Wheel Base, Name, Width, Dist, Minimum Distance, Maximum Distance, Trigger Class, Trigger List, Spacing, Presence, Avel, Asize, Aedges, Abvel, Amvel, Aspace.

GRIDSMART data is downloaded in .csv format. The data consists of individual vehicle details such as time of detection, direction of the vehicle bounds to, speed in kmph, length of the vehicle and turning movement of the vehicle.

Figure 22: (a) Data storage server at IIT-M, (b) Wireless data communication antenna.

CHAPTER 6
DEVICE DESCRIPTION AND TESTING

6.0 General

Each of the above identified technologies needs to be evaluated for their performance under Indian road conditions to ascertain their applicability. The following sections describes in detail the field installation, calibration and analysis of each of these equipments.

The performance of sensors was evaluated using two statistical measures, namely Mean Absolute Percentage Error (MAPE), and Mean Absolute Error (MAE), expressed as

$$MAPE\ (\%) = \frac{1}{n} \sum_{i=1}^{n} \frac{|Actual\ value - Observed\ value|}{Actual\ value},$$

$$MAE\ = \frac{1}{n} \sum_{i=1}^{n} |Actual\ value - Observed\ value|.$$

6.1 Traficam Collect-R

6.1.1. Device Description

The Traficam Collect-R sensor is a product of Traficon. It has a highly sensitive CMOS sensor coupled to video recognition software that detects the presence of a vehicle in a given lane. It works on the principle that a virtual loop is created in the field and vehicles passing inside the loop are recognized using image processing technology.

Figure 23: Traficam Collect-R

a) Features of Traficam Collect-R

It can monitor Traffic Flow and can distinguish 5 levels of service using the flow speed and the zone occupancy.

It does not require cutting of road surface for installation and the output from collect-R can be integrated into a Traffic Signal Controller.

It includes special filters to prevent false detections caused by road markings, shadows and reflections in wet weather.

It can detect and count vehicles in as many as 4 lanes simultaneously.

It can store up to 8000 lines of data into a circular memory. This corresponds to traffic

data of one week from two data zones including vehicle classification at an integration interval of 5 min.

Collect-R provides traffic data such as

a) Vehicle count (per lane and per vehicle class).
b) Vehicle speed (per lane and per vehicle class).
c) Occupancy
d) Headway + Gap
e) Classification (3 classes)

Integrated data (integration interval can be user defined).

The following table shows a typical set of data generated by Traficon Collect-R.

Table 1: Data set generated by Traficon Collect-R

Time	Lane	Headway (meters)	Concentration (Vehicles/Km)	Class	Vehicles	Gaps (Sec/10)	Speed (Km/h)
8:01:00	1	29	29	1	19	18	54
8:01:00	1	29	29	2	4	25	68
8:01:00	1	29	29	3	2	10	48
8:01:00	2	32	25	1	10	29	61
8:01:00	2	32	25	2	11	11	65
8:01:00	2	32	25	3	4	18	61
8:01:00	3	35	24	1	7	26	54
8:01:00	3	35	24	2	4	23	61
8:01:00	3	35	24	3	2	14	71

b) Software Components of Traficam Collect-R

Collect-R uses three software components for operation:

a) Traficam Collect-R PC Tool: Used for configuring the equipment.
b) Traficon Serial Server: Used for connecting the equipment with the computer.
c) Traficon Data Tool: Used for downloading the data to PC.

1) Traficam Collect-R PC Tool

The PC tool helps configure the device using a specific name for the device (e.g. Chennai), choosing the units to be displayed (metric or imperial). Other major configurations are described below.
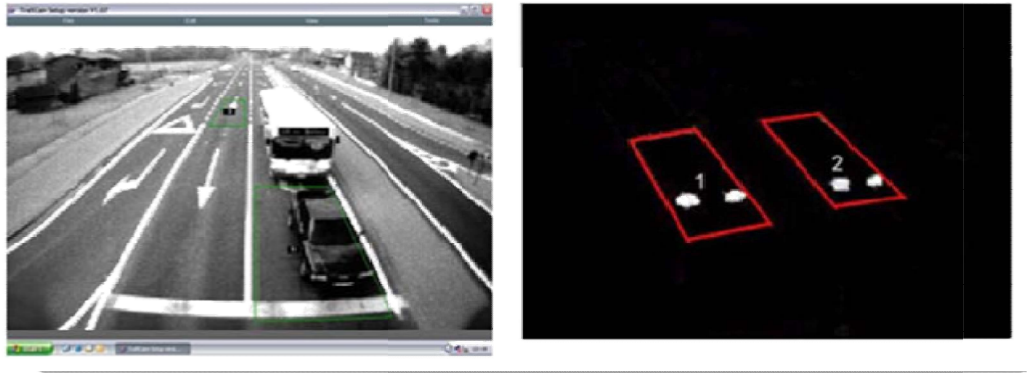

Figure 26: Configuration of Traficam Collect-R PC Tool.

Virtual loops: Configuring the number of virtual loops which can have a maximum value of 4 corresponding to the 4 lanes. Direction of the virtual loops is in accordance with the normal direction of traffic and length of virtual loops can be defined. The length corresponds to the real field dimensions and need to be provided as accurate as possible. The speed and classification data accuracy is very sensitive to the loop length. Nevertheless, the count is not affected by the zone length entered in the setup tool. The width of the virtual loop should be smaller than the lane width. To minimize the vehicles being missed due to lack of lane discipline, in the present study the loops were made as wide as possible, almost to the width of each lane.

Integration Interval: This is the interval in which the data are calculated and displayed. All events like Speed alarm also work on the basis of this integration interval which can be varied from 10 sec up to 1hr.

Classification Threshold: Up to three user-defined vehicle types can be classified based on vehicle lengths. In the present study, it was decided to classify into two wheelers and autos (below 4m length), light motor vehicles (vehicles within 4 and 7m), and heavy motor vehicles like buses, truck (vehicles above 7m in length).

Traffic Data Table: The display window serves as verification after setup of the device. The table lists the number of vehicles per data zone and the individual speed of the last vehicle in the data zone. When a vehicle passes through a zone the corresponding column in the table changes its color.

Live Stream Window: A low quality stream can be used to view vehicle detection in real-time and evaluate the accuracy of the information that is shown in the traffic data table with respect to the number of vehicles and the individual speed of the last vehicle.

When the information in the traffic data table does not provide realistic values, redefining the length of the virtual loop will improve the accuracy of detection. The disadvantages of live streaming include

- Reduction in the detection performance of Traficam.
- Difficulty in examining the accuracy of detection due to poor image quality

- During live streaming PC Tool application cannot be operated and hence the data will not be available concurrently. It can be stored by the Data Tool and transferred to the database afterwards.

2) Traficon Serial Server
The Traficon serial server connects the equipment and the PC. Once the Traficon serial server is started, the Traficon Data Tool can be used to download the data through the server. It is also used to configure the modem.

3) Traficon Data Tool
This is used to download data stored in the Traficam to the PC. Both current traffic data and past data (history) can be downloaded.

The order in which these can be used is:
Open Traficam Collect-R PC Tool, configure the unit and set a timestamp.
Disable "live view" and "streaming video" prior to shutting down the tool.
Check if the Traficam Collect-R PC Tool is closed when storing the traffic data. If the "live view" in the PC Tool is on, the data in the Collect-R database will be lost.

Ideal conditions for Traficam
- Traficam has to be placed in such a way that that it is oriented downwards looking.
- During night vehicles are identified based on head lights so it should be oriented towards upcoming traffic.
- To avoid occlusion, it has to be installed overhead. The minimum height of installation is 6m.
- It should be aligned to avoid sunlight exposure and it should not cover the horizon also.
- The sensor is developed for lane disciplined traffic, for Indian conditions detections zones has to be adjusted so close to incorporate movement over two lanes or between lanes.

6.1.2. Installation Procedure:

a) Study location
The location chosen for the study was Indira Nagar, Chennai. It is a six lane bi-directional

traffic with shoulders on either end.

b) Camera Orientation

Traficam Collect-R is a downwards oriented device looking towards upcoming traffic and thus must be mounted at the right height to minimize occlusion. Occlusion is a dimensional problem and has to be carefully handled. Occlusion occurs when a vehicle blocks out part of the camera's field of view, as can be seen in the figure below.
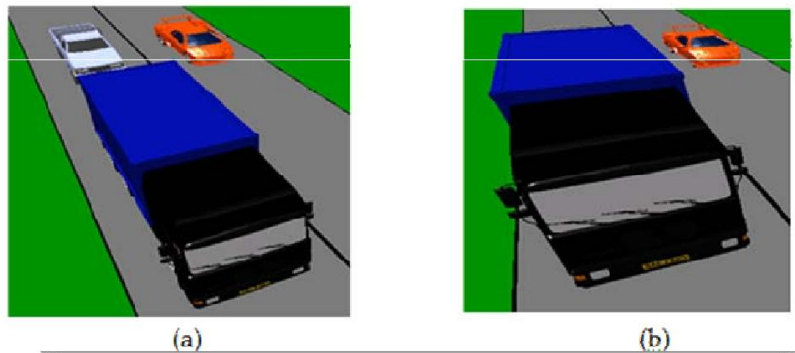

Figure 24: Illustration of occlusion

Figure 24(a) shows the view of a Traficam snapshot image when the Traficam is mounted high. The car behind the heavy vehicle is within the virtual loop of the Traficam and so it can be detected. In Figure 24(b), the Traficam is mounted little lower or in a flatter mode, the car behind the heavy vehicle is not visible and hence cannot be detected. Thus, the camera must be mounted at an optimum height, directly overhead. The minimum installation height is 6 m. If overhead mount is not possible, it is placed next to the fastest lane.The Traficam Collect-R may be mounted in horizontal or vertical position and in a region with minimum exposure to direct sunlight. At night the device detects the headlights of vehicles. The detection zones should cover the headlights in night [Figure 25].
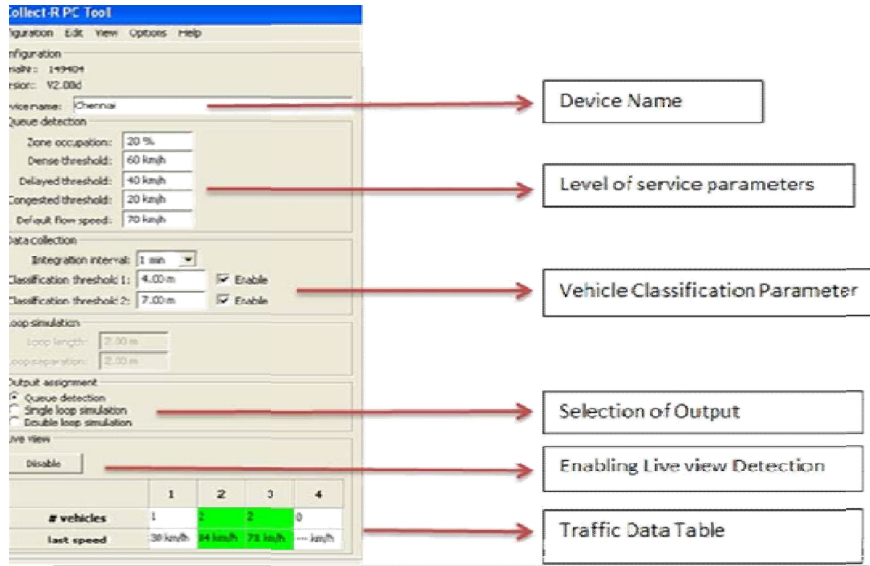
Figure 25: (a) View of Traficam facing Horizon (b) Detection of headlights within the virtual loop

6.1.3. Configuration Procedure

In order to increase the performance of Traficam, configuring and calibrating the sensor under Indian traffic conditions were done. The following steps were employed to configure the Traficam

a) Equipment Connectivity
The connectivity between the laptop and the equipment with the software was established. Problems arose in this step when connection failed during broadcasting [Figure 26].

Figure 26: Connectivity problem between laptop and equipment

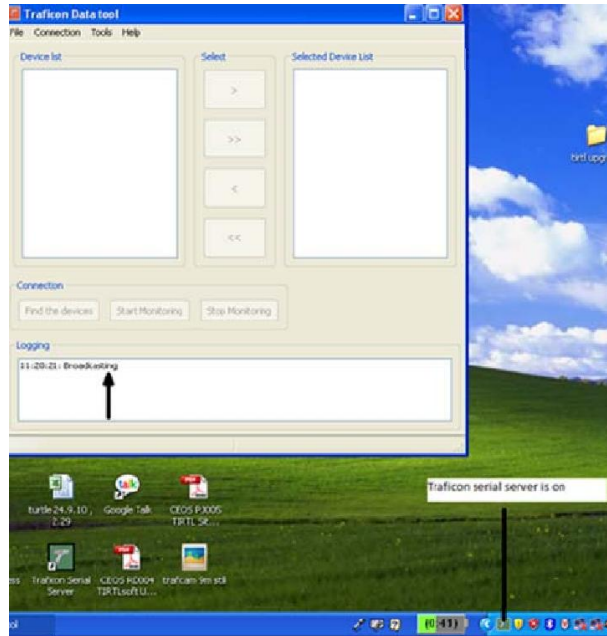The probable reasons for this connectivity error were:
1. The serial server should be started only after the Traficam collect-R is closed. Sometimes it appears that the server does not close completely, and there is no way to check for complete closure.
2. Sometimes multiple serial servers run simultaneously due to improper closure of the server in one instance.

After discussions with technical staff, it was inferred that
- There was a bug in the software.
- Network connection such as WLAN or LAN was required to connect the equipment to the network.
- The PC should be equipped with a Microsoft loopback adapter to ensure connectivity directly between the computer and the equipment.

After removal of the bug, establishment of a network connection and inclusion of a loopback adapter, the connectivity was established without errors. Remote data collection through modem was also established for continuous data collection. MOXA modems were found to be compatible with collect-R equipment.

b) New Updated Software
Software was updated since the earlier version allowed only two user-defined vehicle classifications and three were required for the research. The later version allowed one more classification and in addition eliminated the connectivity bug and included a new Traficon serial server that could verify the connectivity of COM port for both Modem

and equipment, separately. This version also included a "Find Device" option in the Traficon Data Tool which clearly indicated the reception or failure of data.
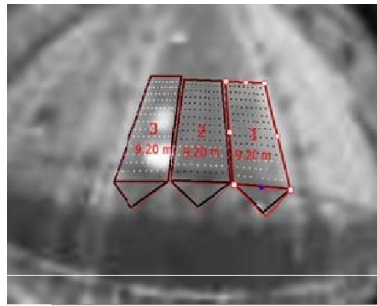

Figure 27: Live streaming of Detection Optimizing Detection

c) Examining the accuracy of detection

The live streaming option in the Collect-R PC tool was used to check the accuracy of detection in real time. The vehicle count was carried out manually from this live stream and the corresponding data generated by collect-R was checked using these numbers. The streaming image was of poor quality, making accurate detection in real time was also difficultThe Collect-R is designed to prioritize detection of vehicles. Heavy traffic leads to consumption of more CPU power. During such times, the other tasks (like communication) are delayed so that there is no compromise on the task of detection.

d) Shift in Data Storage

Initial checks on count accuracy showed both under counting and over counting happening in different intervals. The undercount and over-count observed during repeated trials lead to the suspicion that there was a one-minute lag in Traficam data.

To allay/confirm this doubt, a field test was conducted on 14th October 2010. The following tasks were carried out during this field study:

- The vehicles were manually counted.
- Numbers shown in the Traffic Data Table viewer of the Collect-R PC Tool were noted down.
- Traffic data stored by the system were collected at the end of observation period.

A comparison of the above three showed that the numbers shown in the traffic data table viewer matched better with the field data than the stored information. To solve this problem, the logs (.xml output of Data collection output) on the Collect-R were enabled, through which vehicles can be checked second by second. It was found that the Collect-R counts the data during the first interval and writes on the consecutive interval, thus incurring a one-time step shift per time lag in data storage and is described below.

Since Traficam provides integrated data, the data is transmitted at the end of the integration interval. Thus, the stored data will be delayed by the user defined integration

interval. Thus, if the vehicles are manually counted between 14h23 and 14h24, it represents the Collect-R data with the timestamp 14h24, as this data was received at 14h24. Figure 28 shows the difference between the Traficam count and manual count with and without data shift. Without data shift the graph shows a wide range of undercount and over-count variation. After the data shift, the difference between manual count and Traficam reduced and the corresponding percentage error dropped from 61 to 17%.

Figure 28: Undercount & over count variation for a loop length of 5.5 m.

The percentage error before shift was 61% and that after shift was 17%.

Thus, the timestamp in the data file is the time of conclusion of the integration interval, i.e. if the integration interval is 60 seconds, the data with timestamp 3.15.00 will be the data from 3.14.00 to 3.15.00. Thus, it is possible that the data with timestamp 3.15.00 is already in the file when the time on the computer shows 3.15.13.

e) Time Synchronization between PC & Traficam
While carrying out the manual testing, a time mismatch was observed to occur between the camera, laptop and Traficam Collect-R. When the laptop was disconnected from the Traficam, the displayed times were matching. However, after connecting the devices, the laptop clock was ahead of the clock on the camera. To rectify this problem, the "time sync" option can be used and the clock of the Collect-R can be set to the same time as the computer (laptop) clock to which the Traficam is connected.

f) Loop configuration
Initial checks on count accuracy showed both under counting and over counting happening in different intervals. The under-count/over-count was difficult to eliminate due to the absence of lane discipline. Vehicles driven between lanes create double counts and those driving too close to each other created undercounts. Specifically, the lack of

lane discipline leads to the following scenarios in the virtual loop:
- Vehicles enter a loop, change lane (loop) within the loop to overtake another vehicle (Figure 29 a).
- Vehicles travel between two lanes, in the conjunction area and enter two loops simultaneously (Figure 29 b).

Two types of vehicles – e.g. car and two wheeler or 2 two wheelers, enter a single loop simultaneously (Figure 29 (c) and (d)).

Figure 29: Different traffic scenarios captured in the study area.

If a vehicle changes lanes while driving in a loop it could be detected in both detection zones depending on the time that the vehicle has spent in a single detection zone. Traficam makes measurements based on image processing while the vehicle drives over the detection zone. If the time spent on a single zone is low, the measurements corresponding to that zone are filtered out. However, if the vehicle has spent more time on a single zone than the lower limit, it will be detected in that zone as well as the next zone it entered.

Initially, the virtual loop length was 9m with a narrow loop width as shown in red in Figure 30. Initial results with this alignment were erroneous with more undercounts.
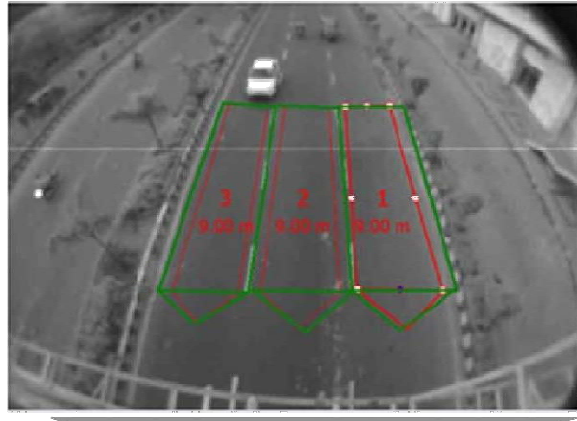
Figure 30: Loop Width Correction for missing vehicle between loops

Such an arrangement suits countries that have better lane discipline where only one vehicle moves in one lane at a time, followed by the consecutive vehicle. For India however, narrow loops are unsuitable due to the three manifestations of lane indiscipline mentioned earlier and hence the width of the virtual loop was extended to meet the edges so that no vehicles is missed. The extended loop is shown in green.

The length of the virtual loop was calibrated by trial and error to have maximum accuracy by comparing the volume count for different loop lengths. The loop length can vary between 5 and 12 meters.

For 1-minute accuracy, undercount and over count must be taken into account. The graph in Figure 31 shows the variation of undercount and over count for different loop lengths. It is evident that 9.2m loop had fewer undercounts and over counts than other loop lengths. Hence, trials were carried out with varying loop lengths and performance was evaluated. A video shot on 18.10.2010 with different loop length were analyzed and based on the performance, the following changes were made in the Collect-R PC tool.

- The detection zones were made to overlap, so that motorcycles driving in between lanes were also detected.
- It was ensured that the Traficam Collect-R PC Tool is closed during evaluation of detection, since streaming video and snapshots reduce the CPU capacity of Collect-R and can adversely affect detection results.

Figure 31 shows the variation from actual volumes for varying loop lengths. Ideal scenario will have zero error. The corresponding error in percentage is plotted in Figure 32. It can be observed that loop length 9.2 m produced least error. The actual volumes on each of these tests are shown in Figure 33 and Table 2. On comparing MAPE values for the series of surveys with different loop lengths, it is seen that the 9.2 m loop length exhibits minimum MAPE.
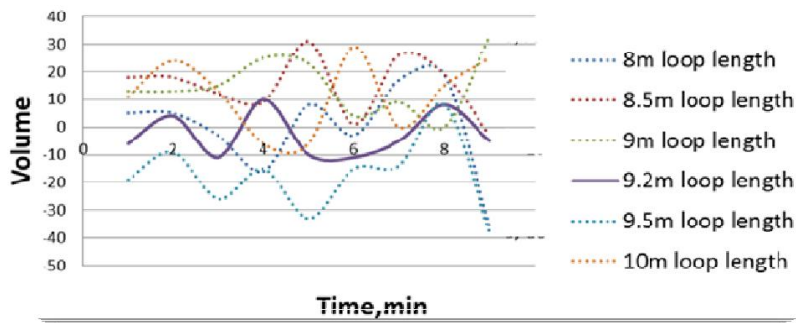
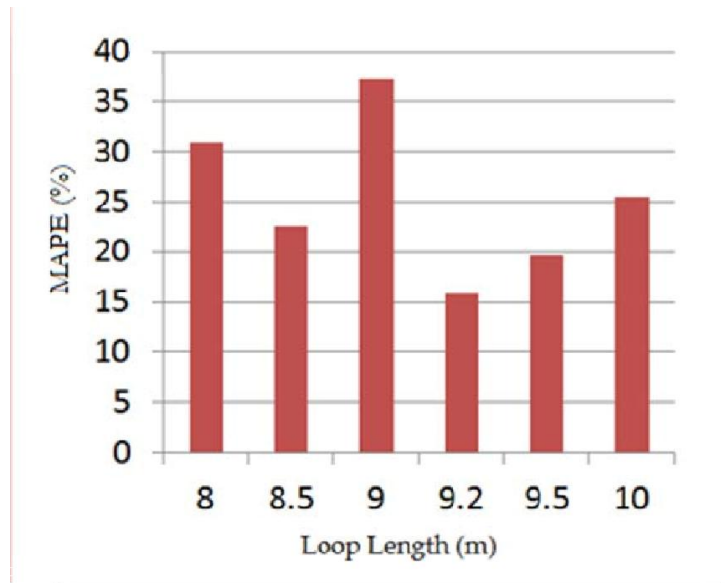**Figure 31:** Undercount & Over-count variation for different loop length

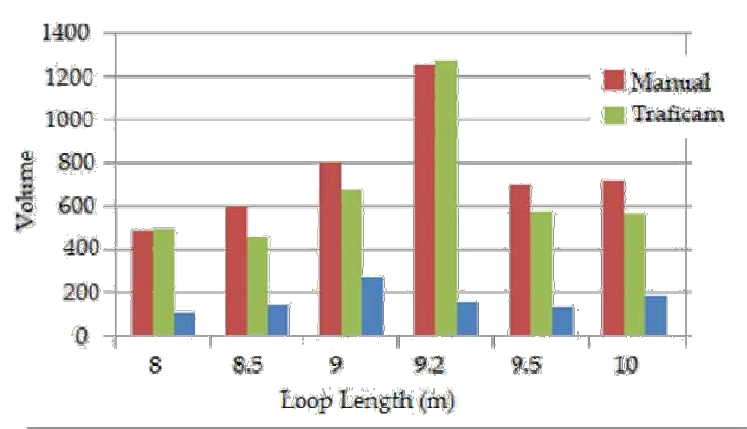**Figure 32:** MAPE for volume count for different virtual loop length

Figure 33: Total volume count of Traficam & manual and the difference between them

Table 2: Performance comparison with varying loop lengths

LOOP LENGTH(m)	MANUAL COUNT	TRAFICAM COUNT	ABSOLUTE DIFFERENCE	MAPE(%)
8	495	499	112	30.91
8.5	594	457	143	22.54
9	802	680	276	37.19
9.2	1253	1276	161	15.88
9.5	699	576	137	19.58
10	720	567	185	25.51

It can be seen from Table 2 that the loop length of 9.2 m produced good accuracy with an absolute difference of 161 of 1253 vehicles & MAPE of 15.88. Hence, loop length of 9.2 m was used in the rest of the analysis.

The same loop configuration procedure was done for speed also. Speed evaluation was carried out by extracting original speed of vehicles from the video as the time to cross two lines marked in the computer screen at a known distance apart. The following observations were made:

- The speed data are more reliable than the volume count.
- Since the speed is calculated based on the entry and exit on the same loop, the results depend on the exact length configuration with respect to real field.

The speed accuracy was also checked for varying loop lengths and 9.2 m gave the best result as before (Figure 34).
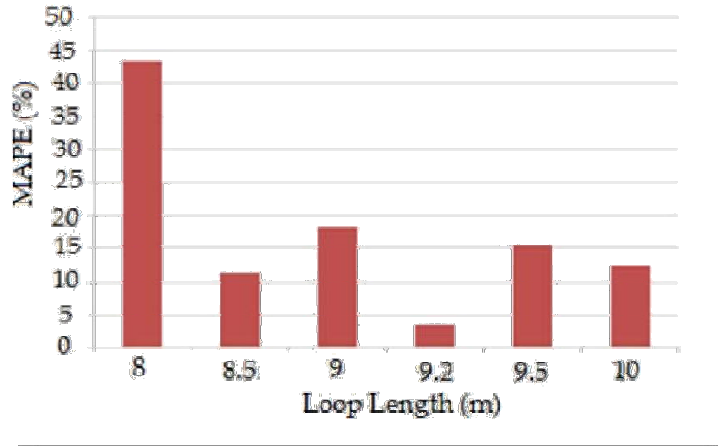
Figure 34: MAPE for Speed evaluation for different loop lengths

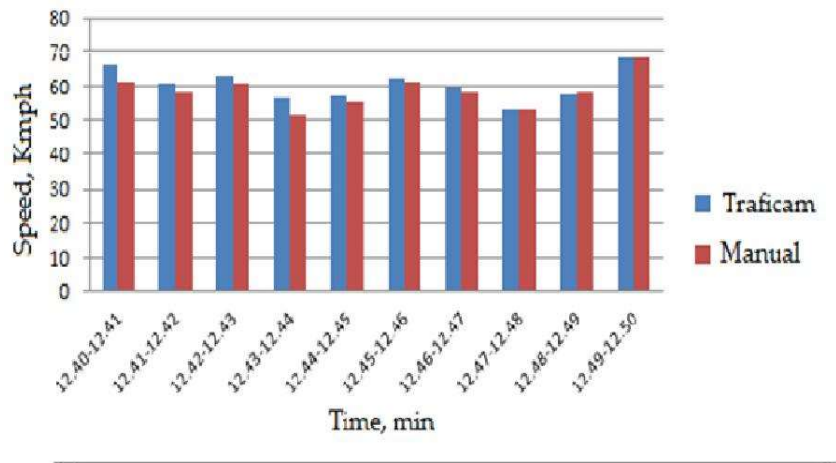With 9.2 m loop length, the accuracy of speed data was checked and one sample result is shown below.

Figure 35: Vehicle speed of Traficam & Manual data for 9.2m loop length

g) Level of Service

Apart from data collection, Collect-R can be used to obtain direct alarms on congestion and level of service. Traficam can give five different level of service, based on occupancy and speed. The thresholds for these parameters are user defined and can be changed according to the traffic conditions. The LOS alarms indicate the fluidity of traffic on the road. There are 4 different trigger levels for the 5 different LOS states. When traffic is fluid the state is "LOS 0" and dense traffic corresponds to "LOS 4".The following levels were set for the study:

- When Occupancy <20% , the level is "Service 0" (Normal traffic)
- When Occupancy >20%, Speed >60 Km/hr, the level is "Service 1" (Dense traffic).
- When Occupancy >20%, 40Km/hr<Speed <60 Km/hr the level is "Service 2"

(Delayed Traffic).
- When Occupancy > 20%, 20 Km/hr<Speed <40Km/hr, the level is "Service 3" (Congested Traffic).
- When Occupancy > 20%, Speed < 20 Km/hr, the level is "Service 4" (Stop & Go Traffic).

In the absence of traffic, since the Traficam cannot detect any speed, the default speed is considered and the appropriate level of service (Service 0) is adopted. The shift from LOS 0 to LOS 1 is dependent on the occupancy on the road. By default the value for LOS 0 is 20% but this can be changed by the user. When occupancy exceeds 20%, the LOS1 alarm is activated. The other trigger levels are based on vehicle speeds. When the speed (by default) falls below 60 kmph, the state becomes LOS 2. When the speed falls below 40 kmph LOS 3 is activated, and speeds lower than 20 kmph activate LOS 4. These values can be preset in the PC Tool.

With the finalized loop width, length and other parameters, evaluation of sensor was carried out separately for total count, classified count, and speed . The results are presented in the next section:

6.1.4 Evaluation

a) Evaluation of Volume
Accuracy of total vehicle count was carried out on various days under varying traffic flow conditions. Actual count was extracted from the video collected from the Traficam location and was compared with Traficam count for one minute aggregate intervals and was quantified in terms of MAPE.

Table 3 discusses the characteristics of each of the traffic condition. Table 4 shows the obtained results for Traficam total volume. The sample plots (Figure 36-Figure 38) below show the comparison of actual and Traficam count for one minute analysis.

Table 3: Characteristics of Traffic conditions

Condition	*Traffic*	*Light*
Morning Peak	Dense	Bright
Afternoon Off Peak	Less	Bright
Evening Peak	Dense	Low

Table 4: Analysis of volume from Traficam

Date	Time	Condition	MAPE (%)
28.08.12	10:39 am -11:07 am		35.29

11.10.12	09:21 am -10:00 am	Morning Peak	30.54
25.10.12	09:32 am -10:02 am		14.47
04.09.12	09:38 am -10:09 am		34.43
24.09.12	10:00 am -10:30 am		47.30
19.12.12	08:51 am -09:23 am		53.88
20.12.12	09:39 am -10:02 am		48.43
12.11.12	11:20 pm -12:20 pm	Afternoon Off Peak	43.74
17.12.12	15:58 pm -16:31 pm		43.32
18.12.12	14:02 pm -14:31 pm		25.65
19.12.12	13:05 pm -13:37 pm		34.96
20.12.12	14:37 pm -15:07 pm		37.10
30.08.12	17:00 pm -17:49 pm	Evening Peak	35.10
05.09.12	16:33 pm -16:56 pm		33.49
10.10.12	16:50 pm -17:20 pm		31.10
18.12.12	17:48 pm -18:18 pm		25.51
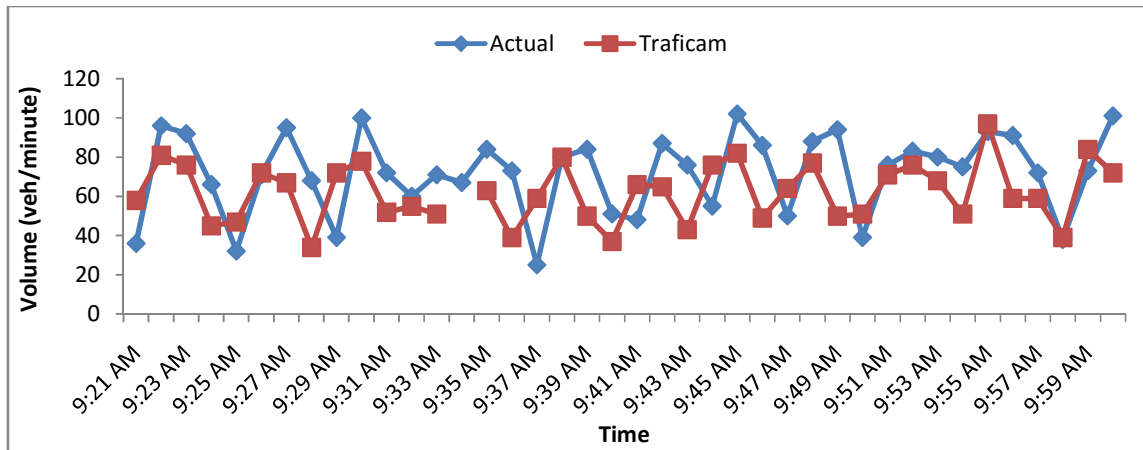
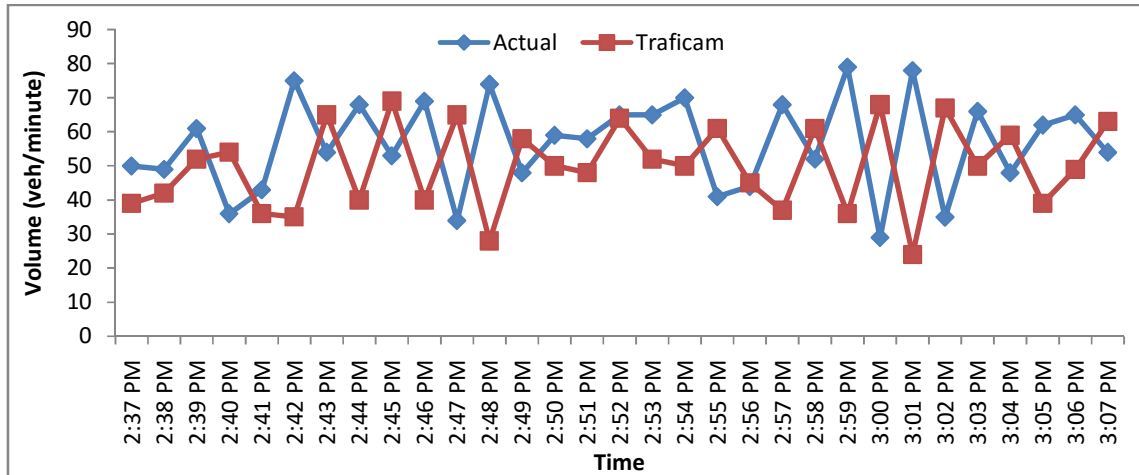**Figure 36**: Sample comparison of Traficam and actual count for morning peak period

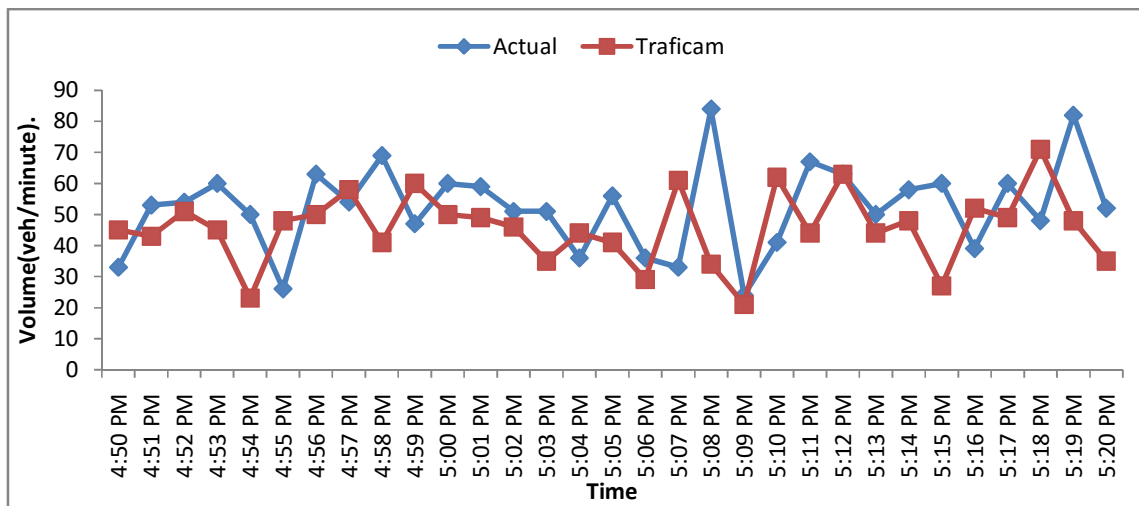**Figure 37**: Sample comparison of Traficam and actual count for afternoon off peak

Figure 38: Sample comparison of Traficam and actual count for evening peak period

b) Evaluation of Classified Volume

Accuracy of classified count was also of interest. The classification is based on the vehicle length. The default classifications in Traficam were giving high errors. Hence the detection zone length was changed based on the actual field measurements. Still, there was significant difference in the classified counts for different vehicle type between Traficam and video counts. Traficam can identify three classes of vehicles based on the threshold values assigned. The table below shows the analysis of classification for varying threshold values. Instead of MAPE, MAE was used for the evaluation of third class because of less number of vehicles. Three threshold values were attempted during the evaluation- 4m-10m, 3m-8m, 4m-7m. Threshold 4-10 indicates length of class1 vehicles are below 4m, class2 is in between 4m and 10m and class 3 above 10m. So two wheelers and three wheelers will come under class1. Class2 includes cars and Light commercial vehicles and Class 3 include buses and trucks. The results obtained during the analysis are shown in the table below.

Table 5: Classification Analysis for Traficam

Date	Threshold	Class1 (MAPE %)	Class2 (MAPE %)	Class3 (MAE)
13.03.12		36.42	71.94	3.36
18.03.12		33.75	44.86	2.52
22.03.12	4m-10m	40.86	48.59	1.8
29.03.12		34.48	33.02	2.17
30.03.12		40.77	61.74	5.75
18.04.12		42.30	19.68	1.48
27.04.12	3m-8m	32.12	41.24	1.9
30.04.12		44.86	33.18	1.8
20.04.12		31.45	45.35	4.33
23.04.12	4m-7m	20.33	35.44	3.96

The sample comparison of volume for different classes of vehicles is shown below in Figures 39, 40, and 41.
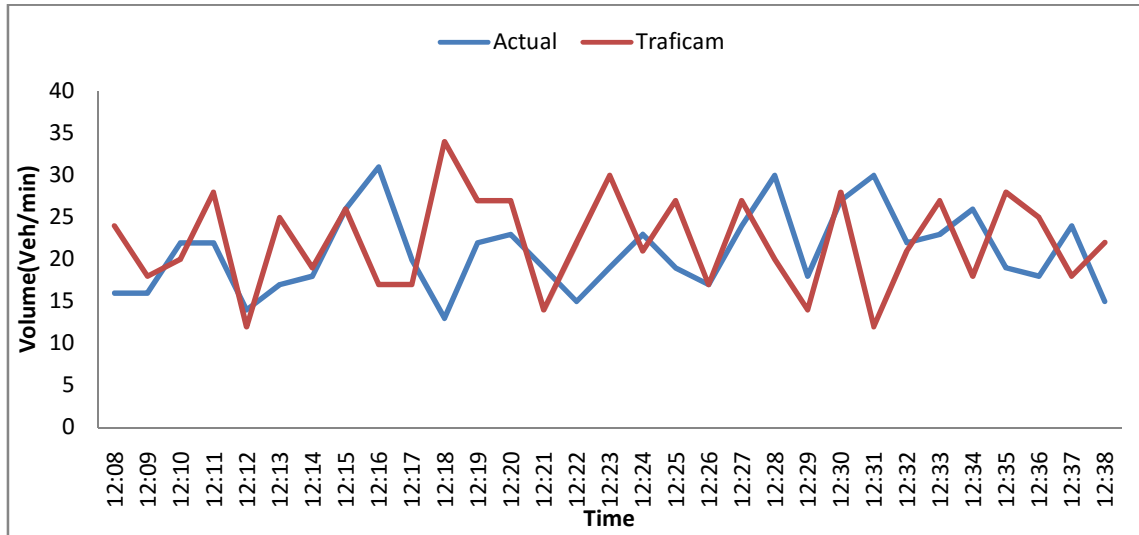

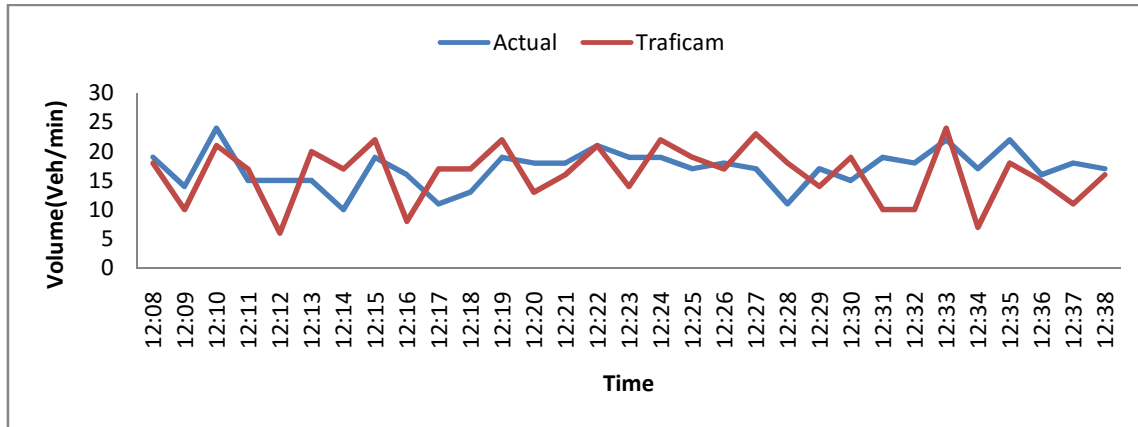**Figure 39**: Sample comparison of Class 1 on October 23, 2011

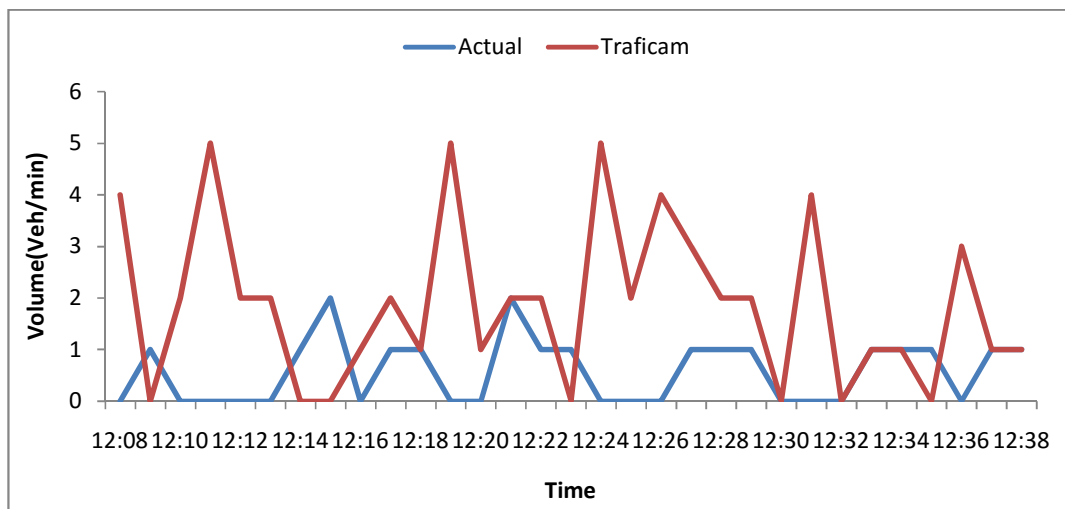**Figure 40**: Sample comparison of Class 2 on October 23, 2011

Figure 41: Sample comparison of Class 3 on October 23, 2011

c) Evaluation of Speed

Like total volume and classified volume, speed from Traficam was also evaluated and is detailed in this section. The actual speed of a vehicle was found directly from the field using laser gun. Individual vehicle speeds were identified and were averaged over one minute interval. This was compared with the Traficam reported speed values. Analysis for average speed was carried out for different days and the results are shown in the Table 6 below. A sample comparison plot is also shown in the Figure 42.

Table 6: Evaluation of Traficam speed

Date	Time	MAPE (%)
21.02.12	10:48-11:20	21.86
09.03.12	12:17-12:34	16.46
22.05.12	09:59-10:17	19.28
25.09.12	15:13-15:36	51.88

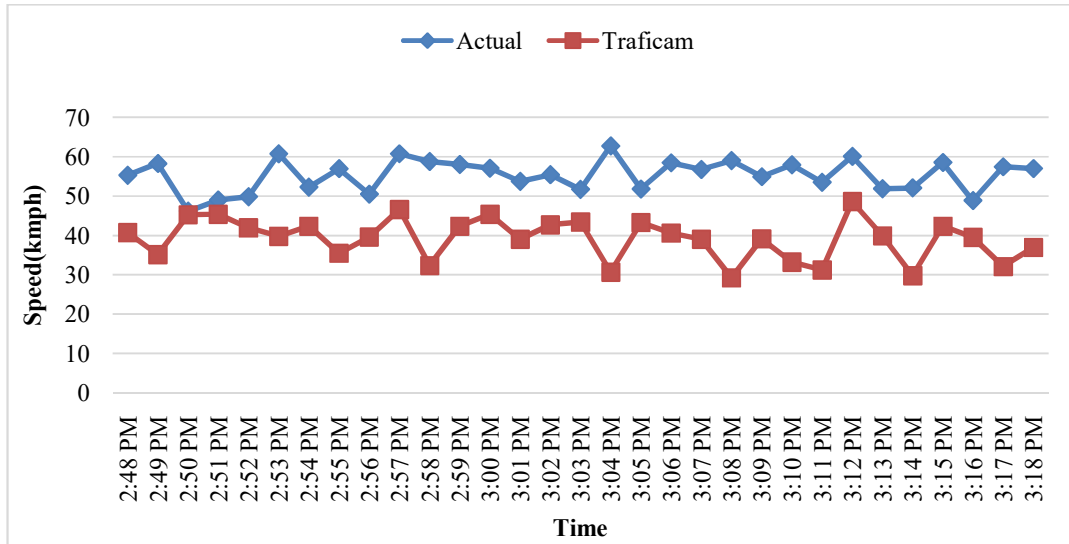| 10.10.12 | 09:37-10:07 | 40.59 |
| 14.12.12 | 14:48-15:18 | 28.75 |

Figure 42: Sample speed comparison plot on September 25

6.2. TIRTL

6.2.1 Device Description

TIRTL is the abbreviation of The Infra-Red Traffic Logger. It is manufactured by CEOS Pvt. Ltd, and marketed by CEOS Industrial. TIRTL consists of a transmitter that transmits two parallel and two cross beams of Infra Red (IR) radiations and a receiver unit on the opposite side of the carriageway that detects disturbances to the infra-red beams caused by wheels of the passing vehicles. Inbuilt intelligent software analyzes the timings of the emitted and received light pulses to classify vehicles. TIRTL gives the information such as time, lane, velocity, class, axels, wheel base, classification, occupancy etc. which can be customized according to the need of the user.

 a) Components of TIRTL
The TIRTL is available as permanently fixable and portable types. The portable version of TIRTL is transported using a suitcase trolley and was used for the study purposes [Figure 43] and the permanently fixable equipment is kept in the aluminum box which can be fitted into both sides of the kerbs of the road for transmitting and receiving. TIRTL operates from -40 to 85º C, is IP67 rated and it is resistant to sunlight, rain, hail, dust and fog.

Figure 43: The portable TIRTL used in this study

Figure 44: Permanent installation site

The main components of portable TIRTL are:

Transmitter
Receiver
Tripods (2 numbers)
12 volts battery (2 numbers)
Laptop
Focus Lenses (2 numbers)
USB converter

In the case of portable TIRTL the transmitter and receiver requires external power supply, which is provided by using two 12 volt batteries. Data is transferred to the TIRTL application in the laptop by connecting TIRTL and the laptop using Ethernet port or

serial port available at the receiver end.

The transmitter unit is paired with a complimentary receiver unit. The transmitter and receiver are similar in appearance. The only identifiable external difference between the transmitter and receiver is that Serial Port B is not present on the transmitter unit. Components of the permanently fixable TIRTL device vary according to the usage and installation from the portable device. Following are the components:

Transmitter
Receiver
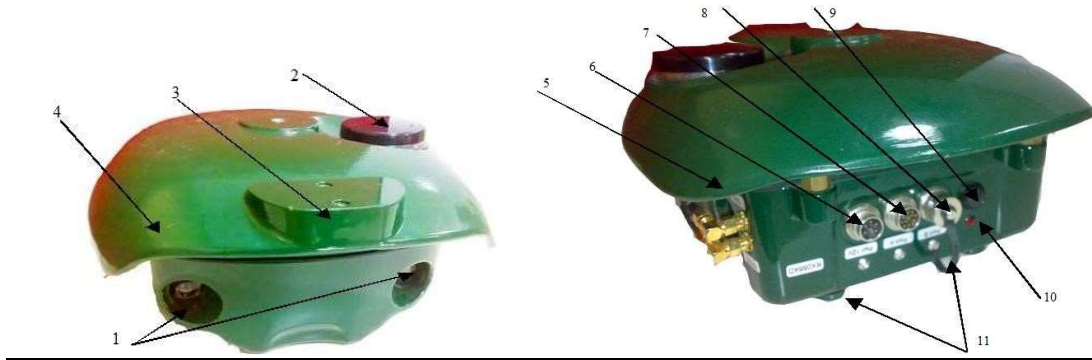GPS and GSM antenna
12V AC power supply
Aluminium Cabinets

Figure 45: Components of Transmitter and Receiver

Table 7: Various components of TIRTL and its descriptions

Item	Features	Description/Purpose
1	Lens	Passage for the infra-red beams.
2	3G/GPS Antenna	Fitted if the unit has the 3G/GPS option
3	Top Sight Mount	Machined surface and alignment pin holes on the top of the sun-shield used for accurate Optical Sight placement.
4	Sun-Shield	Used for portable applications to protect against direct solar radiation exposure.
5	Top Sight Mounted	Machined surface and alignment pin holes on the top of the sun- shield used for accurate Optical Sight placement.
6	Power Connector	5 pin external power connector and fixed line modem

		connection.
7	Serial Port A	12 pin external communications connector (typically RS232)
8	Serial Port B	12 pin external communications connector (typically RS232,receiver unit only)
9	Mode Button	Used to turn the unit on and off.
10	Indicator LED	Conveys information regarding the current operational state of the unit.
11	Battery Door Screw	Unscrewed to gain access to the battery compartment and the SIM card stocked

b) Working Procedure

The TIRTL transmitter's infra-red cones cross each other and form two straight and two diagonal beams. When a vehicle crosses the path of the beams, the TIRTL records two beam events, one from the vehicle entering and the other, leaving the beam pathway. These two events are recorded for all four beam pathways. Thus, eight time-stamped events are generated per axle. The velocity is derived from the timestamps of these beam events. Since, the velocity of each vehicle wheel is known and a timestamp is recorded for each axle crossing each beam, the inter-wheel (or inter-axle) spacing can be determined. Once the inter-axle spacing is known, it is compared with database of inter-axle spacing ranges stored in the unit to determine the correct classification of the vehicle. The results are stored on a per vehicle basis.

1) Vehicle Detection and Wheel size measurement using "Beam Events"

The transmitter emits two straight beams and two cross beams, which get overlapped at the receiver end. Each wheel of the vehicle passing between the transmitter and receiver interrupts each of the four beam pathway.
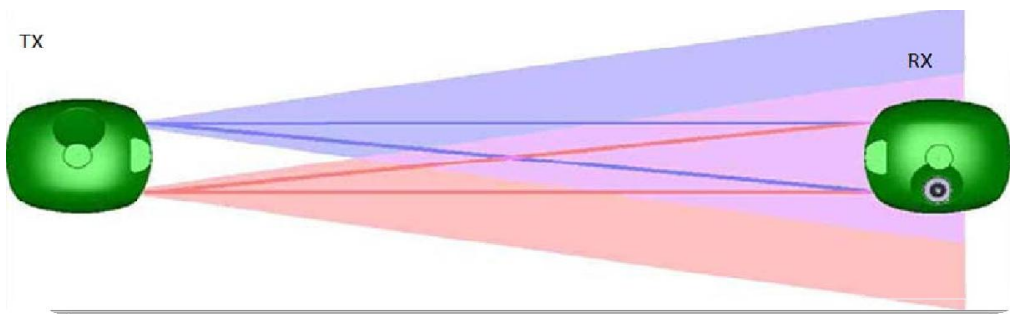

Figure 46: Transmittance and Reception of IR Beams by the TIRTL Duo

As shown in Figure 47, when a vehicle intercepts the infra-red beams, the beams are disturbed, resulting in what is known as the 'Breaking Beam Events'. Similarly, when the vehicle leaves, the beam is reconstructed again back to its normal position called 'Making Beam Events'. Thus, with the passage of each vehicle wheel, a set of eight time-stamped

beam events are generated from the 4 beam pathways at the TIRTL receiver. The precise time of each beam event allows the receiver to compute the velocity and lane of each vehicle wheel as it passes.
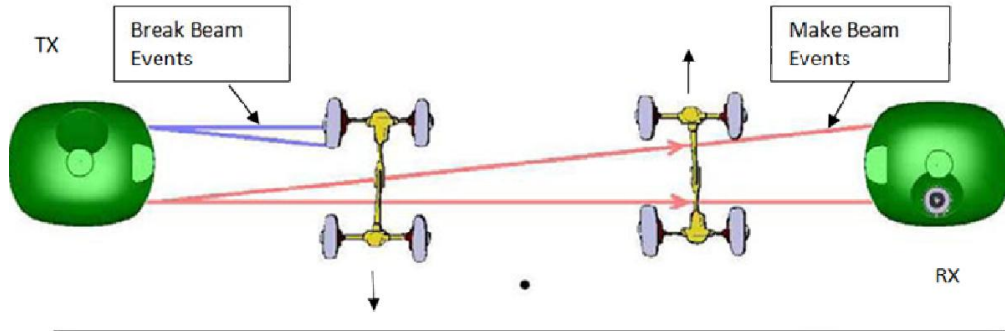

Figure 47: Breaking and Making Beam Events

The wheel size plays an important role in vehicle detection and classification. Each of the infrared beam pathways between the transmitter and the receiver scribes a chord across the passing wheel. The vehicle type and class can be deduced using data on the speed of the vehicle, time between break and make of beam events and traveling lane.

2) Detection of Speed and Vehicle Direction
Figure 48 illustrates a TIRTL installed on a bi-directional roadway as viewed from above. As the wheels of the vehicles interact with the 4 beam pathways, make and break beam events are generated. The speed of a vehicle is determined by the time interval measured (t1 or t2) between like Beam Events on the parallel beams, A and B.
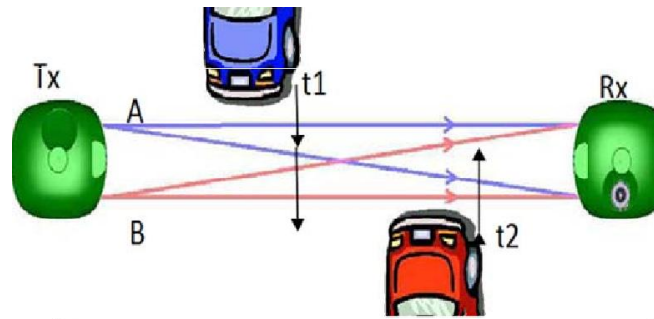

Figure 48: Speed detection using make and break beam events

The direction of traffic is determined by the order in which the beam events occur. In the figure, A to B represents south bound traffic and B to A represents north bound traffic. According to the direction convention, traffic moving from left to right when viewed from the rear of TIRTL receiver is given positive speed sign and the opposite direction speeds are represented as negative speeds. For this to be accurate, the installation details are to be entered correctly in the site information. The site information should reflect the exact orientation of the TIRTL units.

3) Lane Detection

In Figure 49, once the vehicle crosses the infra-red pathway, A, Ax, B and Bx, beam events are generated. For each class of beam events, make or break time intervals are measured. In the figure, t1 and t2 are the intervals between the beam events on the beams A and Ax. t3 and t4 are the intervals between the beam events on the beams A and Bx.
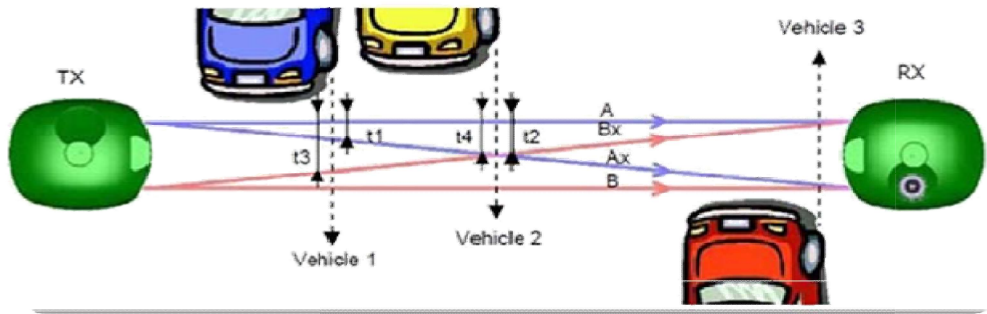

Figure 49: Lane detection in TIRTL

Quantized time difference between the time interval t1 and t2 are used by the TIRTL receiver software to identify the lane in which a particular vehicle travels. The time interval t3 and t4 are used to double-check the lane details of the vehicle.

4) Vehicle Classification

The combination of a break beam event followed by make beam event of the same beam occurring within a single vehicle lane help in detection of an axle. The TIRTL software uses a number of different features of the wheel base of road vehicles to classify vehicles. A classification scheme has been developed by the classification editor according to user requirements and traffic condition. The classification scheme contains a series of patterns based upon parameters associated with vehicle axles.

TIRTL classifies 15 different class of vehicles, which is unique from other devices that classifies to 3 or 4 classes. Also, the outout from TIRL is individual vehicle details than an aggregated information and hence the evaluation can be carried out at individual vehicle level.

6.2.2 Installation of TIRTL

The following steps were carried out during the installation of TIRTL at the installation site.

(a) TIRTL Alignment
Proper TIRTL deployment must meet all of the installation conditions given below:
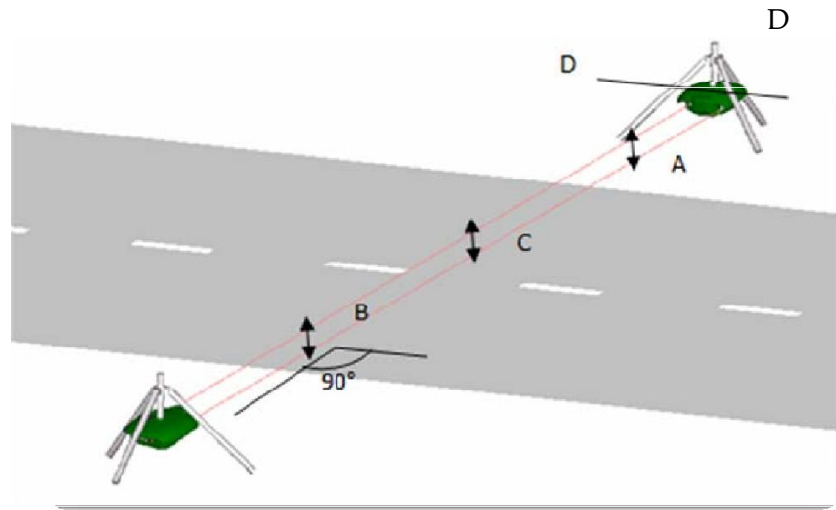
Figure 50: Specifications for installation of TIRTL

The infra-red beams must be at 90° to the direction of traffic.
1. A line (D) drawn between the lenses on each TIRTL must be parallel to the surface of the road.
2. The height (C) of the beams above the peak of the road surface must be of the order of 5 to 6 cm.
3. The height (A and B) of the beams above the edges of the road must be equal, this is important for roads with large camber.

6.2.3. Configuration Procedure

a) TIRTL Software
TIRTL Soft is a Windows-based application developed by the COES for configuring and monitoring individual TIRTLs. TIRTL soft screens allow its users to view the TIRTLs configuration, status and traffic events at any time. Once the installation is complete, the user can connect TIRTL soft in four different modes.

PPP Direct Serial: The physical connections to the serial port of TIRTL
PPP Dial Up Modem: Where an optional modem module has been fitted to TIRTL. The user may be remotely connected via a standard landline telephone connection or via mobile telephone.
Mobile Call: The user connects via a mobile call connection, such as 3G or GSM.
TCP/IP: The user remotely connects via an IP network using PPP.

b) Connecting TIRTL
The following tasks were performed to connect and install TIRTL.

Connection to TIRTL was first established by clicking on the ☎ icon on the task bar or

activating the TIRTL tagged drop down box in the menu bar. The activity log was viewed to confirm that connection has indeed been established.

Once connected, the following actions were taken:

Check status- after clicking the TIRTL status, clicking the update button below the status button provides information on beam level, an important parameter in vehicle detection.

Classification scheme – A correct class scheme need to be uploaded before monitoring. The classification scheme is developed by the classification editor (TirlSoft GUI). A pre-determined vehicle class is available as a .tcf file to meet user requirements and the traffic conditions. The TCF file was loaded through the configuration tab in the main menu.

Site information - the following site orientation details must be inputted before the monitoring activity-
- Total separation
- Carriage way width
- Max axle spacing
- Min axle spacing
- No: of right bound traffic
- No: of left bound traffic
- Traffic direction in accord with the transmitter

Height setup – This displays the graph of the calculated heights of the beam above the road level. The number of groups of dots will depend on the number of lanes that are to be monitored.

There are two groups of dots and 3 zones,
- Dark dots represent the multiple measurement of beam height at the same point.
- Light out laying dots can be ignored.
- A dot in the green zone represents ideal beam height.
- A dot in the yellow zone is moderate.
- If the point falls in the red zone then the TIRTL set up is either too low or too high to operate.

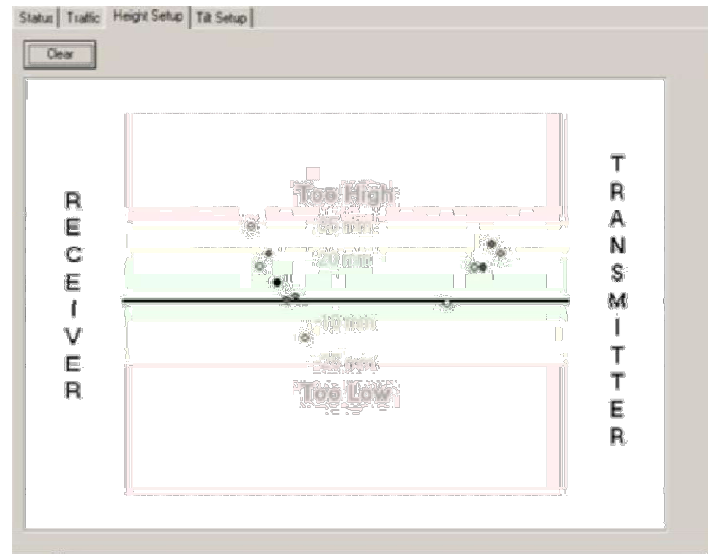The setup must be configured in such a way that the dots should fall in the green zone

Figure 51: Height setup options

The same may be followed for the "TILT set-up" which plays a vital role in gaining the number of IR beams that in a way helps the accuracy.

c) Site selection
The portable TIRTL unit was used at different locations so as to choose the ideal location for TIRTL to be placed permanently. The following content discusses the problems encountered during installations, and detection of vehicles.

A demonstration of the TIRTL under real traffic conditions was made on 17th June 2010 by a team from CMS Bombay. The portable TIRTL instrument was set up near SRP tool junction, Chennai. This junction has four undivided (2 way traffic) lanes.

The following problems arose:
- The shoulders were not of same level which led to delays in field installation of the TIRTL.
- There were difficulties in connecting the laptop to the instrument.
- The class scheme was not able to identify two-wheelers and all other vehicles were identified as LCV.

Following technical support provided by the support team in Australia, a new version of TirtlSoft was installed. After the TIRTL software was updated another survey on 24th September, 2010 on the stretch of a 6-lane, bidirectional road opposite Rajaji Bhavan, Besant Nagar. Here too, the camber was too high and hence only one directional flow (3 lanes) was monitored. The results of the survey are as follows. The total manual count between 2:29 pm and 2:59 pm was 303 and the total TIRTL count was 259.

Vehicle classes such as 2-wheeler, LCV and LMV were being undercounted and 3-

wheelers were over-counted by 19. The over-counting happened due to miss judgment of vehicle class. The TIRTL and video data were compared for every minute and Mean Absolute Percentage Error (MAPE) was found to be 14.18. Although the results were better than earlier surveys, the problem of non-detection of HMV remained.

Another survey was conducted in the 6-lane, bidirectional stretch of road opposite the Rajaji Bhavan on 21st October, 2010. The high camber restricted monitoring to unidirectional (3-lane) flow, where the traffic was much less than the other site. New urban vehicle classification was used in this survey. The results of the survey conducted between 1:09 pm and 2:28 pm are as follows. The total manual count was 203 and the TIRTL count was very close at 204.

A third survey was conducted on 1st November, 2010 on a five lane road with one-directional traffic at the Toll Plaza on Rajiv Gandhi Salai. The traffic volume on this stretch was higher than those in the earlier locations and the types of vehicles were varied, posing a considerable challenge to TIRTL. The same class schemes as the previous were used. The survey was conducted briefly (16:02 pm to 16:18 pm) because of delays in installation.

The total manual count was 652 and the TIRTL count was 510, showing a difference of 142 between the two. The two-wheelers contributed to this large difference. There was an undercount of 77 in two wheelers, a significant number compared to other classes, due to grouping of two wheelers. The MAPE value between TIRTL and manual video monitoring was 20.95.

Another survey was conducted on 24th November, 2010 on the five-lane, unidirectional stretch at the Toll Plaza in Rajiv Gandhi Road between 12:38 pm and 13:00 pm. The traffic volume was high, and the types of vehicles varied. The same classification was used as before. The total manual count was 1496 and TIRTL count was 1434, accounting for a difference of 58. The MAPE when data was compared every minute was 5.19. The TIRTL faced difficulties in identifying two-wheelers.

The next survey was conducted on 3rd December, 2010 near Raj Bhavan between 1.33 pm and 2.04 pm on a four lane road with unidirectional traffic. A new class scheme developed by CMS Bombay was introduced. The total manual count was 2268 and total TIRTL count was 1128, showing a difference of 1140. The MAPE was 48.38. There was significant undercount in TIRTL data and hence was decided to use the previous classification table.

The next survey was performed on 9th March, 2011 at the Toll Plaza in Rajiv Gandhi Road between 12.08pm and 2:26 pm. The total manual count was 1080and total TIRTL count was 1042 leading to a difference of 38. The MAPE was 15.04 this time.

The MAPE values from the various studies using TIRTL at various locations were compared and it was observed that Rajaji Bhavan and Toll Plaza are two ideal locations to operate the TIRTL. Some problems that were incurred during the tests include: difficulty in establishing connectivity between the laptop and instrument, un-suitability of location for survey, difficulty in alignment of the TIRTL, issues with classification and generation of junk data. Thus, Perungudi Toll Plaza, Chennai, was finally selected for the installation of the TIRTL device permanently.

It is a unidirectional 3 lane road with Southbound Traffic travelling from Perungudi to Madhyakailash. It is a free flowing traffic coming out of the toll plaza. Equipment was connected through 3G/GPS antenna with a static IP from ITS lab, IIT Madras. Initially there were issues with the connectivity and the site maintenance. 2G was changed to 3G connection and latching of network has been done for getting a proper band width. Rain water has seeped into the device which was cleared by arranging drainage and the fitting of the cabinet was also taken care of.

Up-gradation has been done by the CEOS in the month of January 2013 for much effective results and reducing number of vehicles identified as Un-classified vehicles in the output. After the up-gradation the evaluation was started and following were the results obtained.

Ideal Conditions for TIRTL

- The infra-red rays should be at an angle of 90 degree with the movement of traffic. Therefore the transmitter and receiver have to be placed at positions satisfying the criteria.

- The height of beam has to be in the range of 5-6cm. Therefore road surfaces with large camber cannot be considered for installing the device.

- The device can perform well under the locations which are less affected by the pedestrian movements in the infra-red beam path.

- The free flow condition maintained by the toll plaza at Perungudi site was well suited for the detection of vehicles by the device. The evaluation result shows that the accuracy of detection of vehicles has reduced significantly under stop and go condition.

6.2.4. Evaluation

a) Evaluation of Volume
Following is the evaluation chart of TIRTL, which was fixed permanently, for 13th Feb

2013, in which different vehicles were evaluated separately and the accuracy for each type of vehicle is tabulated. The table shows performance of TIRTL during both peak and off peak conditions.

Table 8: MAPE for different traffic conditions

Date	Time	MAPE(%)	Traffic
07.03.13	10:45 am -11:46 am	0.29	Peak
21.02.13	09:39 am - 10:41 am	2.35	
21.03.13	10:00 am - 11:01 am	1.02	
13.02.13	03:48 pm - 04:45 pm	0.82	
21.02.13	17:56 pm - 18:54 pm	1.02	Off-peak
28.02.13	07:49 am - 08:50 am	0.32	
28.01.13	11:31 am - 12:30 pm	0.77	
08.03.13	01:07 pm - 02:07 pm	1.02	
05.11.15	2:20 pm - 3:10 pm	1.93	

From the table it can be seen that there is no significant difference in the performance of TIRTL during peak and off peak conditions. The following figure show a sample plot of comparison of actual volume and TIRTL volume.
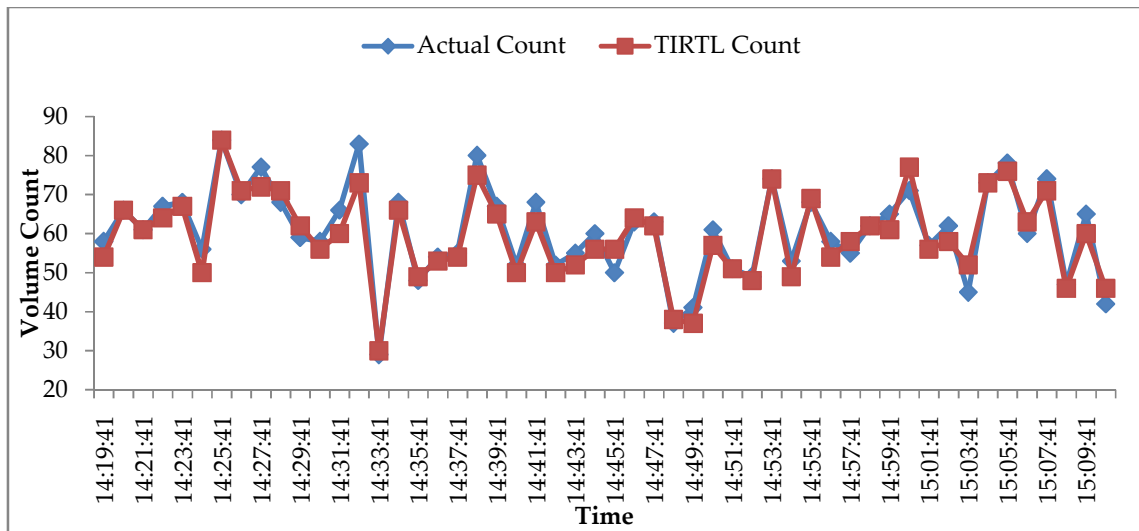

Figure 52: Comparison of actual count and the TIRTL count

b) Evaluation of Classified Volume
Since TIRTL is able to give per vehicle data, the analysis was also conducted based on

individual vehicles passing the intersection. In the previous evaluations, interval was considered for continuous one hour and error was determined. Here, each single vehicle passing the sensor was identified from corresponding video. For quantifying error, average percent error was calculated for every minute and was averaged over the total interval. The results are shown in the table shown below.

TIRTL classifies vehicles in to 15 classes based on the axle length. For the classified analysis, these classes were combined in to four classes by manual identification - two wheeler (2W), three wheeler (3W), Light Motor vehicles (LMV) and Heavy Motor Vehicles (HMV). The table below shows the classified evaluation of TIRTL.

Table 9: Classified TIRTL Evaluation

Date	MAE			
	2W	3W	LMV	HMV
07.03.13	0.93	0.38	0.74	0.32
28.02.13	2.58	0.29	0.29	0.13
05.11.15	2.44	0.73	1.35	0.52

Figures below show sample plots of comparison of TIRTL classified count with the actual classified count.
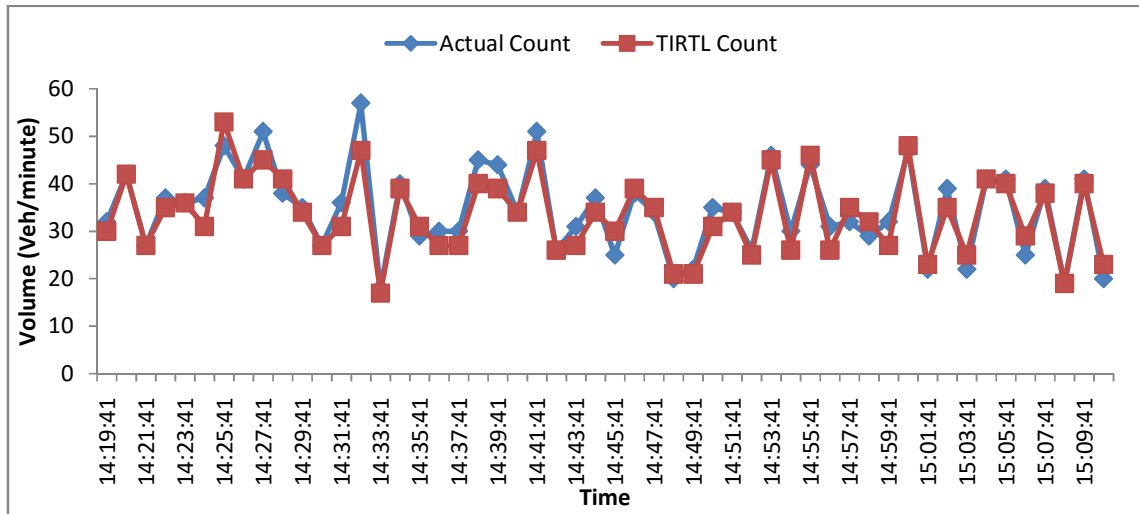

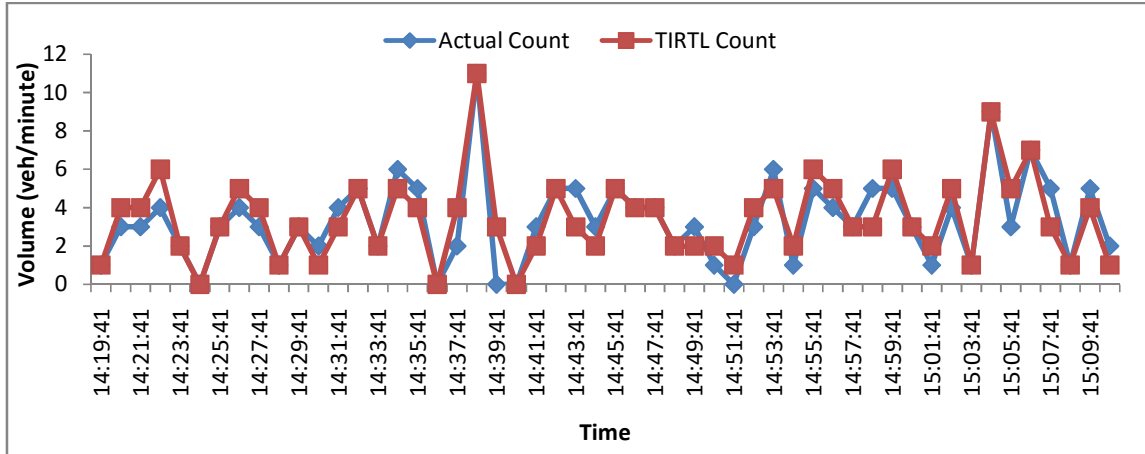**Figure 53**: Comparison of actual 2W count and the TIRTL 2W count

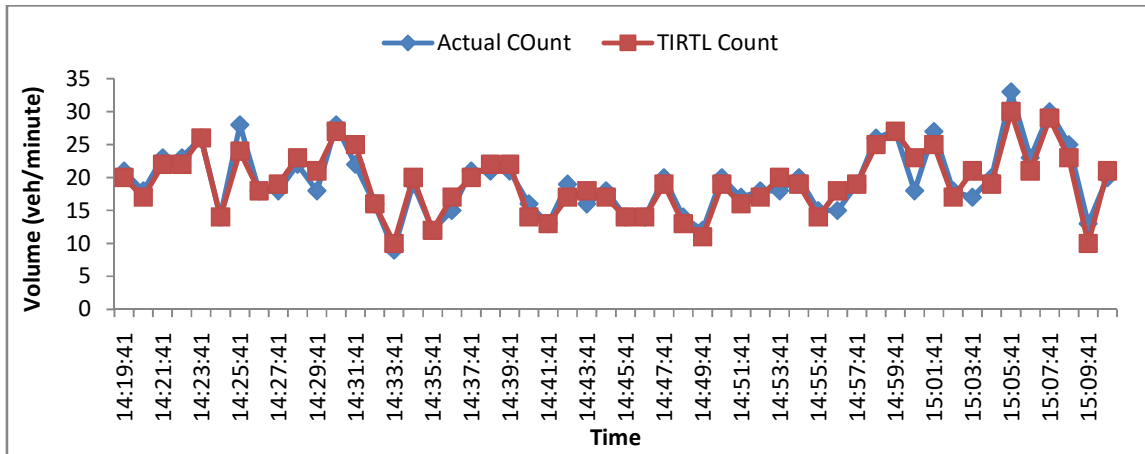**Figure 54**: Comparison of actual 3W count and the TIRTL 3W count

Figure 55: Comparison of actual LMV count and the TIRTL LMV count
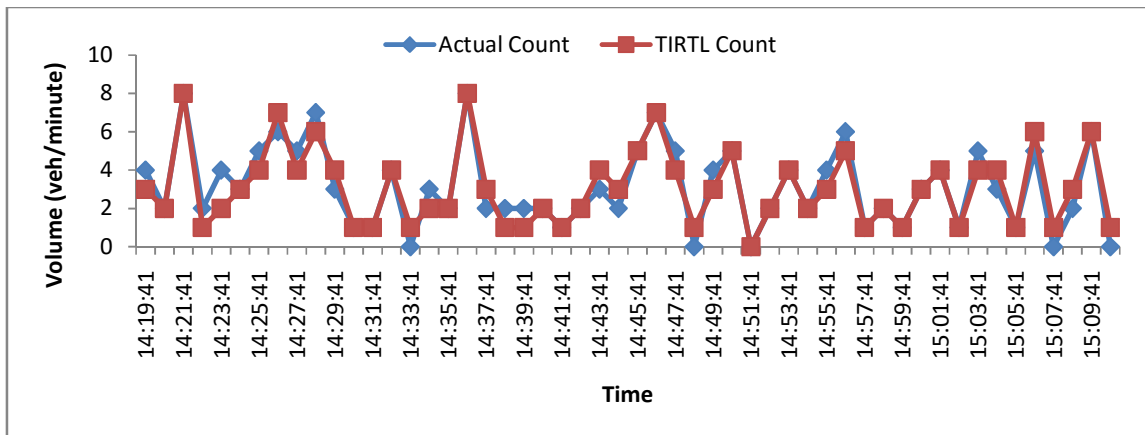

Figure 56: Comparison of actual HMV count and the TIRTL HMV count

c) Evaluation of Volume and classified volume at different locations

Taking the traffic scenario into consideration, portable unit has been taken to various sites with different scenarios to find the efficiency variation in the device, and found that there is a lot of variation in the accuracy. Tables 10 and 11 show the results obtained for both total volume and classified volume.

Table 10: Evaluation of total volume at different locations

Date	Time	Place	Actual count	TIRTL count	MAPE (%)
01.05.13	07:45 am -08:45 am	Tidel Park	2135	1807	15.36
23.05.13	12:40 pm - 1:40 pm	Aquatic complex (Towards Velachery)	3803	3391	10.83
23.05.13	12:40 pm - 1:40 pm	Aquatic complex (Towards Guindy)	2427	2215	8.74
23.08.13	6:08 pm - 6:48 pm	Gurunanak College	1140	971	14.86
08.11.13	5:31 pm - 6:16 pm	Gurunanak College	1346	1181	12.35
04.04.14	9:00 am - 12:30 pm	Sirucheri	4468	4540	1.61

Table 11: Evaluation of classified volume at different locations

Date	Time	Place	2W_MAE	3W_MAE	LMV_MAE
01.05.13	07:45 am -08:45 am	Tidel Park	3.07	0.18	1.7
23.05.13	12:40 pm - 1:40 pm	Aquatic complex (Towards Velachery)	4.73	0.28	2.2
23.05.13	12:40 pm - 1:40 pm	Aquatic complex (Towards Guindy)	1.38	0.02	1.72
23.08.13	6:08 pm - 6:48 pm	Gurunanak College	3.49	0.72	1.03
08.11.13	5:31 pm - 6:16 pm	Gurunanak College	3.39	1.11	0.93
04.04.14	9:00 am - 12:30 pm	Sirucheri	0.97	0.42	0.79

The following observations were made during the evaluation of TIRTL at different locations.

- Two-way undivided traffic was tried near aquatic complex, Velachery for an hour duration. It was found that there was an issue in identifying the HMV and LMV.

- One-way stop and go condition tried at Tidel park junction, Thiruvanmiyur for an hour duration. There was a lot of decrement in the accuracy, which was discussed and found that it was due to the improper stop and go condition in Indian condition. The same problem was observed near Gurunanak College, Velacherry, where the traffic was bi-directional with no median.

- When the pedestrian movement is more, error is found large in the TIRTL results. For example, in Sirucheri during the survey, it was observed that there were a lot of constant pedestrian movements.

- Camber is a greater issue to find a working site for TIRTL.

d) Evaluation of Speed
For the evaluation of TIRTL, individual speed of each vehicle identified by the sensor was compared with speed measured in the field using laser gun for the corresponding vehicle. This involved matching of individual vehicles speeds.

Table 12: Evaluation of TIRTL speed data

Speed Evaluation		
Date	Time	MAPE(%)
13th Feb 2013	15:54:00-16:10:43	4.135
07th Mar 2013	10:45:43-10:48:54	2.938
08th Mar 2013	13:07:06-13:11:18	3.05
05th Aug 2013	15:10:00 – 15:40:00	5.1
06th Aug 2013	16:01:00 – 16:30:00	4.07
07th Aug 2013	14:59:00 – 15:30:00	6.2

Speed analysis, for six days, was done using the laser gun and relating it with the video recorded manually. Each vehicle needs to be chosen according to time and make the

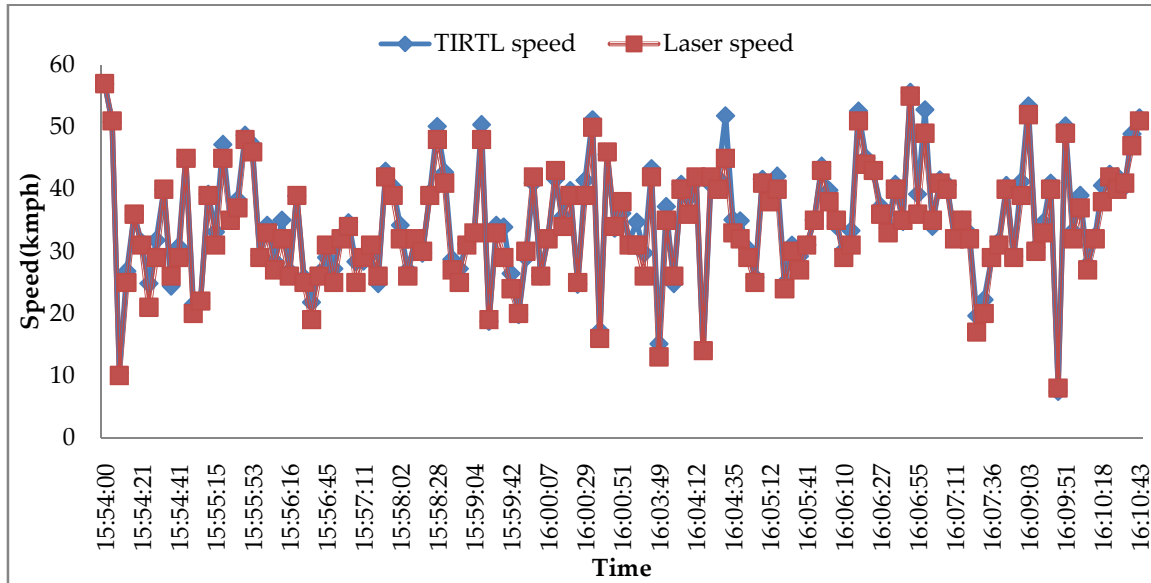relation with the picture of vehicle given by laser gun. Following is a sample plot of the speed analysis.

Figure 57: Comparison of TIRTL speed and actual speed

Note: TIRTL device gives better results compared to many other devices but it needs a customized location. Accuracy depends on the site and the vehicle movement.

The site in which the permanent device was installed has a free flow and there is no issue with the camber of the road too, which is an ideal scenario because of which we are getting such result.

6.3. Wavetronix Smartsensor HD traffic sensor

6.3.1 Device Description

The Wavetronix Smartsensor HD traffic sensor uses 24.125 GHz radio waves to collect and deliver traffic statistics. The Smartsensor HD is capable of measuring traffic volume and classification, average speed, individual vehicle speed, lane occupancy, and presence. Classified as Frequency Modulated Continuous Wave (FMCW) radar, the Smartsensor HD detects and reports traffic conditions simultaneously over as many as ten lanes of traffic.

6.3.2. Installation of Wavetronix

a) Study location

The location chosen for the study was Indira Nagar, as shown in Figure 58. It is a six lane bi-directional traffic with a median separates the two way traffic. Roadway has shoulders on either end.

Figure 58: Study site Indira Nagar

b) Sensor placement

Installation of the Smartsensor HD involves attaching the mounting bracket to a pole, attaching the sensor to the mounting bracket, aligning the sensor and connecting the Smartsensor cable to the sensor. Once the location is identified (preferably locations without buildings and other obstructions nearby), the sensor is fitted at a few meters offset and height. The optimum height and offset is given in the following figure and table.
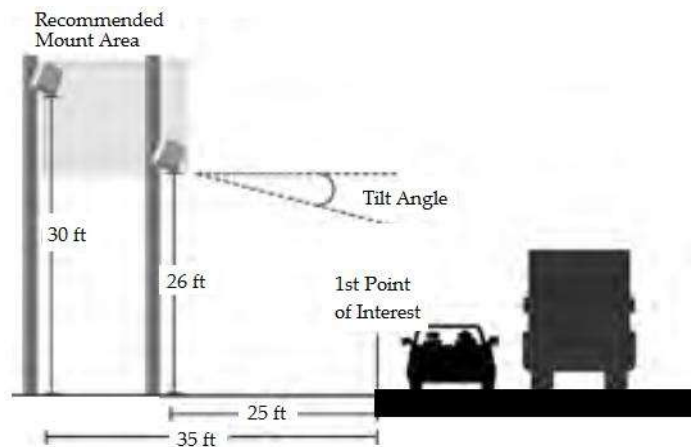

Figure 59: Various distances and parameters for installation of Smartsensor HD

Table 13: Optimum height and offset values for installation of Smartsensor HD

Offset from first lane detected (m)	Optimum mounting height(m)	Minimum mounting height(m)	Maximum mounting height(m)
7.32	7.32	4.88	10.06
7.62	7.92	5.18	10.06
7.92	7.92	5.18	10.36
8.23	8.23	5.49	10.67
8.53	8.23	5.49	10.67
8.84	8.23	5.49	10.97
9.14	8.84	5.79	11.28
9.45	8.84	5.79	11.28
9.75	8.84	5.79	11.58
10.06	9.14	5.79	11.89
10.36	9.14	5.79	11.89
10.67	9.14	6.10	12.19
10.97	9.14	6.10	12.50

c) Aligning the Sensor to the Roadway

Once the sensor is installed it must be properly aligned to get accurate data. The alignment process involves both vertical and horizontal alignment. The sensor is tilted downwards so that it is aimed at the center of the detection area.
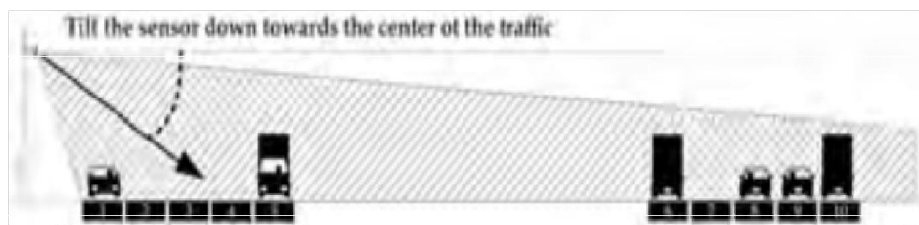

Figure 60: Tilt of the sensor unit

The side-to-side angle is aligned as close to perpendicular to the flow of traffic as possible.
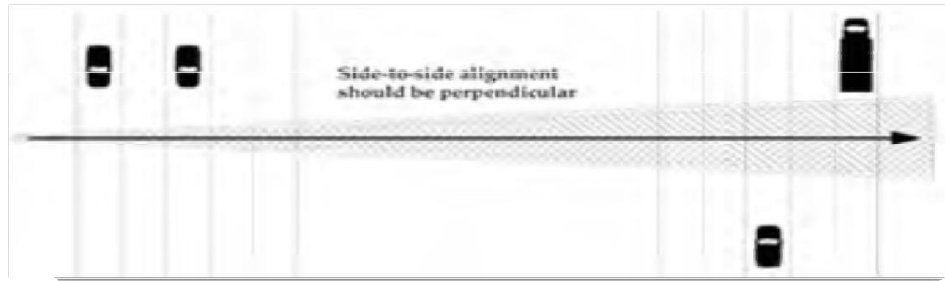
Figure 61: Alignment of the sensor unit

6.3.3 Configuration of Wavetronix

The following steps were followed in order to configure the Wavetronix sensor for the optimal performance.

a) Connecting the Smartsensor Cable
The sensor connector is keyed clockwise and snapped to position to ensure proper connection.

Figure 62: Sensor connector

b) Setting up Communication
Once the SS125 software is installed, it can be used to change settings, view data, and configure the sensor to the roadway. The computer is connected to Smartsensor 125 to initiate a screen shown in Figure 63.

Figure 63: SSMHD Main Screen

To establish connectivity, the Communication window is first launched, The Serial tab is then selected and Port and Speed are set to desired values. The SSMHD software's default is 9600 baud and may be kept as such.
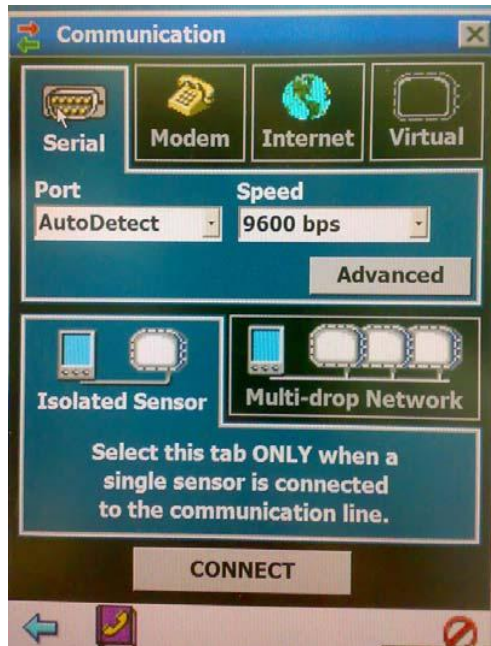

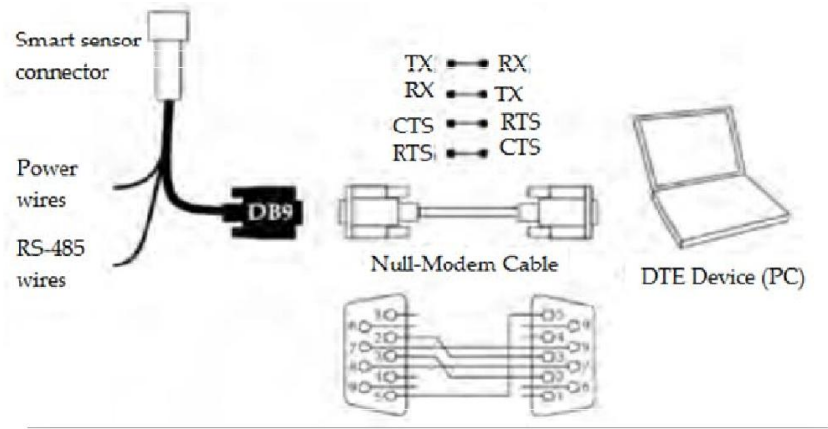**Figure 64:** Connection established

Figure 65: Connections

c) Sensor Alignment

The sensor is aligned before lane configuration. The SSMHD includes an alignment feature that provides visual and audio confirmation when the perpendicular alignment of a sensor is correct. To access the sensor alignment feature, the lane setup is invoked, followed by activating the sensor alignment. The sensor is adjusted according to the image displayed in the Sensor Alignment window. A green arrow means that the sensor is correctly positioned for optimal performance, yellow and red arrows point to incorrect alignment with the roadway. Audio verification may also be checked.
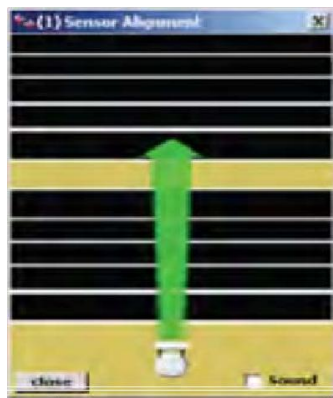

Figure 66: Sensor Alignment

d) Lane Configuration – Automatic

The Lane Configuration screen can be used to automatically or manually configure the roadway, adjust lanes, and control how you see the information on screen. One of the advantages of the Smartsensor HD is the fast and simple lane auto configuration function, where the sensor automatically configures the roadway and sets up the lanes based on passing traffic. This is suitable for lane-less traffic since the lanes are identified by the unit based on number of parallel movements than based on actual lane markings or width.

Figure 67: Automatic Lane Configuration Window

e) Lane Configuration – Manual

The Lane Configuration screen can also be used to manually configure and adjust lanes. The following functions and tools are available on the Lane Configuration screen.
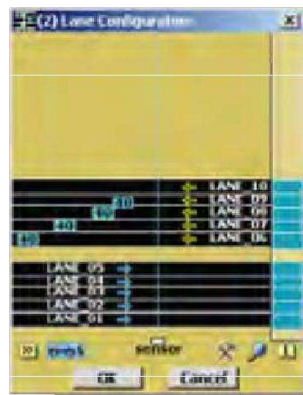

Figure 68: Manual Lane Configuration Window

f) Lane Verification

The Lane Verification option allows monitoring the accuracy of lane detection and adjustment of lane properties for better detection.

g) Data setup and collection

The *Data Setup & Collection* option allows adjustments of interval and per vehicle data, storage and download of data, set bin definitions and enables defining approaches and synchronizing computer and sensor times.

Figure 69: Data collection

h) Interval Data

Interval data refers to the information culled about vehicles that cross the sensor at a set amount of time. This interval of time must be carefully chosen because it affects the duration of data storage onboard. A shorter interval causes the sensor to record data often, leading to faster depletion of the sensor's onboard memory. A longer interval allows the sensor to be operated for longer periods of time

i) Data Storage & Download

The Data Download window allows specification of the time for which stored data will be retrieved and the location in which it will be saved. The Data Storage & Download window comprises the following three sections

Storage Settings – Allows adjustment of the data interval length and mode of data storage.

Storage Status – Shows the storage timeline, storage level and the amount of storage space remaining.

Data Download – Allows retrieval of data from the sensor and storage in the form of a report in a laptop or PDA.
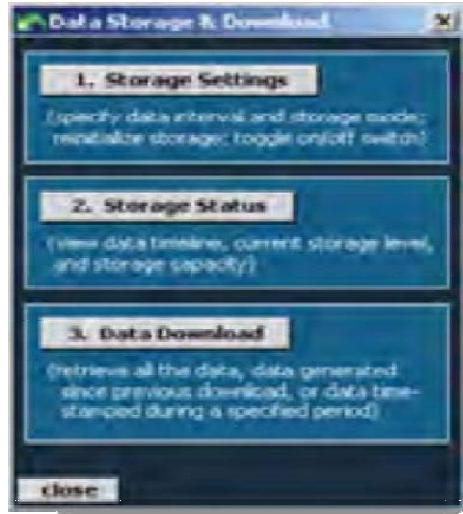
Figure 70: Data Storage and Download

6.3.4. Evaluation

Data collected from the study location were compared with the ground truth values obtained using video. Actual counts were obtained from videos by manually counting the number of vehicles crossing the location of interest. Laser speed gun data were used for speed value comparison. Both directions of traffic were considered for the evaluation.

The collected data were analyzed based on speed and flow. The one-minute interval data from the Wavetronix was compared with that of the video graphic survey. Average speed at every location from the Wavetronix was also compared with that of the laser speed gun. The mean absolute percentage error (MAPE) was used as a measure of effectiveness.

a) Evaluation of Volume

Detailed analysis was carried out for two different traffic conditions- peak and off-peak traffic. Actual count was extracted from the videos collected from the field and compared it with the sensor reported count values aggregated over one minute. The table below shows the MAPE obtained for volume analysis for peak conditions.

Table 14: Evaluation of volume from Wavetronix

Date	Time	Total volume	MAPE (%)
04-06-12	10.03 am-10.33 am	1957	30.47
17-10-12	09.30 am-10.00 am	1360	23.96

18-10-12	09.06 am-09.36 am	1590	36.34
31-10-12	09.00 am-09.30 am	1753	27.88
19-12-12	09.25 am-09.45 am	1020	32.39
20-12-12	09.30 am-10.00 am	1711	29.84
24-12-12	09.00 am-09.30 am	1829	26.83
26-12-12	09.06 am-09.36 am	1855	32.84
27-12-12	09.00 am-09.30 am	1855	28.79
01-01-13	09.20 am-09.50 am	886	27.45

Sample comparison of Wavetronix vehicle count and actual vehicle count for the data collected during a peak hour on 17th October 2012 is shown below.
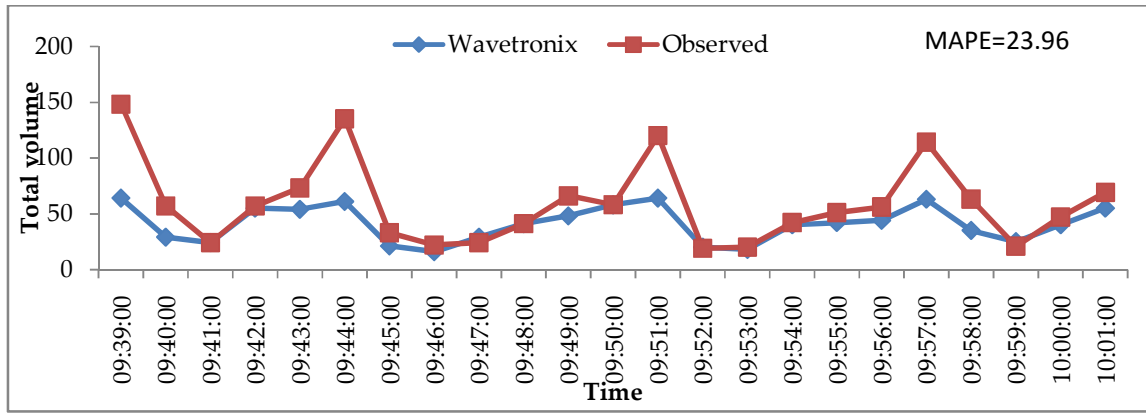

Figure 71: Comparison of Wavetronix count and actual count

Similar evaluation was carried out for off-peak traffic conditions and error was quantified. The table below shows the MAPE obtained for off-peak conditions.

Table 15: Evaluation of volume from Wavetronix for Off-peak condition

Date	Time	Total volume	MAPE(%)

21-08-12	10.30 am -11.00 am	1329	22.86
16-10-12	01.45 pm -02.15 pm	1210	17.17
12-12-12	12.23 pm -12.53 pm	1219	26.83
18-12-12	03.00 pm -03.30 pm	1186	37.15
09-01-13	03.03 pm -03.32 pm	1389	29.41

Sample comparison of Wavetronix vehicle count and actual vehicle count for the data collected during off-peak hour on 16th October 2012 is shown below.
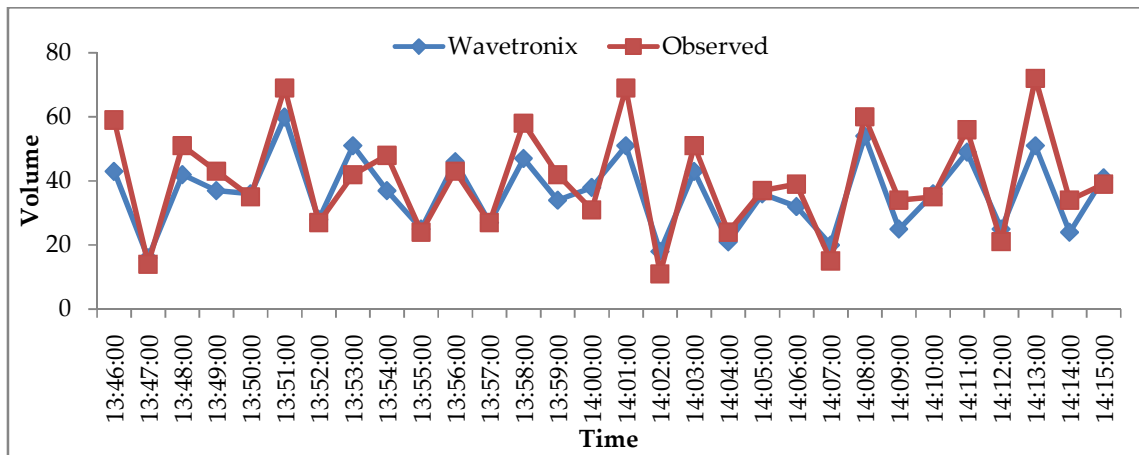

Figure 72: Comparison of Wavetronix count and actual count

b) Evaluation of Classified volume

Similar total volume evaluation, classified volume evaluation was also carried out at the study site location. Classes such as 2 Wheelers (2W), 3 Wheelers (3W), Light motor Vehicles (LMV), and Heavy Motor Vehicles (HMV) were considered. The error was represented in terms of Mean Absolute Error (MAE). Table 16 below shows the results obtained.

Table 16: Evaluation results for classified volume

Date	Time	2Wheeler_ MAE	3Wheeler_ MAE	LMV_MAE	HMV_MAE
04-06-2012	10.03 am - 10.33 am	20.7	1.87	10.1	10.4
16-10-2012	01.45 pm - 02.15 pm	6.83	1.13	4.03	4.17

16-05-2012	10.43 am - 11.00 am	16.44	4.11	14.61	15.67
28-12-2012	09.32 am - 10.00 am	29.52	3.31	1.59	12.69
30-05-2013	02.31 pm - 03.00 pm	10.45	3.48	8.59	6.55

Figures from 73 to 76 show a sample comparison plot actual volume and Wavetronix volume for each vehicle class.
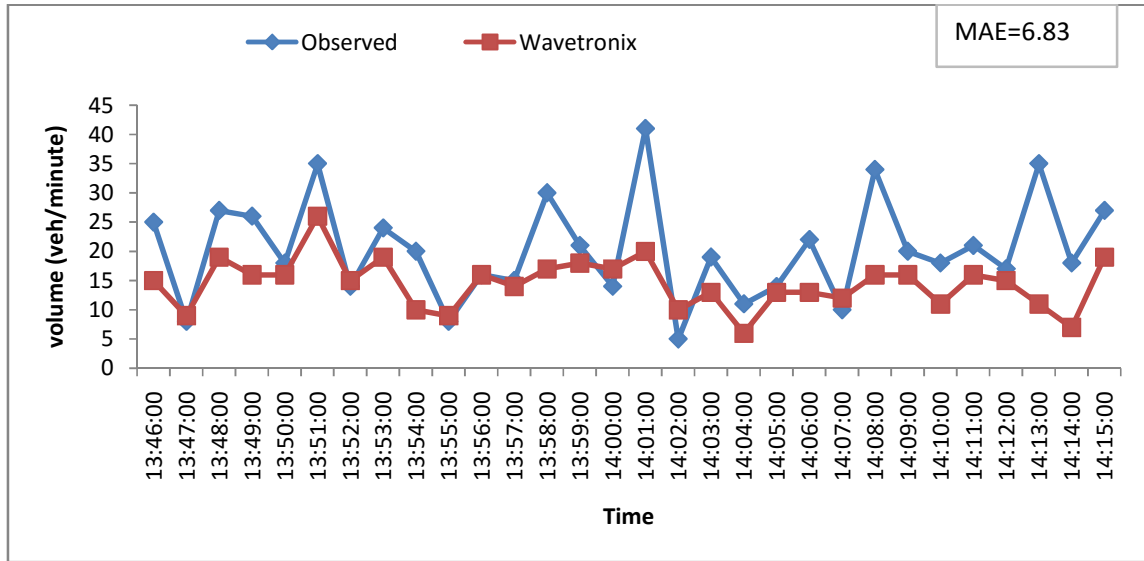

Figure 73: Comparison of Wavetronix 2W count and actual 2W count
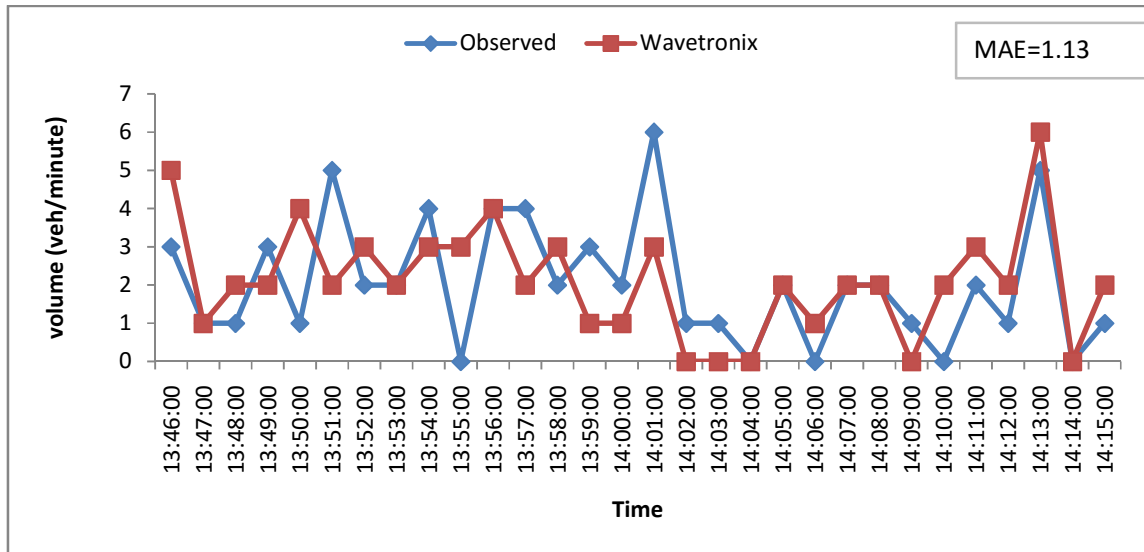

Figure 74: Comparison of Wavetronix 3W count and actual 3W count
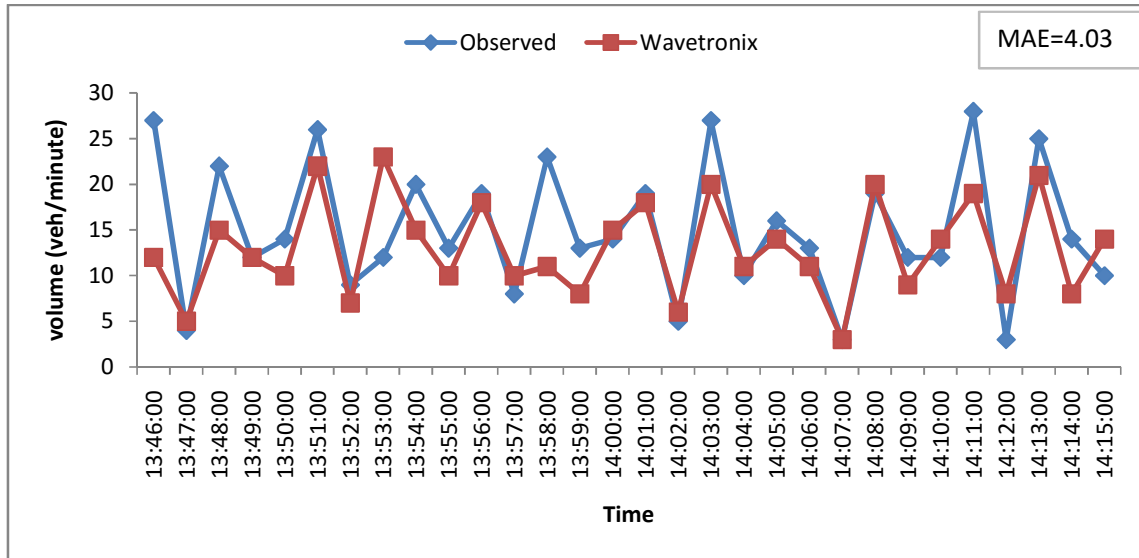
Figure 75: Comparison of Wavetronix LMV count and actual LMV count
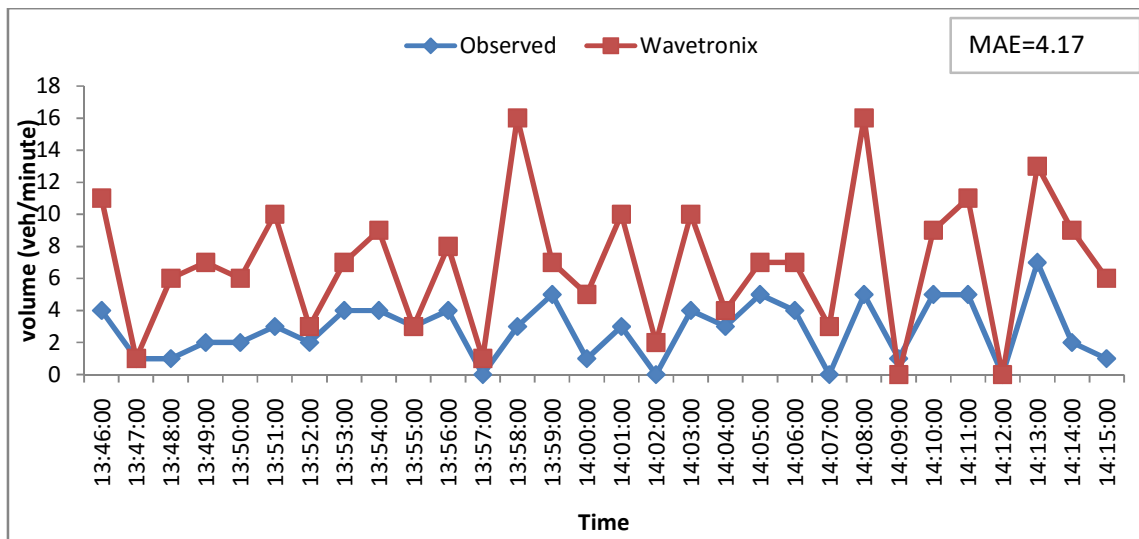
Figure 76: Comparison of Wavetronix HMV count and actual HMV count

c) Evaluation of Volume at different locations

Evaluation was done at different locations, namely National Institute of Fashion Technology (NIFT), VGP, and Indira Nagar, to find the performance of Wavetronix in giving both flow and speed, and the overall error in flow and speed are shown below in Table 17.

Table 17: MAPE in speed and flow for the different locations

LOCATION	MAPE (SPEED)(%)	MAPE (FLOW)(%)
NIFT	9.423	36.37
INDRA NAGAR (Two direction)	12.66	25

VGP	14.03	24.77
INDRA NAGAR (One direction)	7.89	57.5

d) Evaluation of Speed

The individual vehicle speeds were collected from the field using laser gun and was averaged over one minute interval. This average speed was used to compare it with speed obtained from the sensor for one minute aggregate intervals. Table 18 shows the results obtained.

Table 18: Evaluation of speed from Wavetronix

Date	Time	MAPE %
25-09-12	03.38 pm-04.08 pm	08.00
22-10-12	04.18 pm -04.46 pm	05.00
14-12-12	02.15 pm-02.45 pm	06.62
27-12-12	03.11 pm -03.43 pm	08.53
28-12-12	03.10 pm -03.40 pm	08.51
08-01-13	04.20 pm -04.50 pm	09.63
15-01-13	03.45 pm-04.15 pm	07.47
16-01-13	09.55 am-10.31 am	05.51
17-01-13	03.30 pm -04.00 pm	07.87
18-01-13	04.30 pm-05.00 pm	05.07
21-01-13	05.00 pm -05.15 pm	06.61
24-01-13	10.35 am -11.05 am	06.85
30-01-13	03.27 pm -03.57 pm	05.70

A sample comparison of speed from wavetronix with observed speed is shown in the Figure 77.
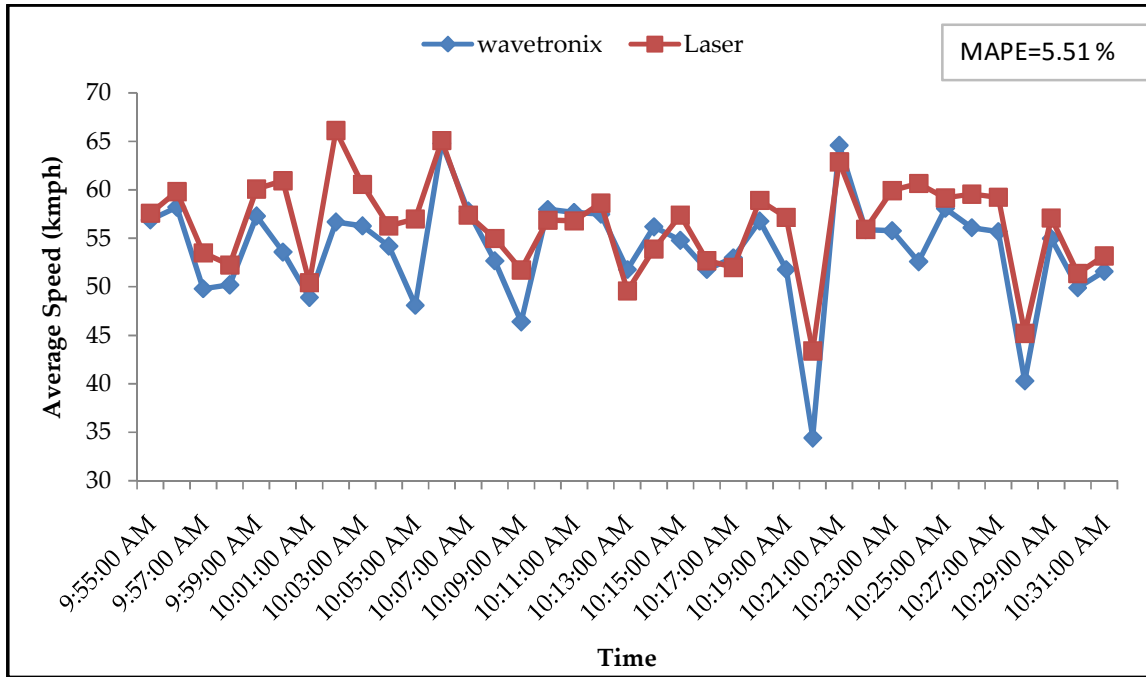
Figure 77: Sample comparison of speed from Wavetronix with observed on 16.01.13

6.4 Trazer

6.4.1 Device Description

Trazer is real time video image processing software developed specifically for heterogeneous traffic conditions. It has computer vision and image-processing algorithms, useful for traffic flow pattern analysis. Trazer works on a video feed to detect vehicles, classify them into various categories, and track a whole lot of statistics such as

a) Vehicle tracking information
b) Occupancy of the road and
c) Classified vehicle counts and velocities

It is developed for midblock sections and can work in both day time and night time. It works in two different modes - the live or online mode and the video or offline mode. The inputs required for the process by the online mode and offline mode are the live feed from the camera and its IP address and video in AVI format respectively (Refer Figure 78)
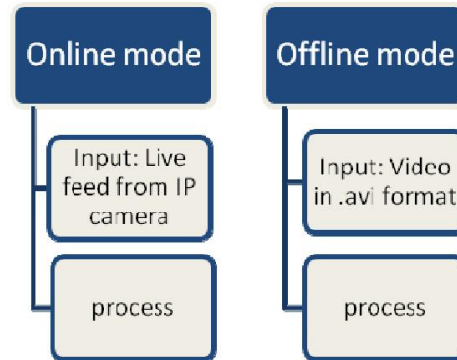
Figure 78: Different modes of Trazer

The real time version of Trazer has two modules namely Trazer App and Trazer CFR.
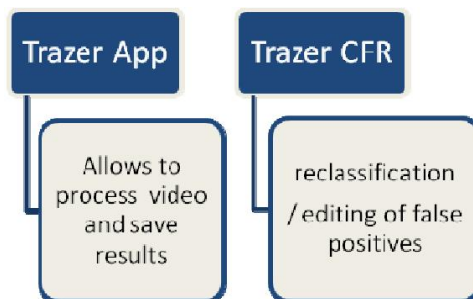
Figure 79: Different modules of Trazer

6.4.2 Installation of Trazer

Trazer is a computer software which can be installed in any windows enabled computer for it to work.

a) Trazer App
The Trazer App module carries out the analyzing of traffic, detection of vehicles and vehicle classification. It can classify the vehicles into four groups as:

LMV – Light Motor Vehicles
AUTO – Three wheeled auto rickshaws
HMV – Heavy Motor Vehicles
TW – Two Wheelers

b) Input Requirement
Trazer can be run in the online mode and the offline mode. The main difference lies in the format of input. The Offline/video mode requires the video in AVI format with ffmpeg codec.

The live mode/online mode requires details regarding the route of the video feed including its

IP Address
Username
Password

6.4.3 Configuration Details

Configuration is the process of making Trazer site/location specific. Configuration need to be carried out separately for day time and night time. The main configuration includes the selection of the following:

a) **Detection Window** – specifies the region where we need to detect vehicles
b) **Homography** – specifies road dimensions, here we need to mark four points onthe road and specify the road dimensions
c) **Occupancy** – specifies two points on the road between which we need to checkthe vehicle occupancy

The following Figures 80, 81 and 82 show the screenshots during each of these phases.

Figure 80: The detection window

Figure 81: The homography co-ordinates

Figure 82: The occupancy points

In addition to the above, we need to specify the classifier details to carry out the vehicle classification correctly. It includes

- Minimum width   minimum width (in meters) for each class

- Maximum width → maximum width (in meters) for each class

- Minimum move → minimum trajectory (in meters) for each class

The first two help in differentiating between various classes, and the third helps in reduction of false positives.

Once the configuration is completed, new project can start running and can generate output data. After creating a new project or loading a project, the following screen will appear.
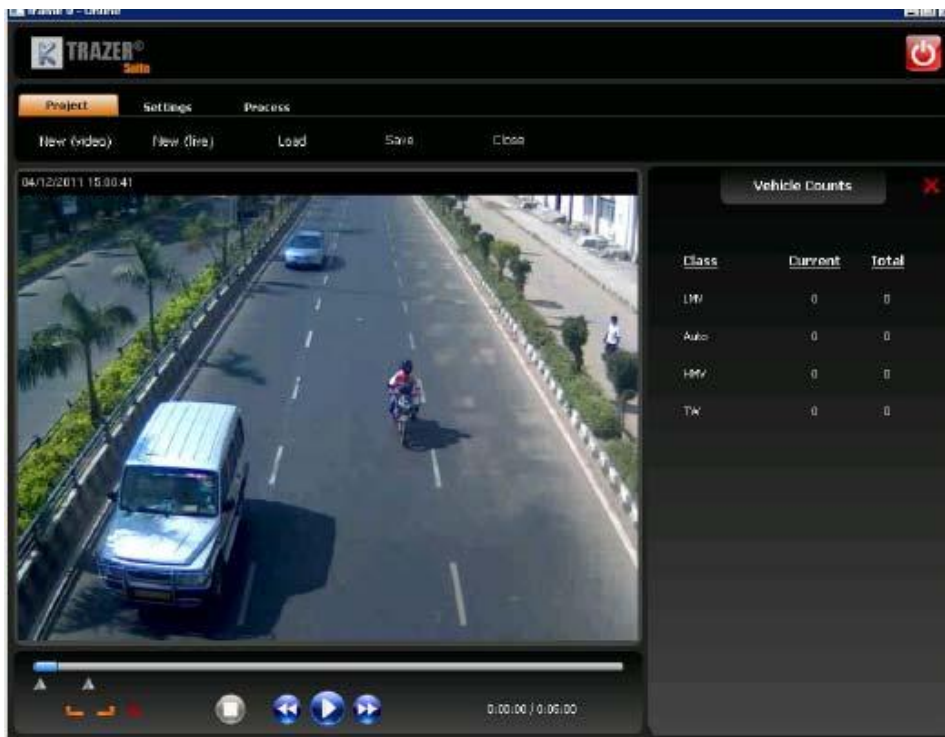

Figure 83: Screen shot of the Trazer Screen

The right hand side of the screen shot shows four classifiers and their counts. During the processing stage, these counts will get updated on the screen as well as in the database.

Figure 84: Screen shot during processing stage

a) Trazer CFR

The Trazer CFR module is provided to improve performance by manual intervention. It allows the user to carry out the following actions to reduce the error in Trazer process.

- To add undetected vehicles
- To delete false positives
- To reclassify wrongly classified vehicles
- To save reports

To use Trazer CFR, a Trazer App project that needs to be processed is required. This project is first uploaded into Trazer CFR. There are two phases of operation. In the first phase, false positives are deleted and wrongly classified vehicles are corrected. During second phase, vehicles that were undetected by the Trazer App are added.

Once the outputs are ready, the data can be saved in user specified formats. The time stamp (time interval) over which CFR must be performed can be specified. This time stamp is the starting and ending time of Trazer App execution.

Three inputs are required:

From time stamp – It specifies the starting time. It includes date (yyyy-mm-dd) and time (hh:mm:ss).
To time stamp – It specifies the ending time. It includes date (yyyy-mm-dd) and time (hh:mm:ss).
NOTE: It uses 24 hour time format.
Interval length - This part of input specifies the length of interval in seconds. Based

upon the interval length, the flow reports will be saved during report generation. Default value of this interval is 10 seconds.

The Trazer CFR yields two intermediate reports - occupancy report and trajectory report and the final compiled report which is called interval-wise statistics. The occupancy report gives the occupancy values of individual vehicles and trajectory report contains the location details of every vehicle at every 1/25 seconds. From these two detailed reports, the compiled Interval-wise statistics is generated. It contains classified count, occupancy and speeds for the specified time interval as shown in Fig. 85.

S. No.	StartTime	EndTime	Counts					Average Velocity					Occupancy			
			LMV	AUTO	HMV	TW		LMV	AUTO	HMV	TW		LMV	AUTO	HMV	TW
1	14:59	14:59:59	0	0	0	0		0	0	0	0		0	0	0	0
2	15:59:59	15:59:59	7	1	5	18		24.81	38.73	16.7	23.59		0.11	0	0.24	0.43
3	16:59:59	16:59:59	11	2	6	34		14.93	25.68	15.48	25.93		0.22	0.23	0	0.23
4	17:59:59	17:59:59	6	0	2	14		24.05	0	9.58	35.61		0.37	0	0.28	0.1
5	18:59:59	18:59:59	8	1	3	25		17.92	29.08	20.72	30.35		0.35	0	0.17	0.25
6	19:59:59	19:59:59	12	3	3	33		8.94	35.28	11.42	27.82		0.51	0.42	0	0.22
7	20:59:59	20:59:59	5	3	2	24		26.11	38.69	29.55	31.3		0.33	0.21	0.63	0.16
8	21:59:59	21:59:59	8	4	6	34		20.25	34.54	19.57	32.01		0.28	0.5	0.07	0.24
9	22:59:59	22:59:59	12	6	9	27		16.56	40.93	15.96	24.29		0.39	0.03	0.04	0.27
10	23:59:59	23:59:59	6	2	3	14		32.03	33.6	19.8	38.03		0.25	0.31	0.46	0.21
11	0:59:59	0:59:59	8	2	6	27		15.89	37.55	17.94	32.25		0.08	0.21	0.21	0.2
12	1:59:59	1:59:59	10	4	4	23		15.07	32.02	24.24	28.11		0.42	0	0.35	0.41
13	2:59:59	2:59:59	5	2	7	19		12.05	27.36	20.56	24.74		0.05	0.2	0.07	0.34
14	3:59:59	3:59:59	6	2	3	20		4.68	23.66	23.76	22.96		0.36	0	0.14	0.26
15	4:59:59	4:59:59	20	7	4	20		12.15	27.8	19.69	22.97		0.72	0.19	0.26	0.25
16	5:59:59	5:59:59	3	3	5	20		23.93	25.61	10.72	25.54		0.07	0.13	0	0.23
17	6:59:59	6:59:59	3	2	1	24		13.04	39.28	24.05	29.44		0	0	0.46	0.37
18	7:59:59	7:59:59	12	3	6	30		21.92	25.25	17.46	22.21		0.23	0	0.37	0.56
19	8:59:59	8:59:59	11	3	10	28		16.1	30.07	15.64	23.57		0.7	0.59	0.05	0.25
20	9:59:59	9:59:59	1	0	3	11		0	0	17.66	23.95		0	0	0	0.32
21	10:59:59	10:59:59	5	0	5	10		23.58	0	13.3	26.46		0.17	0	0	0.25
22	11:59:59	11:59:59	4	2	2	29		20.65	45.72	23.38	33.13		0	0	0.35	0.15
23	12:59:59	12:59:59	6	3	3	12		16.04	21.51	10.78	24.52		0.21	0	0.51	0.43
24	13:59:59	13:59:59	6	1	1	12		42.94	36.76	10.32	34.03		0.07	0	0	0.24
25	14:59:59	14:59:59	7	6	4	23		17.71	16.42	14.11	24.76		0.64	0.52	0.31	0.25

Figure 85: Screen shot of the flow report

Ideal Conditions for Trazer

- Detection window should face the upcoming traffic and front of the vehicle should be clearly visible. So camera has to be kept overhead towards direction of traffic.
- Actual road dimensions should be available as an input to the software.
- Software can perform better in free flow traffic.
- It can perform better in places where bicycles and tricycles are very less. The software doesn't consider this kind of vehicles.
- The real time video has to be in 640x480 or 720x520 pixel size with 25 frames per second. In case of offline mode, avi format with ffmpeg codec is needed.
- High end processor is required for processing the software.

6.4.4 Evaluation

a) Evaluation of Volume
Detailed analysis of the sensor was carried out for the sensor including more number of

days in the evaluation. Peak and Off-peak conditions were separately considered for finding the effect of traffic in detection of vehicles. Actual count was extracted from the video available for the site and was compared with values given by the software. The error was quantified in terms of MAPE and MAE for total volume.

The tables below show the evaluation results for Trazer in both peak and off-peak conditions.

Table 19. Evaluation of Trazer in off-peak traffic

Date	Time	Actual Volume	Trazer Volume	MAPE %
30-08-2012	03.04 pm-03.34 pm	1700	1651	6.5
31-08-2012	02.00 pm -02.30 pm	1850	1719	9.15
15-10-2012	12.30 pm-01.00 pm	2058	1907	7.15
18-12-2012	03.00 pm-03.30 pm	1883	1762	8.61
27-11-2012	03.38 pm-04.08 pm	718	742	6.84

Table 20. Evaluation of Trazer in peak traffic

Date	Time	Actual Volume	Trazer Volume	MAPE %
01-05-2012	12.00 pm -12.30 pm	1464	1268	13.71
18-09-2012	10.30 am -11.00 am	1313	1287	9.08
20-09-2012	11.00 am -11.30 am	2105	2074	4.63
23-10-2012	09.30 am-10.00 am	1623	1462	13.55

Figure 86: Comparison of actual volume and Trazer volume during off-peak condition
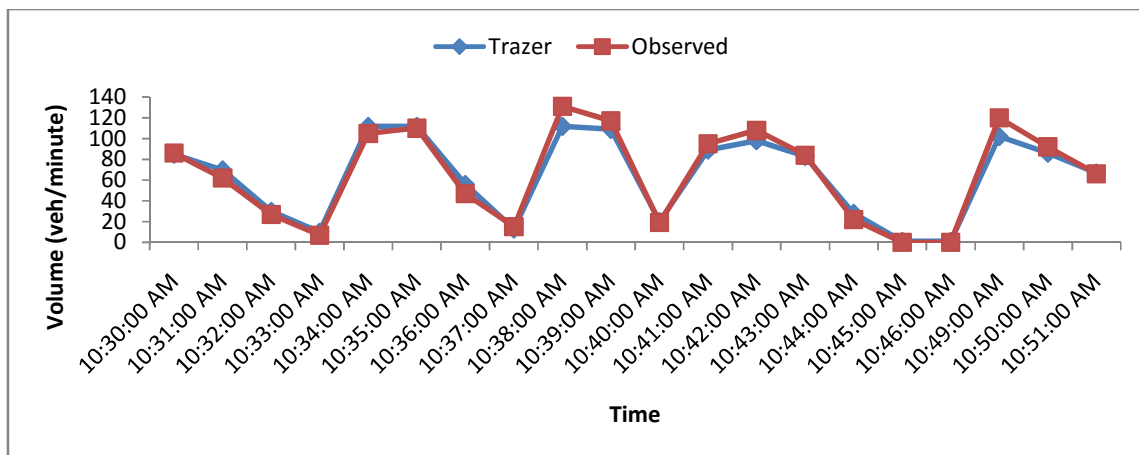

Figure 87: Comparison of actual volume and Trazer volume during peak condition

b) Evaluation of Classified Volume

Classification analysis was also conducted along with the total evaluation. Vehicles were grouped in to four classes- two wheeler, three wheeler, Light motor vehicles and Heavy Motor vehicles, based on the Trazer classification. Error was quantified using MAE (Mean Absolute Error) because of less number of three wheelers and HMVs. Thr following table shows the performance of Trazer in classifying the vehicles.

Table 21: Evaluation of classified volume

Date	Time	MAE			
		LMV	Auto	HMV	TW
30-08-2012	03.04 pm -03.34 pm	2.26	0.84	1.71	2.84

31-08-2012	02.00 pm -02.30 pm	3.4	0.87	2.27	2.63
15-10-2012	12.30 pm-01.00 pm	3.5	0.7	1	2.63
11-12-2012	02.38 pm-03.07 pm	2.57	0.77	0.87	2.33
18-12-2012	03.00 pm-03.30 pm	3.3	0.97	1.5	3.07
27-11-2012	03.38 pm-04.08 pm	3.44	0.44	1.4	-

The following figures show some sample plots of comparison of actual classified count and Tazer's classified count (11-12-12.)
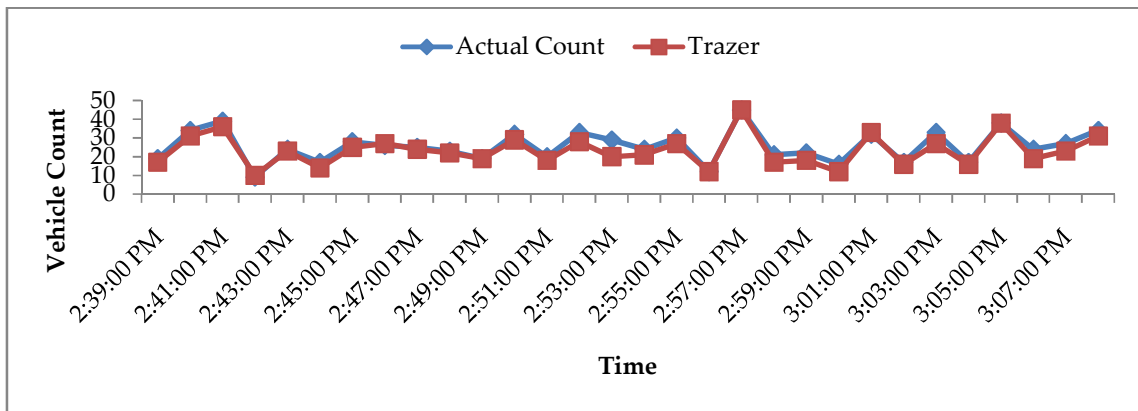

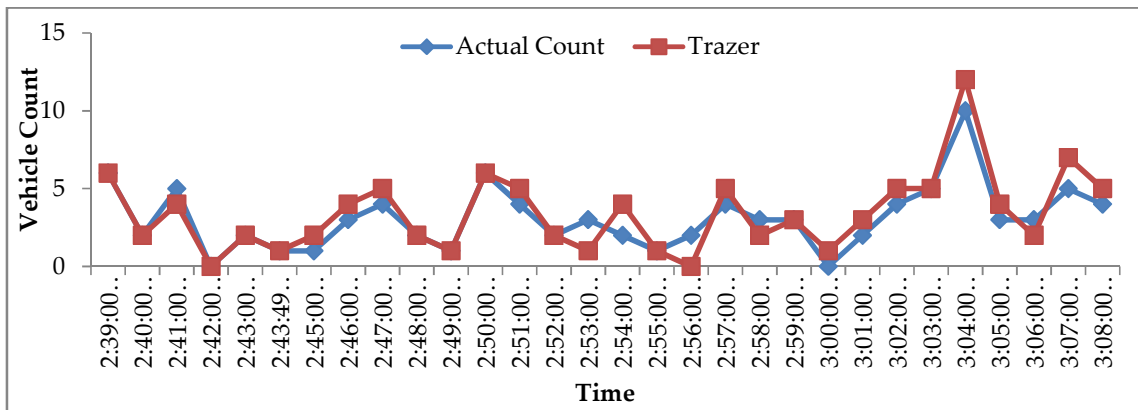**Figure 88**: Sample comparison of actual and Trazer volume (Light Motor Vehicle)

Figure 89: Sample comparison of actual and Trazer volume (3 Wheelers)
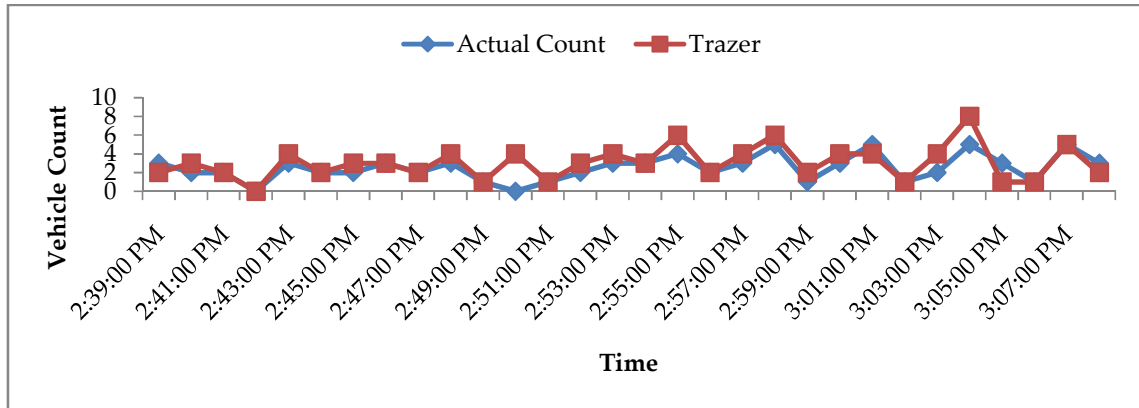
Figure 90: Sample comparison of actual and Trazer volume (Heavy Motor Vehicles)
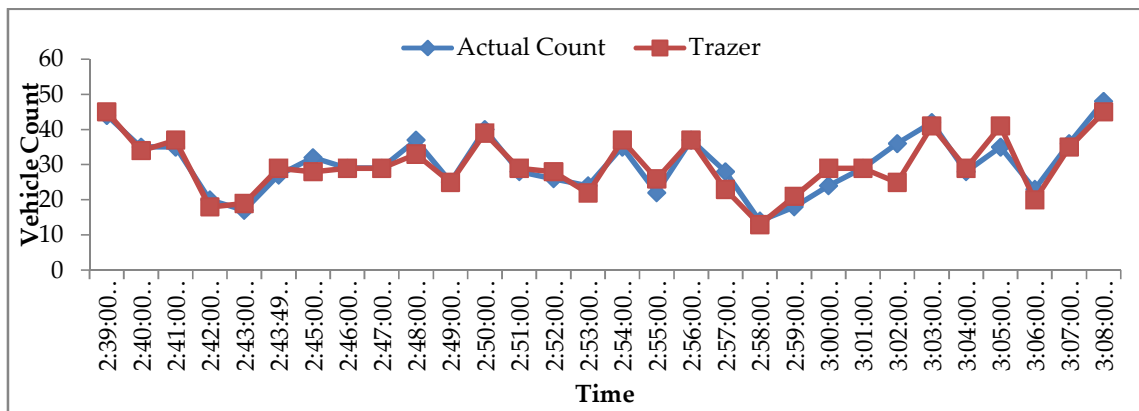

Figure 91: Sample comparison of actual and Trazer volume (2 Wheelers)

c) Evaluation of Volume at different locations

To check the Trazer's performance at different locations, traffic videos from different locations were used. Those videos were run in Trazer software. Performance at various locations was evaluated, and results are shown below.

Table 22: Evaluation results at First Foot Over Bridge:

Date	Time		MAE				MAPE %	Total Observed volume
			LMV	3W	HMV	TW	Total	
30-07-2014	08:15:00 am	08:45:00 am	1.5	1.33	1.37	5.23	6.5	4718
17-12-2014	05:00:00 pm	05:30:00 pm	2.86	1.67	3.44	10.87	19.5	3572
09-10-2015	09:10:00 am	09:40:00 am	9.56	1.47	1.72	7.10	8.97	5042

17-12-2015	11:03:00 am	11:04:00 am	3.86	1.52	2.29	7.93	10.61	4360
18-12-2015	11:00:00 am	11:30:00 am	2.46	1.65	1.76	4.82	6.76	4602
23-12-2015	03:30:00 pm	04:00:00 pm	18.60	1.31	7.90	6.31	10.40	3844

Table 23: Evaluation results at Indira Nagar:

Date	Time		MAE				MAPE %	Total Observed volume
			LMV	3W	HMV	TW	Total	
23-06-2015	09:45:00 am	10:15:00 am	3.43	1.53	0.97	5.8	13.47	2934
23-06-2015	13:10:00 pm	13:40:00 pm	6.83	0.67	1.7	2.3	18.47	2401
19-06-2015	09:10:00 am	09:40:00 am	4.12	2.00	1.93	6.44	13.93	4116

Table 24: Evaluation results at Velachery Bypass:

Date	Time		MAE				MAPE %	Total Observed volume
			LMV	3W	HMV	TW	Total	
31-07-2015	09:58:00 am	10:13:00 am	4.20	1.27	1.50	5.97	6.86	4664
10-08-2015	08:00:00 am	08:30:00 am	1.77	1.13	0.63	7.07	9.23	4432
14-08-2015	08:15:00 am	08:45:00 am	5.48	1.72	1.55	12.28	20.52	4666

Table 25: Evaluation results at Tidel Park:

Date	Time		MAE				MAPE %	Total Observed volume
			LMV	3W	HMV	TW	Total	
28-08-2012	11:33:00 am	12:03:00 pm	4.4	1.4	2.37	6	21.95	3740
30-08-2012	15:03:00 pm	15:34:00 pm	2.26	0.84	1.71	2.84	6.5	3290

Date	Time						MAPE %	Total Observed volume
31-08-2012	14:01:00 pm	14:30:01 pm	3.4	0.87	2.27	2.63	9.15	3700
18-09-2012	14:45:00 pm	15:14:00 pm	2.31	1.69	1.21	3.72	7.02	3695
15-10-2012	12:30:00 pm	13:00:00 pm	3.5	0.70	1.00	2.63	5.17	4116
22-11-2012	14:07:00 pm	14:29:00 pm	2.05	1.09	1.14	2.86	5.99	3646
18-12-2012	15:01:00 pm	15:31:00 pm	3.3	0.97	1.5	3.07	8.61	3766

Table 26: Evaluation results at National Institute Of Technology (108)

Date	Time		MAE				MAPE %	Total Observed volume
			LMV	3W	HMV	TW	Total	
11-08-2015	10:00:00 am	10:30:00 am	2.21	1.70	1.46	7.07	9.23	4432
17-12-2015	11:10:00 am	11:40:00 am	1.86	2.25	2.3	6.34	6.85	2632

Table 27: Evaluation result at Directorate Of Technical Education, Anna University (towards Guindy):

Date	Time		MAE				MAPE %	Total Observed volume
			LMV	3W	HMV	TW	Total	
04-08-2014	10:00:00 am	10:30:00 am	7.00	3.35	3.18	15.47	21.53	4978

d) Evaluation of Volume in Live and Offline mode

To check the performance difference between live and recorded video, the live video feed from a location, First Foot Over Bridge, was ran through the software. The same videos were then ran through the software in off line mode, and the performance was checked. The following table presents the results obtained from the analysis.

Table 28: Evaluation results at First Foot Over Bridge- Live mode

Date	Time		MAE %				MAPE %	Total volume
			LMV	3W	HMV	TW	Total	
06-01-2016	03:34:00 pm	04:04:00 pm	1.70	1.63	1.33	4.47	12.65	3348
22-01-2016	09:00:00 am	09:30:00 am	4.56	1.76	1.52	6.59	07.54	5168
25-01-2016	11:30:00 am	12:00:01 pm	6.12	1.76	1.85	10.86	12.00	4170
27-01-2016	08:30:00 am	08:58:59 am	4.52	1.95	1.96	6.48	13.14	4721

Table 29: Evaluation results at First Foot Over Bridge - Offline mode

Date	Time		MAE %				MAPE % Total	Total volume
			LMV	3W	HMV	TW		
06-01-2016	03:34:00 pm	04:04:00 pm	2.00	1.57	1.30	2.93	5.98	3348
22-01-2016	09:00:00 am	09:30:00 am	2.12	1.65	2.00	5.50	6.49	5168
25-01-2016	11:30:00 am	12:00:01 pm	2.46	1.44	2.62	2.56	6.24	4170
27-01-2016	08:30:00 am	08:58:59 am	2.29	1.95	2.32	3.79	5.44	4721

Comparing the results obtained in offline mode and live mode, it can be seen that the performance of Trazer is poor in live mode.

e) Evaluation of Volume after Upgradation

To address the issue of Trazer's poor performance in live mode, Trazer software was upgraded to the latest version. After the upgradation another set of evaluation was done and the results are presented in the tables below.

Table 30: Evaluation results at First Foot Over Bridge-Live mode

Version	DATE	Time		MAE %				MAPE %	Total volume
				LMV	3W	HMV	TW	Total	
Old	22-01-2016	09:00:00 am	09:30:00 am	5.07	2.23	1.96	11.63	21.81	5168
New	22-01-2016	09:00:00 am	09:30:00 am	4.56	1.76	1.52	6.59	07.54	5168
Old	27-01-2016	08:30:00 am	08:59:59 am	6.57	1.74	3.05	25.10	39.03	4721
New	27-01-2016	08:30:00 am	08:59:59 am	4.52	1.95	1.96	6.48	13.14	4721

| Old | 28-01-2016 | 08:30:00 am | 08:59:59 am | 7.00 | 2.09 | 3.52 | 44.03 | 49.87 | 5174 |
| New | 28-01-2016 | 08:30:00 am | 08:59:59 am | 5.14 | 2.50 | 2.61 | 14.54 | 24.75 | 5174 |

It can be seen from the Table 30 above that the performance of Trazer in live mode was increased significantly after the upgradation.

f) Evaluation of Speed

The vehicle speed given by Trazer is also evaluated. To evaluate the vehicle speed, five days were selected and the average speed of the vehicles for every one minute, for the specified time period, is then compared with actual average speed. The actual average speed is calculated by taking average of the speed of the vehicles obtained using the laser gun in that time period. The results are tabulated below,

Table 31: Speed evaluation for different days

Date	Time	MAPE %
27-09-12	04.30 pm - 04.50 pm	35.07
01-10-12	03.20 pm - 04.00 pm	19.19
11-10-12	03.30 pm - 04.00 pm	22.76
24-12-12	03.15 pm- 04.00 pm	20.08
17-05-13	06.30 am - 07.00 am	28.91

A sample comparison plot of Trazer speed is shown in Figure 92 below,
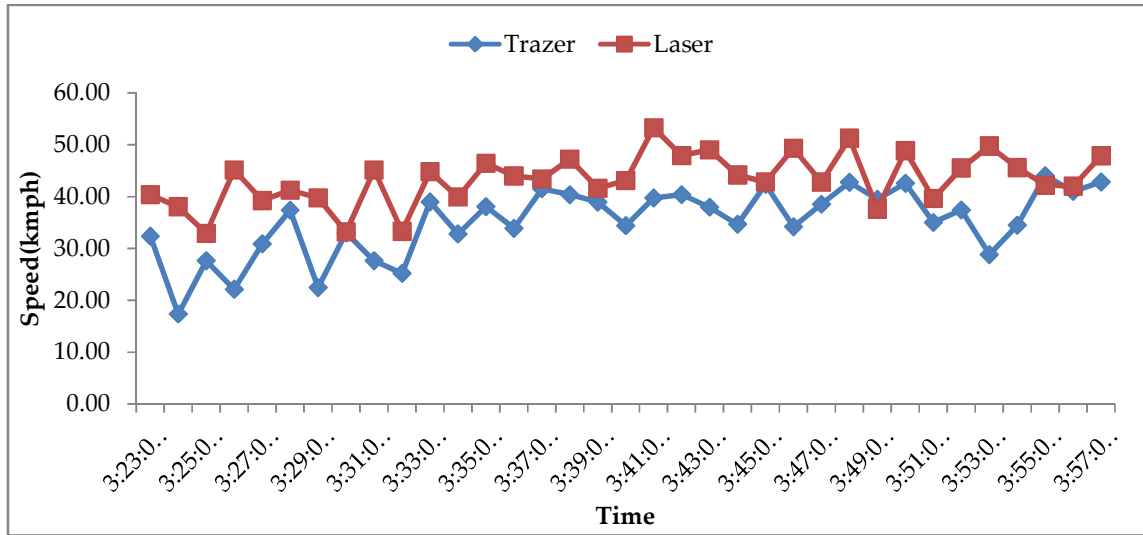
Figure 92: Comparison of Trazer speed with actual speed

6.5. GRIDSMART:

6.5.1 Device Description

GRIDSMART is a vision based vehicle tracking system and consists of a fish eye camera, a processor and an application software. This system is developed especially for intersections to optimize the signal timing.

The fish eye camera has 360° view and will cover the entire intersection along with the legs of the intersection. The video feed from the fish eye camera is fed into the processor which will process the video and identify all the vehicles by giving them unique ID and tracks them till they disappear from the camera view. The information about every vehicle is stored in a file once the vehicle disappears from the camera view.

In a multi legged intersection, each leg is marked with appropriate directions and allowable turning movements, in the form of zones. Zones are selected area on the road within which vehicles are detected. Once the vehicle enters a particular zone it will be assigned a unique ID and a 3D image of the vehicle is created in order to track it until it leaves the camera vision. GRIDSMART is able to give approach-wise turning movement counts, queue length, speed of each vehicle and vehicle length. The individual vehicle output data can be downloaded for the specified time of day either by zones or by approaches using the utility software called "GRIDSMART Client". Each of these are detailed below.

a) GRIDSMART Components

GRIDSMART has three important components that make the sensor works are as follows,

a) A Fish eye Camera

b) A Processor or CPU

c) "GRIDSMART Client" -An interface software

1) Camera

The sensor uses a high resolution CMOS sensor that is fitted with a bell type fish eye lens allowing the camera to capture the whole intersection. The resolution of the camera is 5-mega pixel CMOS sensor. The camera supports up to 10 frames per second. The power to the camera is given by a long single grade Cat5e, which is connected to the GRIDSMART processor. The camera has a view of 180 degree horizon to horizon. A weatherproof enclosure for the camera is provided to prevent it from damage. Figure 93 shows a typical enclosure used in the field.

Figure 93. Fish eye camera

2) GRIDSMART Processor (CPU)

The CPU is designed to capture and process the images from one or more cameras. The windows based processor is placed in a cabinet near the intersection and contains all the electronics and a software to interact with the processor. A LED display in the processor shows operational information such as the camera is functioning, and current phase, if it is connected to the signal. The power and communication between the CPU and camera is given through a single Cat5e cable. Figure 94 shows the processor unit.

The processor contains specially designed software called GRIDSMART Client, which allows the user to configure the intersection and download the data. The CPU provides 24 inputs and outputs. The input/output is optically isolated to provide protection against transients as well as to prevent ground loops. A Synchronous Data Link Control (SDLC) interface can be used to communicate with the signal controller.

Figure 94: GRIDSMART controller

There are multiple ports available in the processor that equips users with different options to interact with processor. The CPU contains a network interface to facilitate the users to connect to the processor remotely. There is also a local port available in the CPU to use laptop to access the GRIDSMART client by using a standard network cable. Two USB ports provided in the CPU is used to collect data or update the software without even opening the software.

For image data collection, a NTFS formatted hard drive of capacity more than 128 GB is used. Video will be stored frame by frame as an image file in the hard drive till it is taken out. Flash drives can be used to download count data. Additionally, a standard VGA monitor, USB keyboard and a mouse can be connected directly to the CPU to manage the operations.

3) GRIDSMART Client

GRIDSMART client is a software, which allows user to interact with the processor to create new sites, configure them and download data. The software can be downloaded from GRIDSMART cloud and can be installed in the processor. Figure 95 shows a sample image using GRIDSMART Client.
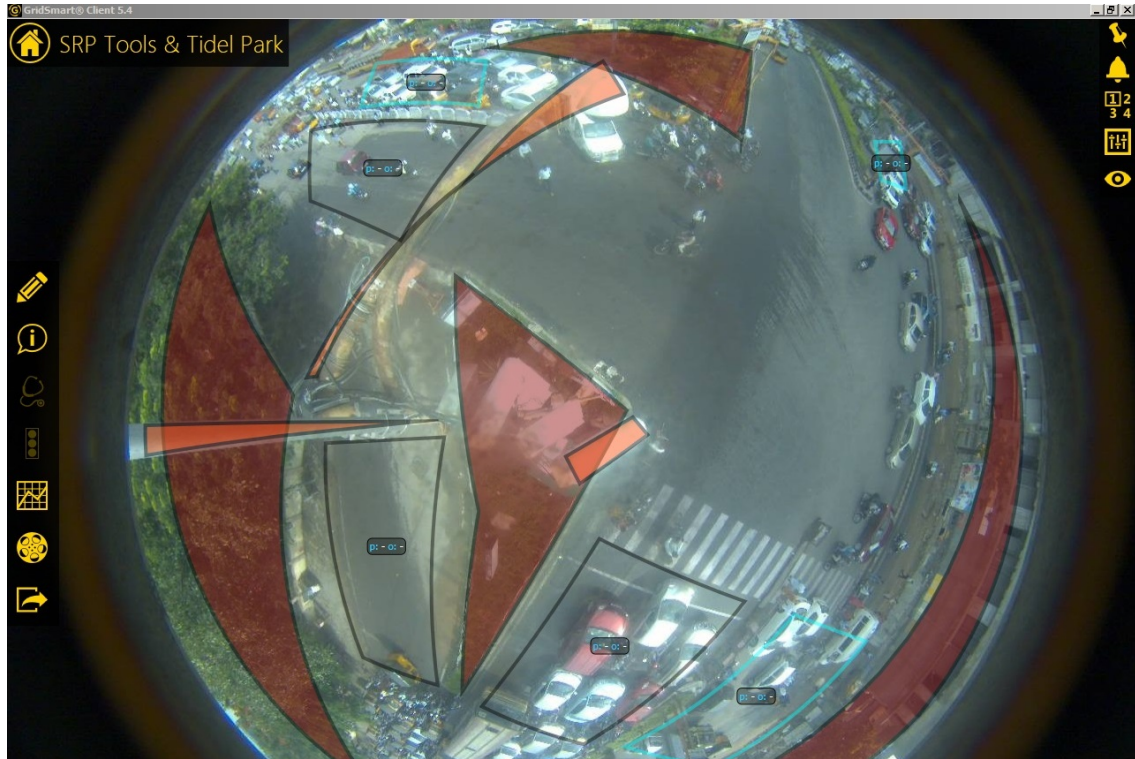
Figure95. A sample image from the camera

Once the software is downloaded and installed, clicking the configure icon on the left side of the image will take the user to the assignment section. That section will have options such as vehicle zone, object mask and road mask, as shown in the figure below.

Figure96: Image with differnt zones and object masks

b) GRIDSMART data

Once the sensor starts processing, individual vehicle data will be stored in reports. The data can be downloaded using the Auto reports option. The data can be downloaded either approach wise or zone wise for a specified time interval or time of day given by the user. The data can be exported to .pdf, .xls, .rtf, .tif, .mhtml. The user can choose appropriately from any of the formats above.

Figure 97 shows a sample data from GRIDSMART for one approach.

	A	B	C	D	E	F	G	H	I	J	K	L	M
				SecondsSinceLast	SecondsIn	SecondsSinceLast		SpeedOn				Queue	
1	Date-UTC	ApproachType	Name	Exit	Zone	Green	TurnType	Exit	DayMode	CarLength	LightState	Length	AllowableTurnType
2	2015-10-22T04:01:22.4000000	Southbound		-1	-1	-1	Right	22		15	None	0	Right
3	2015-10-22T04:01:42.9000000	Southbound		-1	-1	-1	Right	13		9	None	0	Right
4	2015-10-22T04:02:52.6000000	Southbound		-1	-1	-1	Right	29		63	None	0	Right
5	2015-10-22T04:03:37.0000000	Southbound		-1	-1	-1	Straight	20		24	None	0	Right
6	2015-10-22T04:04:28.1000000	Southbound		-1	-1	-1	Right	11		28	None	0	Right
7	2015-10-22T04:05:00.6000000	Southbound		-1	-1	-1	Right	23		17	None	0	Right
8	2015-10-22T04:07:58.0000000	Southbound		-1	-1	-1	Right	9		17	None	0	Right
9	2015-10-22T04:08:00.1000000	Southbound		-1	-1	-1	Right	27		33	None	0	Right
10	2015-10-22T04:09:43.2000000	Southbound		-1	-1	-1	Right	21		17	None	0	Right
11	2015-10-22T04:09:50.1000000	Southbound		-1	-1	-1	Straight	25		65	None	0	Right
12	2015-10-22T04:10:42.0000000	Southbound		-1	-1	-1	Straight	20		46	None	0	Right
13	2015-10-22T04:11:07.0000000	Southbound		-1	-1	-1	Straight	28		19	None	0	Right
14	2015-10-22T04:11:55.9000000	Southbound		-1	-1	-1	Straight	24		13	None	0	Right
15	2015-10-22T04:12:47.0000000	Southbound		-1	-1	-1	Right	25		59	None	0	Right
16	2015-10-22T04:15:14.2000000	Southbound		-1	-1	-1	Right	18		65	None	0	Right
17	2015-10-22T04:16:03.3000000	Southbound		-1	-1	-1	Right	25		19	None	0	Right
18	2015-10-22T04:18:08.3000000	Southbound		-1	-1	-1	Straight	31		12	None	0	Right
19	2015-10-22T04:19:20.2000000	Southbound		-1	-1	-1	Straight	21		17	None	0	Right
20	2015-10-22T04:22:56.4000000	Southbound		-1	-1	-1	Right	26		18	None	0	Right
21	2015-10-22T04:23:37.1000000	Southbound		-1	-1	-1	Straight	17		17	None	0	Right
22	2015-10-22T04:24:17.3000000	Southbound		-1	-1	-1	Right	29		17	None	0	Right
23	2015-10-22T04:24:28.1000000	Southbound		-1	-1	-1	Straight	17		21	None	0	Right
24	2015-10-22T04:26:05.6000000	Southbound		-1	-1	-1	Right	5		12	None	0	Right

Figure 97.:Sample GRIDSMART output data

6.5.2 GRIDSMART Installation

The camera should be mounted in such a way from the centre of the intersection to capture all legs of the intersection. For better performance, it is recommended that the camera mounting height should be between 30 feet and 40 feet and the distance of the camera pole should not be more than 75 feet from the centre of the intersection and no more than 150 feet from any stop bar. The following figure shows the ideal camera positioning for better performance of the sensor.
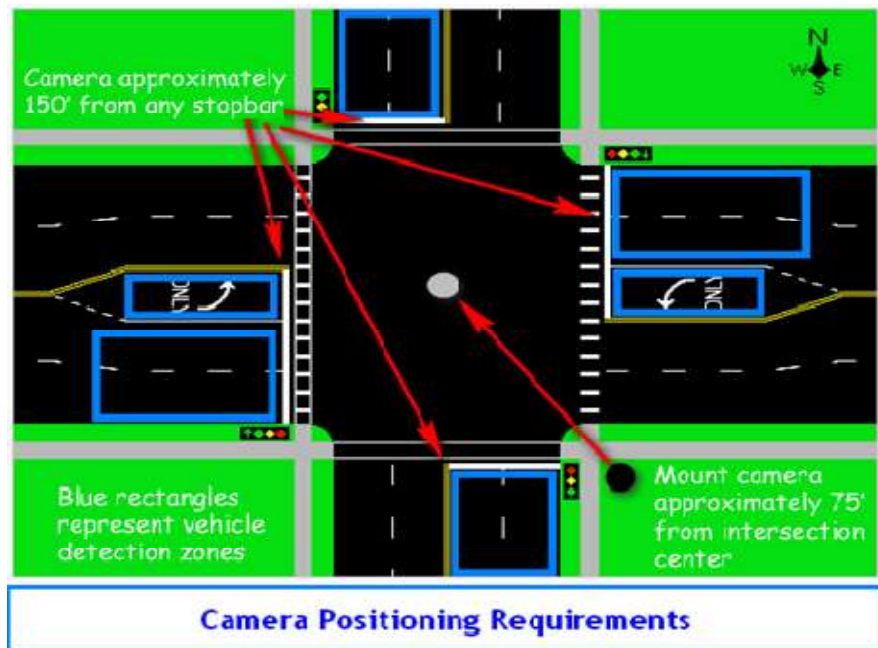
Figure 98. Positioning of the camera

Once the camera is aligned, the video feed of the intersection is given to the GRIDSMART processor. The video will be then processed by the GRIDSMART software, and the data will be generated at the end of the day.

6.5.3 Configuration of GRIDSMART

a) Setting up a new site

The following section details the step by step procedure for creating a new site using GRIDSMART client software.

Site Details

After the installations of camera and the processor in the site, a new site can be created using the GRIDSMART client. A new site can be created by clicking "Factory Default" first. Details of the site location, such as Street address, City name and Pin code, need to be provided. Once the details are entered, it can be saved by giving the password provided by the manufacturer.

Road Masks

Once the details of the site are given, a thumbnail picture of the camera with the name given to the site appears. Live feed of the camera can be checked. Next, road mask setting needs to be carried out. Road mask is an option to mask the roads that are not used by the vehicles by covering it with a layer. It can be done by pressing Road Mask option in configure menu.

Object Masks

Like road mask, object mask is done to cover the objects in the camera coverage, which could block the view of the vehicles moving. Object mask option is next to road mask option in the configure menu.

Vehicle zones

Vehicle zones or detection zones are specified in each of the legs. The zones can be of any shape or size. The zones are defined by selecting points within the intersection view to create a detection area. Once the zones are created, the phases associated with the zone can be given. However, if the sensor is not coordinated with signal, the phases cannot be specified. The direction of the normal traffic flow is specified inside the zone to avoid false calls. For example, each zone will have the direction of the traffic, such as northbound, southbound etc., and the turning movement, namely right, left or straight.

In the vehicle zone, the allowed traffic movement direction is specified by pointing the arrow parallel to the allowed moving traffic. And in each zone, details such as, vehicles bound direction and allowable vehicles turn type is given.

Publish

"Publish" is the option which would save the settings specified by the user and adjust the processor to work with respect to the settings given. After all the settings are done, the settings are published. Normally, the sensor will take certain amount of time to process the video after the new settings are given.

Revert

If the user wants to go back to the previous setting, it can be done by pressing the "Revert" button in configure menu.

b) Remote connectivity

Remote network connection can be established using external modem. The input for the modem can be taken from the network port in the CPU using standard LAN cable. SIM card can be used to enable the remote connectivity.

VNC can be created to access and control the CPU remotely, if there is any changes to make in the configuration settings. By giving the assigned IP and port for GRIDSMART and the password will give access to the GRIDSMART processor.

6.5.4 Evaluation

a) Evaluation of Volume

In order to check the performance of a sensor, an evaluation has to be carried out, matching the data given by the sensor and the field data. Data from GRIDSMART is collected using "Reports" option in the main menu. After selecting the date and time, for which duration the data is to be downloaded, the data can be downloaded using the "Export" option.

Field data can be downloaded in the form of camera images using the NTFS formatted hard drive by plugging it into the processor. The camera images will start to be stored once the hard drive is recognised by the processor till the hard drive is removed. To get the video streaming from the images downloaded, "Replay" option can be used. The path of the folder which contains the images should be given for it to replay the video. From the video, the user can manually count the vehicles for the desired approach and turning movements.

On 13th April 2016, data were collected between 1:30 PM and 2:00 PM, similarly as explained above the, for the same time, video is saved as images so as to count manually. Northbound straight through traffic, Southbound straight through traffic, Westbound straight through traffic and Eastbound right turning traffic are considered for GRIDSMART data with the field data. First, the vehicles are counted for 30 minute period depend on its turning movement. Total vehicle count is then compared with the GRIDSMART count during the same time. The error, APE (Absolute Mean Error), is calculated and taken as the error observed. The result of the analysis is shown in the next section.

The following table presents the results of the evaluation.

Table 32: Summary of evaluation of GRIDSMART for different turning movements

	Northbound Straight	Southbound Straight	Eastbound Right Turn	Westbound Straight
Actual Count	1244	1552	215	821
GRIDSMART Count	860	1356	202	645
APE	30.87	12.63	6.05	21.44
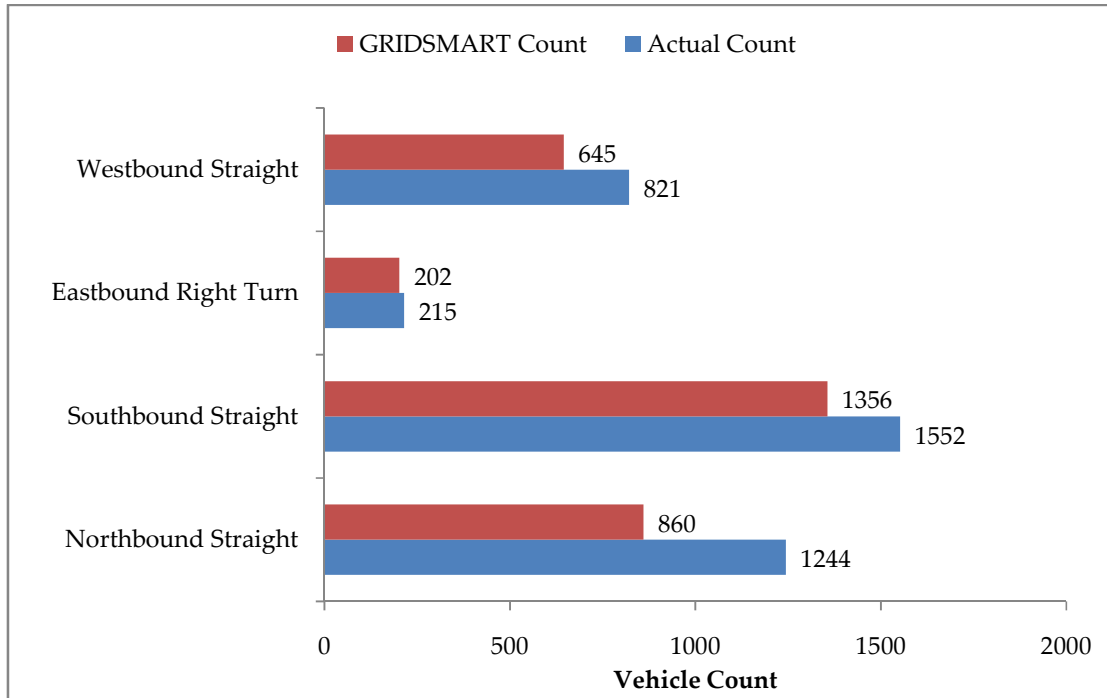
Figure 99: Comparison of actual count and GRIDSMART count of different turn traffic

In addition to the above evaluations of the performance of existing technologies, new sensors were developed for the Indian traffic conditions and are discussed in the next section.

CHAPTER 7
DEVELOPMENT OF NEW SENSORS

7.0. Development of new technologies for Indian traffic conditions

This section presents the development of an inductive loop detector, designed especially for Indian traffic conditions.

7.1 Multiple Inductive Loop Vehicle Detection System for Indian Traffic

Among the traffic flow sensors mentioned above, the inductive loop detectors [22-23, 54-57] are widely used as they provide good sensitivity coupled with a cost effective solution. Existing inductive loop detectors are mainly suitable for vehicular traffic that conforms to lane discipline, and these sensors will not function properly when there are parallel movement of vehicles, as shown in Figure 100, within the same lane (same loop area), e.g., roads with vehicles occupying any available road area without restricting to lanes, and heterogeneous traffic with vehicles of widely varying characteristics (from non- motorized vehicles such as bicycles and animal drawn vehicles to trucks and tractor trailers) occupying the same road space.
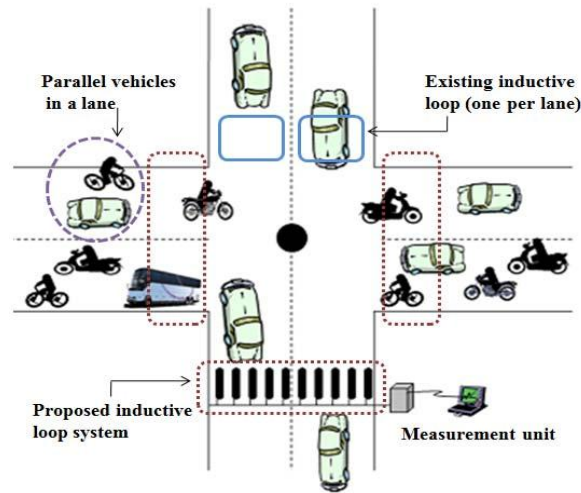
Figure 100: Illustration of an inductive loop based vehicle detection scheme at a junction

Moreover, a loop designed to detect large vehicles (e.g. bus) cannot reliably detect a small vehicle like bicycle. Thus the existing loop detectors are suitable only for the lane disciplined and homogeneous traffic conditions.

The present work proposes a new and simple inductive loop sensor structure that senses both large and small sized vehicles and differentiates the large one from the small. The sensor provides a unique output signature for each type of vehicle. The sensor output information is such that it is not only possible to detect and classify the vehicles in an

unstructured traffic system but also possible to compute individual vehicle's speed and occupancy time. Details of the new inductive loop structure, principle of measurement, prototype system developed, experimental set-up and results of field tests are discussed in the following sections of the report.

7.1.1 The New Inductive Loop Sensor

Figure 101 shows the schematic diagrams of three possible inductive loops for vehicle detection.
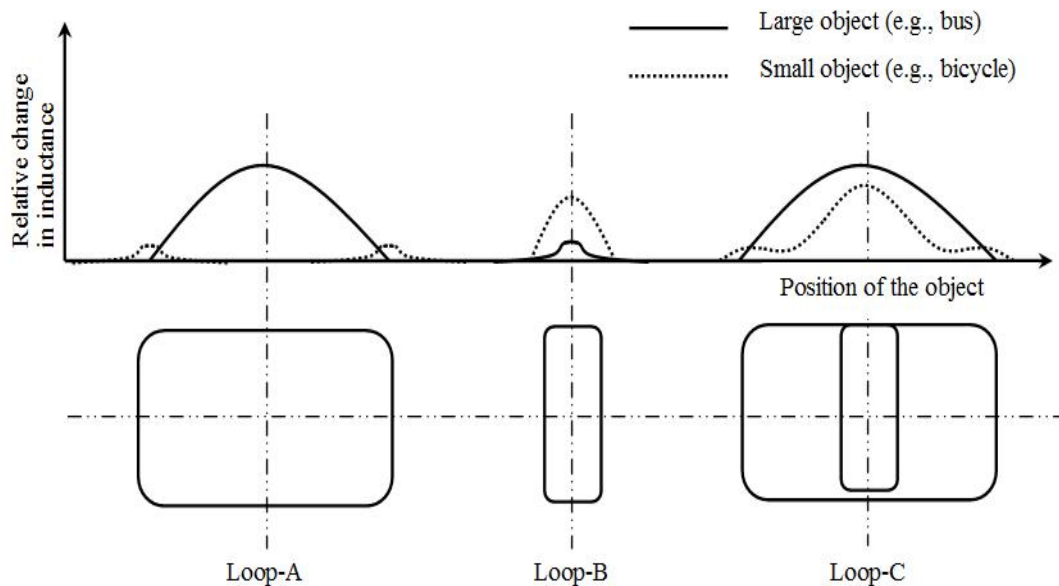
Figure 101: A pictorial representation of the relative change in inductance for the inductive loops A, B and C.

The continuous curve in the plot shows the relative change in inductance when a large metallic object (such as a bus), moves from left to right, at a vertical distance of about 60cm from the plane of the loop. The dotted curve shows the change in inductance when a small metallic object (e.g., bicycle) moves from left to right. In this case, the object is moving at a distance of about 8 cm above the plane of the inductive loop.

The coil structure with large area indicated as 'Loop-A' in Figure 101 is the one in use for lane based homogeneous traffic and is well suited to detect large, more or less uniformly sized vehicles such as car or bus or truck. When such a large vehicle goes over the loop, the change in the inductance LP of the loop will be as indicated by the curve (continuous line) drawn on top of the Loop-A section in Figure 101. However, if a small vehicle such as a bicycle goes over this loop the change in the inductance of the loop will be small, and it is detectable only when the object is directly above the coil position, as indicated by the

curve drawn with a dotted line in Figure 101, above Loop-A. In all other positions, the resultant change in the inductance of Loop-A will be negligible. On the other hand, for a coil structure as indicated in 'Loop-B', with a smaller cross-sectional area compared to loop-A, the relative change in the coil inductance (shown by the curve drawn in dotted line) will be appreciable when a small vehicle approaches, close to the plane (vertically) of the loop. But the relative change in inductance (indicated by the continuous line, on top of Loop-B) will be small for a large vehicle (bus or truck) moving over loop-B. Thus, loop-A is mainly sensitive to large vehicles and loop-B is sensitive to small vehicles that go very close (i.e., vertical distance from the loop plane) to the loop.

The proposed loop, 'Loop-C' in Figure 101, is formed using a continuous conductor wound as illustrated (shown more clearly in Figure 101), to form an outer loop and an inner loop. The loops are formed in such that a current flow through the coil produces a magnetic flux in the outer loop to be in line and aiding the flux produced by the inner loop, at the center of the loop. When a large vehicle like a bus moves over Loop-C, the loop will give a relative change in inductance similar to loop-A and when a small object like a bicycle goes over the loop, it gives a relative change in inductance similar to loop-B. Thus a large vehicle (e. g., bus) and a smaller vehicle close to the loop (e.g., bicycle) can be detected reliably with the proposed Loop-C shown in Fig. 101. A detailed three-dimensional view of the proposed loop is shown in Fig. 102. The loop coil can be placed below or on the surface of the road. The loop is connected to the measurement system as indicated in Figure 102.
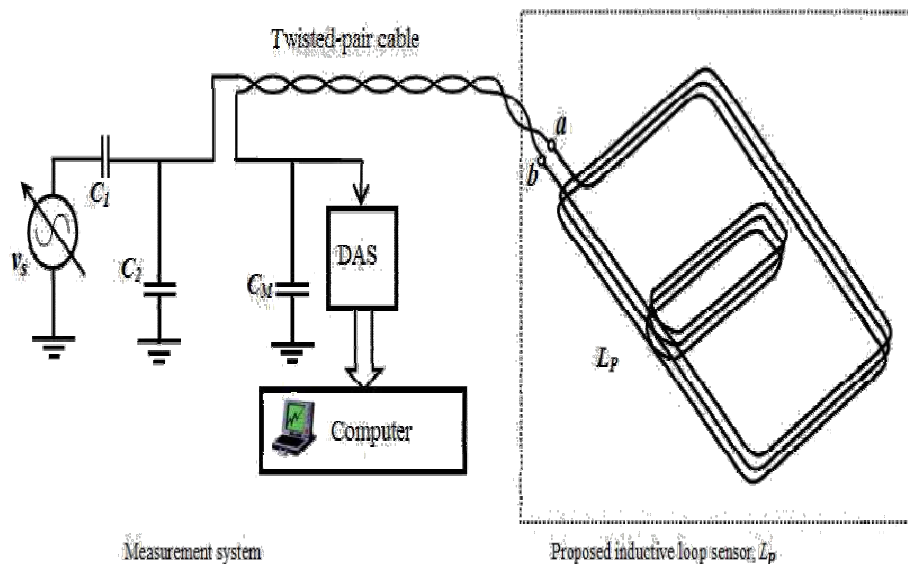
Figure 102. The new inductive loop suitable to sense small as well as large vehicles

The capacitances $C1$, $C2$ and CM along with the inductance LP of the loop coil form a

resonant circuit. This circuit passes the signal at the resonant frequency to the measurement system and attenuates all the unwanted frequency components that may be picked-up by the loop. The measurement system and the loop with inductance *LP* are connected together using a twisted-pair cable. The voltage across the capacitor *CM* is given to a Data Acquisition System (DAS). The data acquired by the DAS is sent to a computer and a suitable algorithm, implemented in the computer using a virtual instrumentation environment, detects the type and speed of the vehicles and counts the number of vehicles being sensed.

7.1.2 Multiple loop detector system

For detecting vehicles that flow in an un-organized fashion with no-lane discipline, multiple loops having the structure as indicated in loop-C (refer Figure 101 and 102) are placed on the road side-by side as indicated in Figure 103.
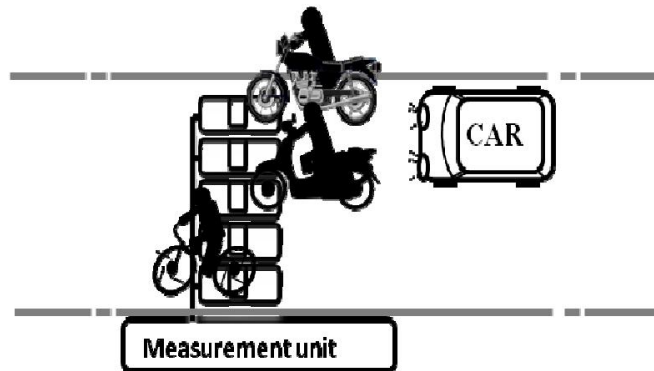
Figure 103: Multiple inductive loop system.

Unlike the present system of having one loop per lane, many loops as practically possible are placed in a lane. Consider, there are N such loops placed covering the road width, resulting in N-inductances. Fig. 104 shows the equivalent circuit representation of the proposed multiple inductive loop system. *L1, L2… LN* is the inductances of individual loops. Since *L1, L2… LN* are of the structure Loop-C, each of the coil is sensitive to both small (e.g. a bicycle) and large vehicles (e.g. a bus). Thus use of *N* loops as indicated in Fig. 104, facilitates the sensing of *N* individual bicycles at a time. If a large vehicle such as a bus goes over the loops, more than one loop will have noticeable change in inductance simultaneously, thus enabling the sensing of a large vehicle as well. If we consider that the wheels of a bus go over the outer loops *L1* and *L3*, the change in inductance for *L1* and *L3* will produce similar signature for the voltages *VC1* and *VC3*, which will be different from the signature of the middle loop *L2*. These signatures and the magnitude of change in inductance are used to detect the presence of a moving bus accurately. The signature of the signals for the above mentioned condition will be different from that of, for example, three bicycles running in parallel. Hence, such conditions also can be distinguished.
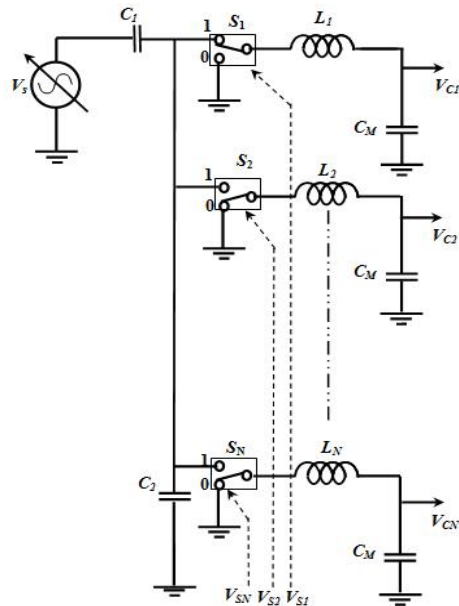
Figure 104: Equivalent circuit of multiple loop system. Voltage signals *VC1*,
VC2…,VCN are continuously recorded using a data acquisition unit.

The signal conditioning part (introducing resonance) of the measurement system used for the multiple loop system is similar to the one employed for a single loop system as Shown in Figure 104. Individual inductance values of the loops, in a vacant condition, will be nearly equal to each other as the dimensions and number of turns used to construct each loop is identical. The voltages *VC1*, *VC2*, …, *VCN* are given to the data acquisition system. These voltages change as a function of the change in inductance of the corresponding loop when a vehicle goes over it. The signal acquired by the DAS is filtered and RMS values of each signal are computed and displayed. In the multiple loop system the number of channels used to acquire the data is equal to the number of loops used. In order to avoid the problems owing to the cross-sensitivity between the loops, at a time, only the loops with odd or even numbers are energized and their responses measured. A minimum distance of few centimeters is kept between the adjacent loops for ease of separation during installation. Switches *S1, S3, S5*, etc. are controlled by signal *VS1* while *S2, S4, S6*, etc., are regulated using control signal *VS2*. The loops with switches in position 1 will be at resonance and work normal and give the expected output. For the circuit in Figure 104, the switches can be set to position 0 or 1 using the switch control signals shown in Figure 105. If required, each loop can be energized and measured individually by operating the corresponding switch and this can be performed in a sequential manner for the loops at a very high rate so that measurement from each loop is completed in-time to capture the data for vehicles moving fast. In such a case, the switch positions (0 or 1) of *S1, S2,….,SN* are controlled using individual control voltages

VS1, *VS2,...., VSN* respectively.
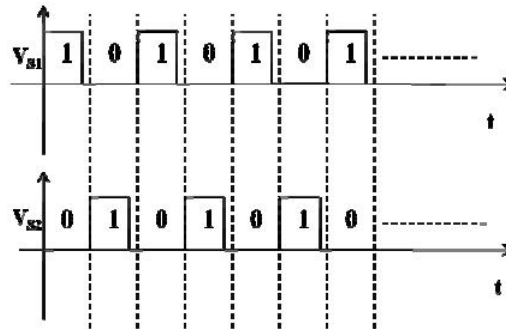
Figure 105: Switch control signals. Switches with odd numbers are controlled using VS1 while that with even numbers are regulated using VS2

A high quality factor (Q) resonant circuit is preferred for each loop in Figure 104 for the best performance. But the practical switches *S1*, to *SN* have its-own 'ON' resistances and hence the Q of the circuit and the sensitivity gets limited. This issue can be overcome with a modified circuit as given in Figure 106. In this circuit, when a loop , say i^{th} loop, needs to be deactivated (i.e., based on odd or even loop number or in a sequential basis as explained in the above paragraph), an additional low impedance Z*B* (e.g., a resistor RB) is connected in parallel to the corresponding *CM*, by setting the ith switch *Si*to position 0. In this condition, the loop '*i*' will be detuned from resonance resulting in a negligible change in the corresponding loop output signal *VCi* when a vehicle approaches. The loops with switches in position 1 will be at resonance and operate normal and give the expected output. For the circuit in Figure 106 also, the switches can be set to position 0 or 1 using the switch control signal shown in Figure 105.
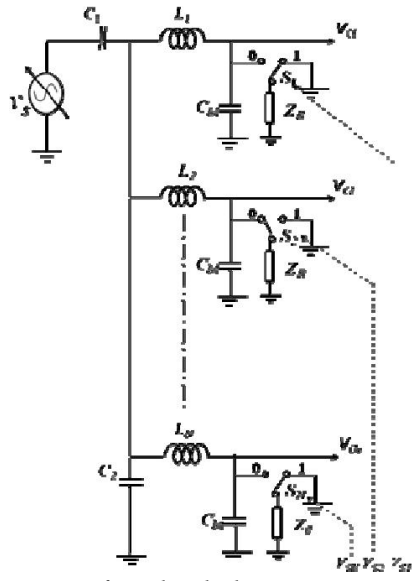
Figure 106: Equivalent circuit of multiple loop system with improved switching arrangement.

A prototype system of the proposed scheme has been built and tested. Details of the prototype developed and test results are discussed in the next section.

a) Experimental Set-up and Results

In order to test the practicality of the proposed scheme a prototype multiple loop detection system with six loops (N = 6) has been designed, built and tested. A snap shot of the experimental setup, developed and employed in the field testing, is shown in Figure 21 (earlier). Each loop has 5 turns and a nominal inductance of 100 μH. The dimensions of the single loop are given in Figure 107. The signal source *VS* was realized using a variable frequency sinusoidal source with 10 V peak-to-peak amplitude followed by a power operational amplifier using the IC OPA541. The capacitance values used are: *C*1= 0.056μF and *CM* = 0.068μF. This results in a resonance frequency of about 65 kHz and the frequency of excitation for the system was chosen to be the same.
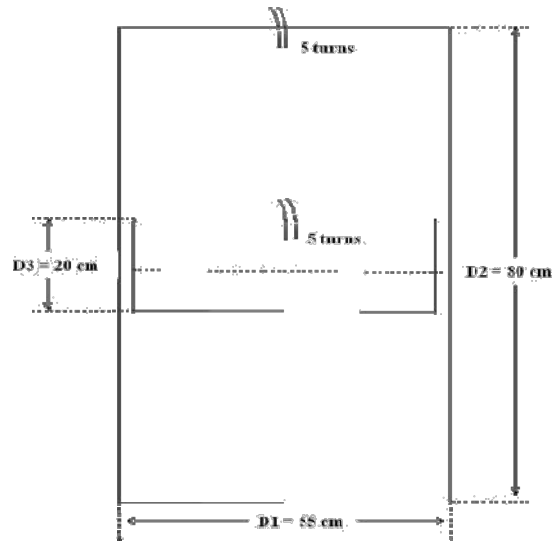
Figure 107: Dimensions of the outer (width, D1= 55cm and length, D2= 80 cm) and innerloops (length D3 = 20 cm). The number of turns is equal for both the loops. The inner and outer loops are in series.

The switches were realized using ICs MAX4053. The output voltages *VC1*, *VC2,…..VC6* were acquired using a 16 bit data acquisition system USB 6216, manufactured by National Instruments. The signals were sampled at a rate of 400 kSa/s. A test has been conducted to obtain a sensitivity map of the new loop. In order to perform this, a cylindrical conductive (mild-steel) test object with a diameter of 10 cm and a height of 2 cm was selected. Then, a sheet of paper with suitable size was taken and a length of 100 cm and width of 60 cm were marked. This was then divided into 60 individual boxes by drawing lines for each 10 cm in the length-wise and width-wise in the paper. This paper was then kept on the loop-1 with both of its centers coincided and the line in the paper in length- wise was in parallel to the direction of loop length. The object was kept in each box (one at a time) marked in the paper at a height of 18 cm and corresponding readings were recorded. The recorded data has been normalized with the maximum output observed among those positions (boxes) and plotted to obtain the sensitivity map of the loop as given in Figure 108. It can be seen from the map (refer Figure 108) that the loop has good sensitivity to even a small object not only at the outer periphery (as can be expected for a loop like Loop-A in Figure 101) but also in the inner regions due to the special structure of the loop with the inner-loop. The developed system was then tested in two stages. In the first stage, a single loop (*L1*) was selected and output corresponding to various types of vehicles was recorded and compared. The recorded data for a bicycle, motor cycle, car and a bus are given in Figure 109. Vehicles moving at various speeds were also tested and the signatures were compared. From Figure 109, it can be seen that each type of vehicle gives a unique signature output, which makes detection as well as segregation easy. Figure 109 also shows that the loop detects small vehicles like bicycle as well as large vehicles (bus), as expected.
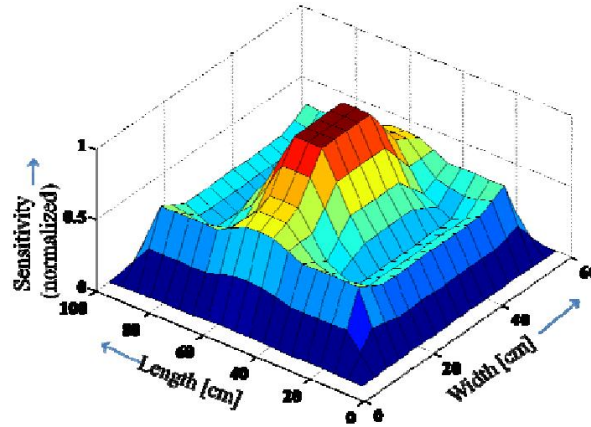
Figure 108: Sensitivity map of the new inductive-loop. Experiment is performed using a cylindrical metallic object with a diameter of 10cm and height of 2cm. The object was placed at a height of about 18 cm from the plane of the loop.
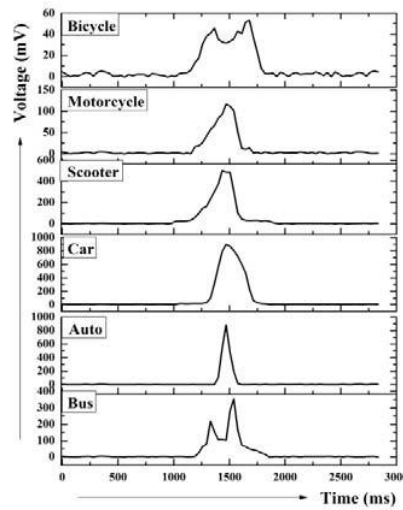

Figure 109: Results from single loop experiment. This shows the output signal (signature) observed for different types of vehicles.

Similar experiments were carried-out with the multiple loop detector and the outputs from all the six loops were recorded and analyzed simultaneously. Figure 110 shows the output when a motor cycle and a bicycle run in parallel. The motor cycle goes over loop-1 while bicycle goes over loop-3 and no vehicle over other loops. Figure 111 shows the results obtained for a bus which was covering the loops *L*1 to *L*3.
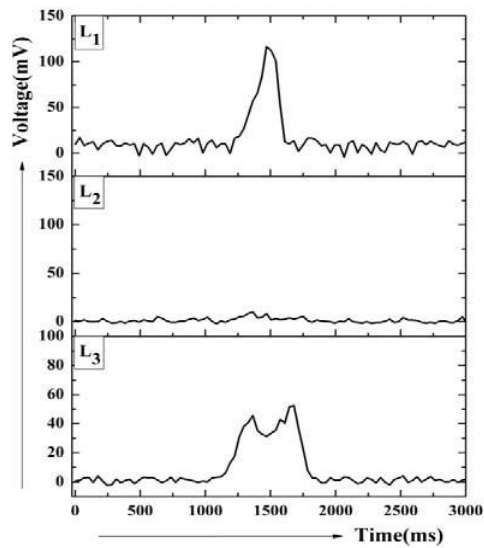
Figure 110: Results from the multiple loop detector. In this case, a motor bike and a bicycle were running in parallel. The motorbike went over loop-1 (L1) while bicycle went over loop-3 (L3) and no vehicle over other loops, for e.g., loop-2 (L2).
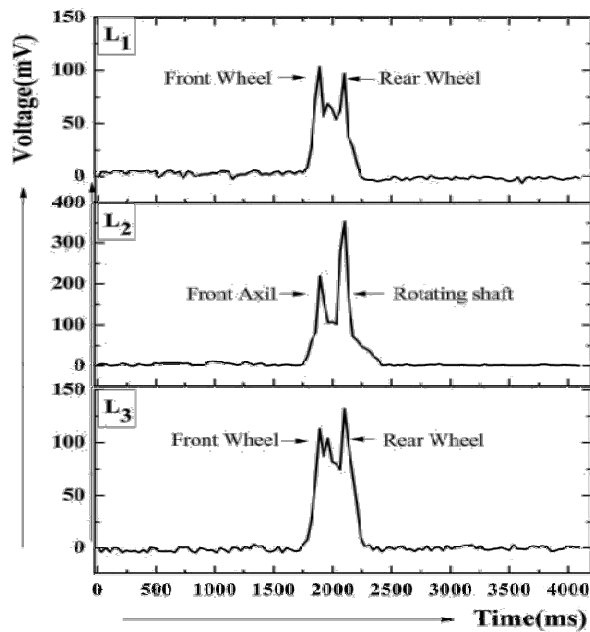
Figure 111: Signature of bus obtained from the multi loop vehicle detector.

Figure 112 shows the test results obtained from all the six loops simultaneously while

various types of vehicles such as bus, car, motor cycle, scooter, etc., were passing through the road in a heterogeneous and no-lane manner. The signatures produced by each vehicle can be seen in Figure 112. A snap-shot of the front-panel of the virtual instrument developed to perform the measurements, to process the data and display the results such as type and number of the vehicles detected is shown in Figure 113. The speed of the vehicle can be obtained accurately by using double-loop detector system [8]. The speed of the vehicle can also be computed from the data length for which a detectable change in output is observed, as the length of the vehicle (as the system detects the type) is known. From the output signal, the calculated speed and the length of the vehicle, the time of occupancy for that vehicle is ascertained. It is found from the above experiments that all important types of vehicles that go through the roadways can be detected and distinguished.
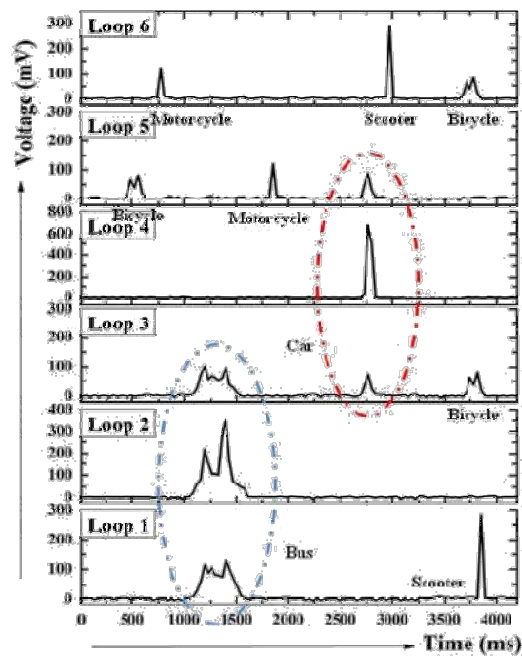
Figure 112: Results from the multiple loop detector with six loops (N = 6) recorded when various types of vehicles were moving simultaneously in the road.
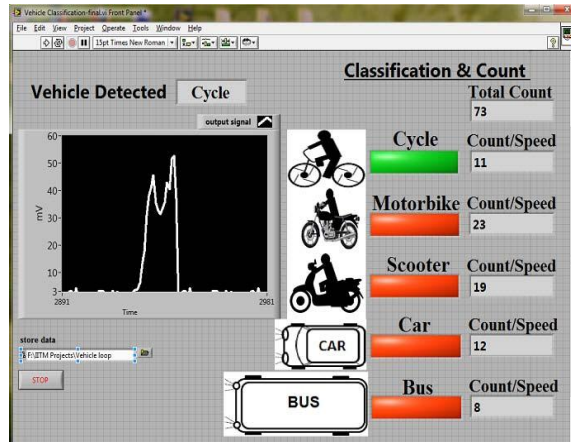
Figure 113: Front panel of the virtual instrument developed to acquire data (output signals from each loop), process it for detection and counting of vehicles.

The results show that the multiple inductive loop system sense and segregate the number of vehicles and their type. The developed inductive loop sensor detects large (e.g., bus) as well as small (e.g., bicycle) vehicles thus making it suitable for heterogeneous traffic conditions. The proposed multiple loop system is useful for roads with any type of (lane or no-lane disciplined and homogeneous or heterogeneous) traffic. The data provided by the measurement system is in digital form and hence it is easy for transmission to traffic management centers for real-time applications. The developed system enables ITS implementations in countries with heterogeneous and lane-less traffic resulting in better management of existing roadways with reduced congestion.

7.1.3 A Modified Multiple Loop System with Simple Loop Configuration

A new configuration of the loops, where all the loops are connected in series that considerably reduces the system complexity and improves reliability, was attempted next. Each loop has a unique resonance frequency and the excitation source given to the loops is programmed to have frequency components covering all the loop resonance frequencies. When a vehicle goes over a loop, the corresponding inductance and resonance frequency will change. The shift in frequency or its effect in any/every loop can be monitored simultaneously and the vehicles can be detected and identified as bicycle, motorcycle, scooter, car, bus, etc., based on the signature. Another advantage of this scheme is that the loops are in parallel resonance and hence the power drawn from the source will be at minimum. A prototype multiple loop system has been built and tested based on the proposed scheme. The developed system detected, classified and counted the vehicles accurately. Moreover, the system also can compute and provide the speed of the vehicle detected using single set of multiple loops. Accuracy of the speed measurement has been compared with actual values and found to be accurate and can be used for real time Intelligent Transportation System (ITS) applications under heterogeneous and less lane-disciplined (e.g., Indian) conditions. Details of the modified loop configuration, principle of measurement, experimental set-up and results are

discussed in the following sections. The performance of the developed system when employed for measurement of count and speed of the vehicles detected is also detailed.
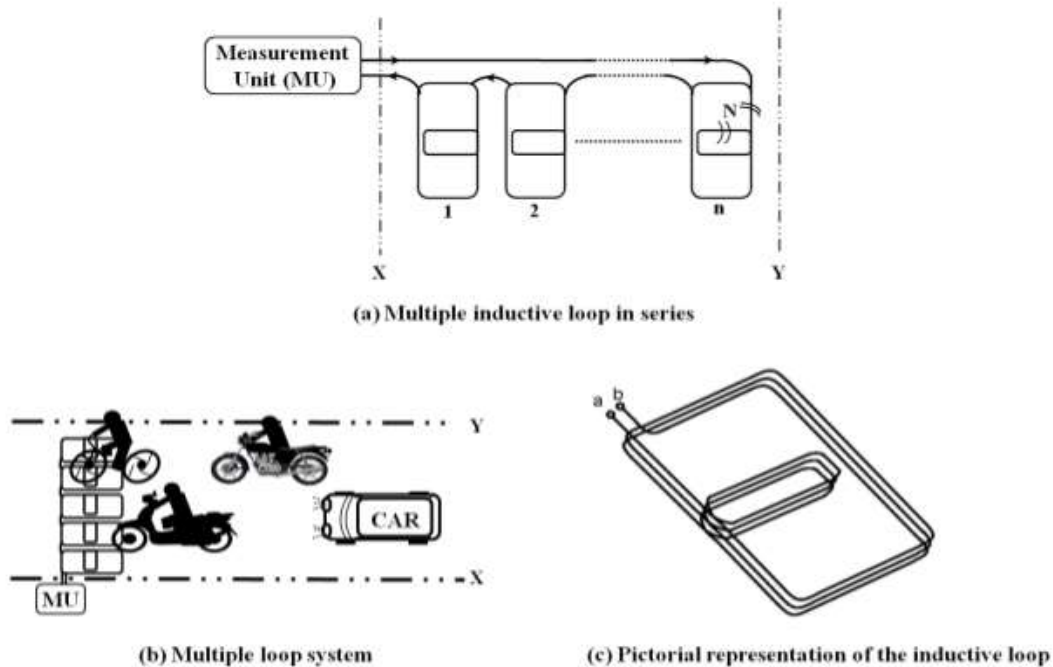

(a) Multiple inductive loop in series

(b) Multiple loop system

(c) Pictorial representation of the inductive loop

Figure 114: Multiple inductive loop system. (a) The loops connected in series, (b) the multiple loop system in a roadways and (c) detailed view of the loop structure.

As shown, there are 'n' number of loops covering the full road width X-Y. A simplified diagram of the system is given in Figure 114 (b). The loop employed has a special structure [6], as shown in Figure 114(c). This loop structure has the advantage of being sensitive to various types of vehicles such as bicycle, motorcycle, car, bus etc. Each individual loop has 'N' number of turns and has an inner and outer loop as illustrated in Figure114(c). All individual loops have identical dimensions. The loops are in series and connected to the measurement system as indicated in Figure 114(a) [31]. An equivalent electrical circuit of the system is shown in Figure 115.
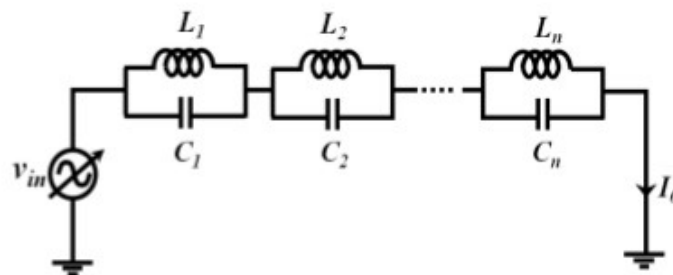
Figure 115: Electrical equivalent circuit of the proposed series connected inductive loops

It can be considered that the mutual inductance between the individual loops is much less compared to its self inductance. L1 and C1 indicate the self inductance and capacitance (included externally) of loop-1. Similarly, L2, C2, ..., Ln, Cn indicate the corresponding values for loop-2,...., loop-n, in order. Consider, Vin(ω) is a sinusoidal source with a constant amplitude and variable frequency 'f'. Then the current I0(ω) flowing through the circuit can be expressed as,

$$I_0(\omega) = \frac{V_{in}(\omega)}{\frac{j\omega_1}{1-\omega^2 L_1 C_1} + \frac{j\omega_2}{1-\omega^2 L_2 C_2} + \cdots + \frac{j\omega_n}{1-\omega^2 L_n C_n}} \qquad (7.1)$$

where ω = 2πf rad/s. As can be seen from equation (7.1), there will be 'n' number of parallel resonance frequencies f1, f2, ..., fn for loops 1, 2, ..., n respectively, where f1= $1/2\pi\sqrt{L_1 C_1}$, f2 = $1/2\pi\sqrt{L2C2}$, ..., fn = $1/2\pi\sqrt{LnCn}$.When a vehicle approaches the sensing area of the loops, the inductance of the loops that are covered by the vehicle will change. As the inductance change, the corresponding resonance frequencies will change and this can be detected using a measurement system. As the dimensions of the individual loops are known, the type of the vehicle detected can be distinguished from the number of loops that show a shift in resonance frequency. The amount of shift in frequency and the way frequency changes (signature) [32] - [34] as the vehicle moves over the loop can also be effectively used to improve the identification/classification process.

a) Measurement System

Figure 116 shows a simplified diagram of the multiple inductive loop sensors with the measurement system. The signal Vin is generated in such a way that it contains all the (resonant) frequency components f1, f2, ... fn. This can be achieved using an arbitrary function generator or a digital-to-analog converter controlled by a computer. A known resistance RS is connected in series to the loops as indicated in Figure 116 to measure the circuit current I0. A capacitance CSh is connected in parallel with RS to attenuate unwanted higher frequency components (before giving it to the data acquisition system) that may interfere with the system.
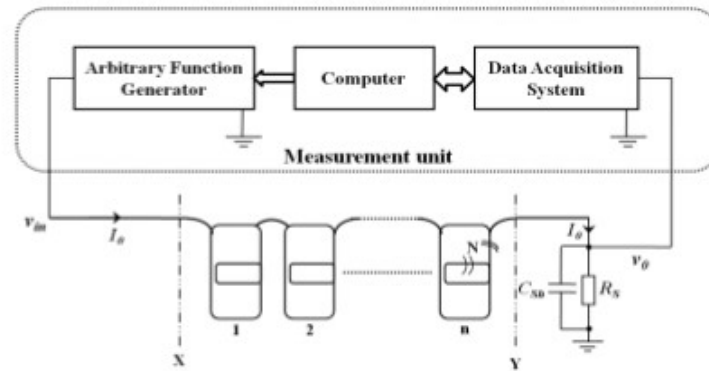
Figure 116: Functional block diagram of the system

Before performing the actual measurements, the system needs to be calibrated using the same set-up indicated in Figure 116. In order to do this, the frequency 'f' of the signal Vin(ω) is varied, starting from f < f1 to f > fn and the magnitude of the output V0(ω) will be recorded. This has to be performed in a vacant condition. From this data, the resonance frequencies for a vacant condition can be found and stored. Once the resonance frequencies are known, we simplify the excitation pattern (Vin) to a waveform which is the sum of instantaneous values of 'n' number of individual sinusoidal voltages having frequencies equal to the resonant frequencies of the loops. The output signal V0 is recorded using a data acquisition system and a computer. The change in amplitude of the output signal V0 corresponding to each resonant frequency is found using suitable filters that separate the responses for each resonant frequency and then computing the RMS of the output of the filter on a cycle-by cycle basis (this can also be achieved by employing a Fast Fourier Transform analysis).

The calibration procedure mentioned above needs to be applied in a regular interval to achieve best results. This can be set as auto-calibration, in which the system will recheck resonance frequencies of the multiple loop system and modify the excitation pattern automatically. In the case of an abnormal frequency pattern, the system can notify the control center and appropriate action can be taken. Auto-calibration will be done in off-peak hours, when no vehicle is present. This can also be initiated routinely by the control center.

A simulation study has been conducted using a SPICE package to verify the principle of measurement. A system with five loops (n = 5) having L1 = L2 = L3 = L4 =L5 = 100 μH and parallel capacitors C1 = 340 nF, C2 = 272 nF, C3 = 204 nF, C4 = 136nF and C5 = 68nF were used for the study. An AC analysis has been carried-out for a frequency range of 10 kHz to 100 kHz and the magnitude response of the circuit has been recorded. The amplitude of Vin was kept as 1 V during the simulation. The parallel resonance points were found to be 25 kHz, 29 kHz, 33 kHz, 41 kHz and 58 kHz for loop 1, 2, 3, 4, and 5 respectively. Another set of simulations were performed, for the same frequency range, by varying the values of inductance's of all the inductors (L1 to L5) simultaneously in steps of 4 μH. The

ratio of magnitudes of output and input (V0=Vin) were plotted and shown in Figure 117. It can be seen clearly that all the parallel resonance frequencies shifted (as expected) owing to the change in the inductance of the loops. Next section discusses the details about the prototype system developed and results obtained.
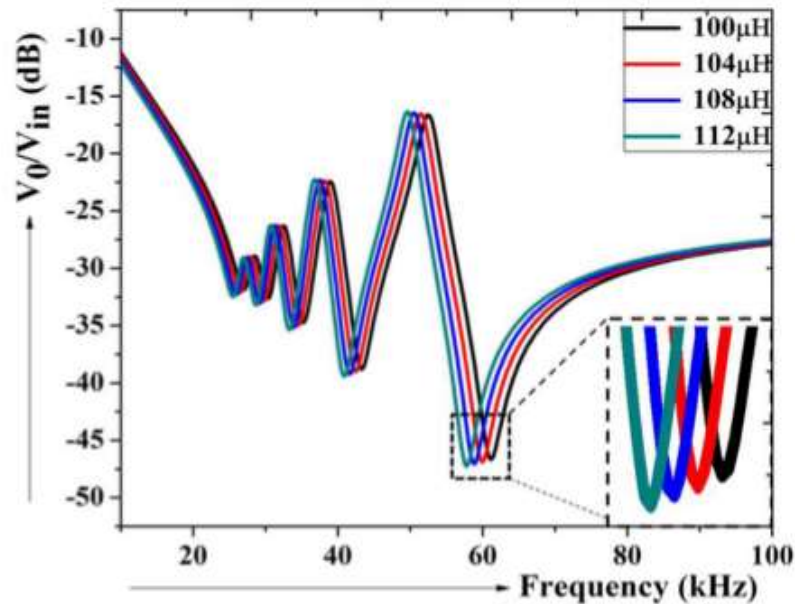

Figure 117: Results from the AC analysis performed using SPICE on the equivalent circuit of the multiple inductive loop detector. Five individual parallel resonances (and shift) can be observed.

7.1.4 Experimental Set-up and Results

In order to test the performance of the new scheme, a prototype system has been developed. The details of the prototype and test results are presented below.

a) Prototype and Experiment - I

A prototype multiple loop system has been developed with three loops (n = 3, stitched to a carpet) and tested in the field for its ability to detect various types of vehicles. The inductive loop used in the prototype system has five turns and inductance of 100 μH. The loops were connected in series as explained in the earlier section. Capacitors C1, C2 and C3 were connected in parallel to loop inductance's L1, L2 and L3 so that each loop has an individual parallel resonance frequency (f1, f2 and f3). The capacitors used were C1 = 204nF, C2 = 136nF, C3 = 68nF and the resonant frequencies obtained were f1 = 23 kHz, f2 = 43 kHz, f3 = 64 kHz. The excitation signal Vin to the circuit was generated using an arbitrary function generator AFG3021B from Tektronix. Sine waves of frequencies f1, f2 and f3 were individually generated in a computer, then a sum of these instantaneous

waveforms was loaded to an arbitrary function generator. The signal from the function generator was amplified using a power operational amplifier IC OPA541. The output V0 from the circuit was acquired using a 16 bit data acquisition system from National Instruments (USB 6216) at a sampling rate of 400 kSa/s [30].

The developed system was tested in three stages. In the first stage, a test was conducted to observe the shift in the resonant frequency in the presence of a conductive object in the vicinity of the loop. In order to do this, the magnitude response of the output was recorded for a frequency range starting from 10 kHz to 100 kHz with a step size of 180 Hz. The amplitude of the signal Vin was kept at 1 V during this measurement. The test was conducted first in a vacant condition and then by placing a conductive metallic sheet of 90 x 40 cm at a height of 10cm from the plane of the loop-2 of the prototype multiple loop system. Figure 118 shows the magnitude plot for the above two cases. It is clear from Figure 118 that the parallel resonant frequency (f2 = 43 kHz) of loop-2 alone shifted (to f02 = 44 kHz) in the presence of a conductive object above that loop. Thus, a shift in the resonant frequency can be observed whenever a metallic object enters the sensing vicinity of the loop.
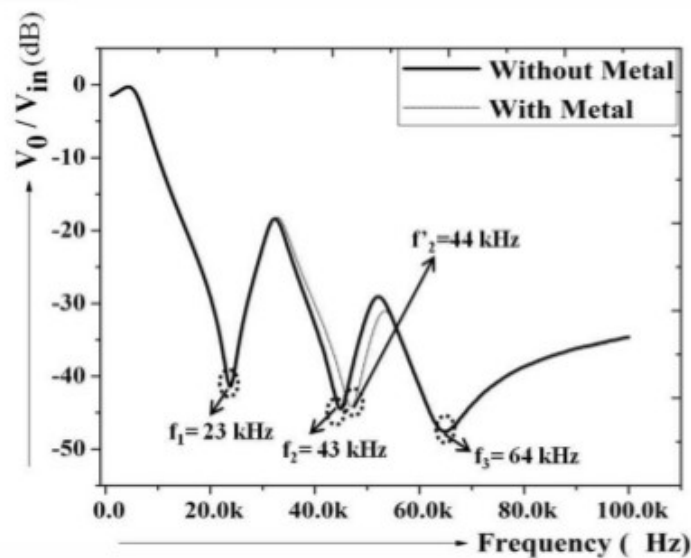

Figure 118: Magnitude of the (measured) Bode plot from the prototype multiple loop system with three inductive loops. The shift in resonant frequency can be seen when a metallic sheet was kept about 10cm above one of the loops (1oop-2).

In the second stage, a single loop (L1) was selected and output for different vehicles like bicycle, motorcycle, scooter, car, auto rickshaw and bus were recorded. The signatures observed are given in Figure 119. Figure 119 clearly shows that each of these vehicles have a unique signature in terms of signal shape and amplitude. It also shows that the loop is sensitive to small vehicles like bicycle as well as large vehicles (e.g. bus). In the

case of a bicycle, the change in output was large when the front or rear wheel was over the loop (as indicated in Figure 119) compared to the output when middle part of the bicycle was above the loop. For a bus, the loop gives more output when wheels and axle were above the loop compared to other portions of the bus, which are 1=2 m or more above the pavement surface. Thus, for both of these vehicles, the signatures (not amplitude) look almost similar as expected. Number of loops covered by a bus was three (in the prototype) while bicycle covered only a single loop. This information helps the classification process. In the case of a car, the gap between its body and pavement is very small. The effect of close proximity of a car body is large, hence the effect due to presence of wheels is not clearly visible.

In the third stage, more experiments were carried-out and the outputs from all the three loops were acquired simultaneously. Figure 120 shows the response for a motorcycle (over loop-1) and a bicycle (over loop-3) running parallel with no vehicle over loop-2. The signature of the bicycle has two peaks which correspond to the (two) wheels of the bicycle. Figure 121 shows the readings obtained for a bus running over the multiple loop detector. In this case, for the loop-1 and loop-3 the first peak corresponds to the front wheel and the second peak corresponds to the rear wheel of the bus. In loop-2 (middle loop), the first peak corresponds to the front axle and the second peak corresponds to the rotating shaft and rear axle which are close to the road surface. Figure 122 shows the signature obtained for a tricycle which covers one (middle) loop fully and two (side) loops partially. The first small peak is due to the presence of front wheel over the middle loop (L2) and second peak is due to the rear wheels (above loop L1 and L3) and metallic body (above loop L2) of the tricycle. Figure 123 shows the output obtained when a bicycle, motorcycle and scooter were running in parallel over the multiple loop detector. It also shows that the cross sensitivity between the loops is very small as no variation in output signal is observed from a loop when the near-by loops are occupied.
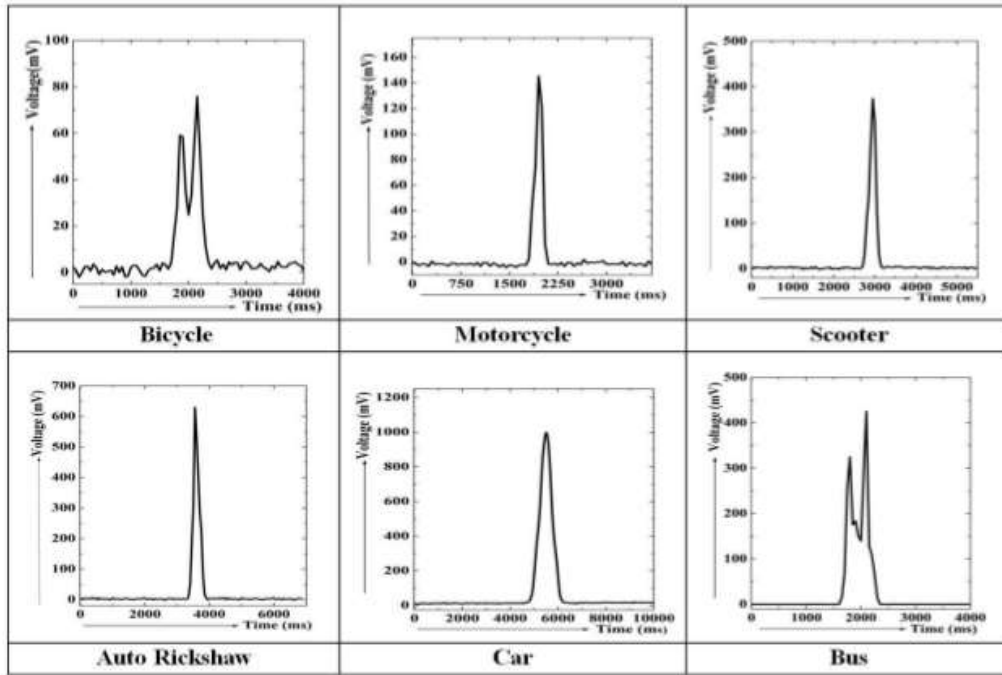
Figure 119: Output signal and signature obtained from a single loop for various vehicles.
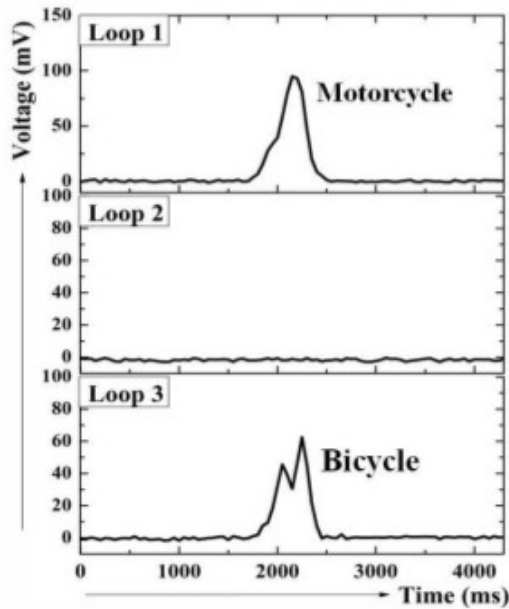

Figure 120: Results from multiple loop detector. Signature obtained when a motorcycle and bicycle run parallel over the multiple loop detector.
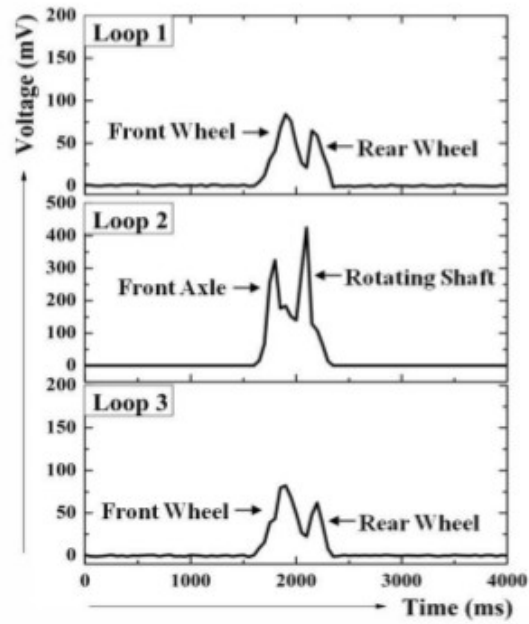
Figure 121: Signature obtained when a bus traveled over the multiple (three) loops.
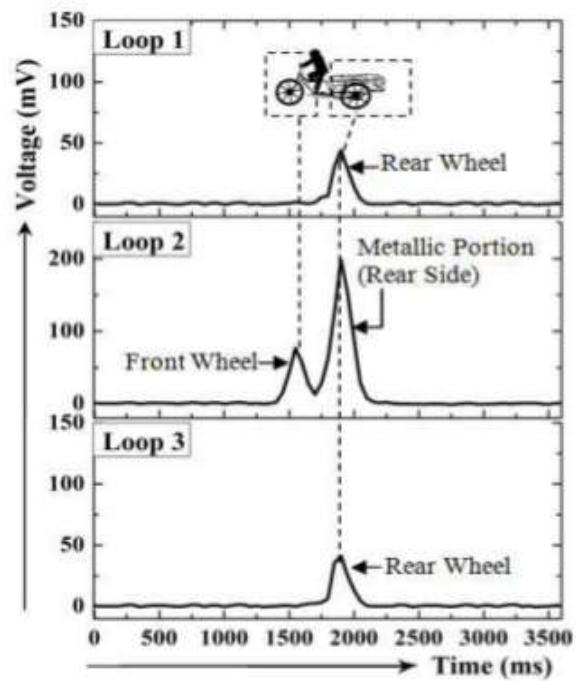

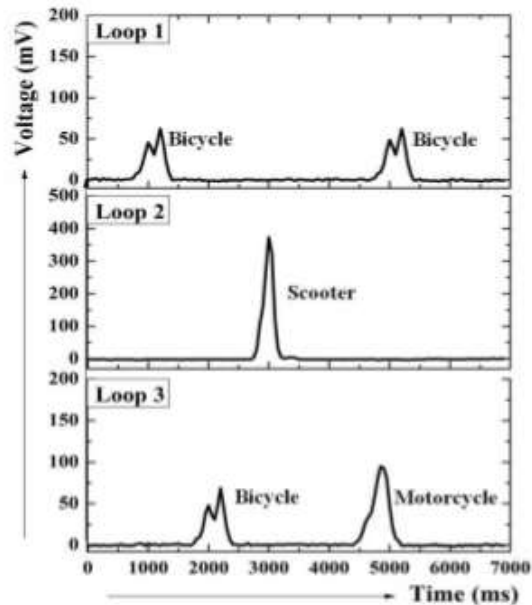**Figure 122**: Signature obtained for the tricycle from the multiple loop system with three loops.

Figure 123: Signature obtained from all the three loops when there was a continuous movement of vehicles

b) Prototype and Experiment - II

As the performance of the first version of the prototype with three loops was promising, we decided to test the scheme further in an extended scale. The prototype version-I developed has been extended with six identical inductive loops covering the full road width. All the six loops were connected (electrically) in series, as in the previous case, and each loop resonates at individual frequencies. For the prototype developed, the inductance of each loop was $L_1 \_\approx L_2 \approx L_3 \approx \_L_4 \approx \_L_5 \approx L_6 = 100 \_H$ and corresponding parallel capacitors were $C_1 = 680$ nF, $C_2 = 220$nF, $C_3 = 100$nF, $C_4 = 56$nF, $C_5 = 33$nF and $C_6 = 22$nF respectively. This resulted in six parallel resonance frequencies $f_1 = 20$kHz, $f_2 = 35$kHz, $f_3 = 52$kHz, $f_4 = 69$kHz, $f_5 = 93$kHz and $f_6 = 112$kHz. Figure 124 shows a photograph of the experimental set-up. Figure 125 shows the data recorded when a bus followed by three bicycles (in parallel) were moving above loops 1 to 3 while a car followed by two motorcycles and a scooter (in the middle) were moving, almost at same speed, above loop 4 to 6. Figure 126 shows a small section of the data recorded (corresponding to each loop) during the field test.

Figure 124: Inductive loop detector covering the entire road width.
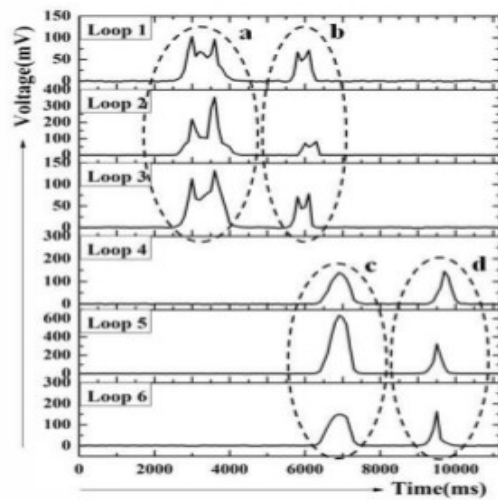

Figure 125: Signatures obtained for various vehicles from the multiple loop detector stretched over the entire road width. (a) Bus, (b) Three bicycles moving in parallel, (c) Car and (d) Two motorcycles and a scooter in the middle.
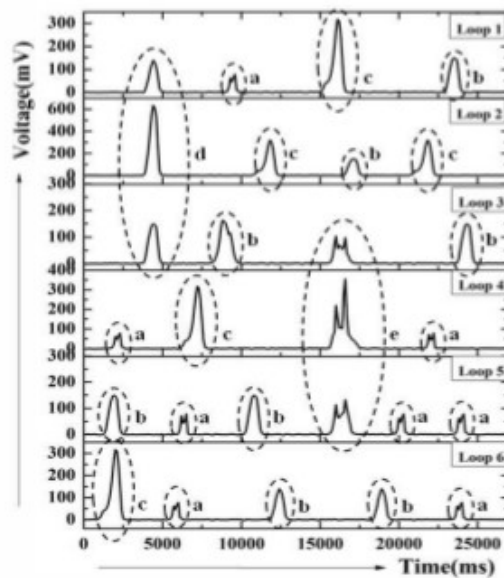
Figure 126: Vehicles detected during a short duration. a = Bicycle, b = Motorcycle, c = Scooter, d = Car and e = Bus respectively

From these results it can be observed that each type of the vehicle has a unique signature with respect to the (a) amplitude and (b) the shape of the signal in relation with time (signature) and (c) number of loops a vehicle occupies. A suitable algorithm can be used to automate the classification process. We used a threshold based scheme and the system accurately counted and classified the vehicles detected by the proposed multiple inductive loop configuration.

7.1.5 Speed Measurement

It has been reported that the speed of a vehicle can be measured, with good accuracy, using single [32], [33], [34], [35] as well as dual [36], [37] inductive loop systems if the traffic is homogeneous and lane-disciplined. This section discusses the functionality and performance of the new multiple loop system (developed for heterogeneous and lane less traffic) when it is employed to measure speed of different types of vehicles. The speed measurement has been conducted using single as well as dual sets of multiple inductive loops. The dual set is similar to the standard dual loop system except that each set here consists of multiple loops so that it works well in a lane less and heterogeneous traffic.

As the multiple loop system can detect the type of the vehicle, based on the signature and amplitude of the output signal and number of loops covered by the vehicle, it is possible to compute the speed using a single set of multiple inductive loop detectors

itself (e.g., set-1 alone in Figure 127, where Figure 128 shows a dual loop system). Since the length of each type of vehicle is known (once the type is detected), the speed can be computed using the time a vehicle takes to pass the loop length, which is also known. The time taken by the vehicle to cross the loop length can be obtained from the duration for which the output from the loop is higher (in amplitude) than a preset threshold.
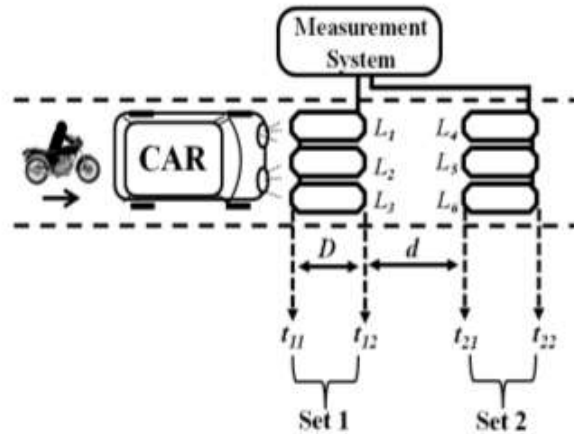

Figure 127: A schematic of the dual multiple loop system for the speed measurement. This test was performed to verify the accuracy of speed measurement using the new loop system.

For computation of speed, it also requires the sampling frequency of the data acquisition system employed. Figure 128 shows the prototype system to test the speed using dual multiple loop detector system.
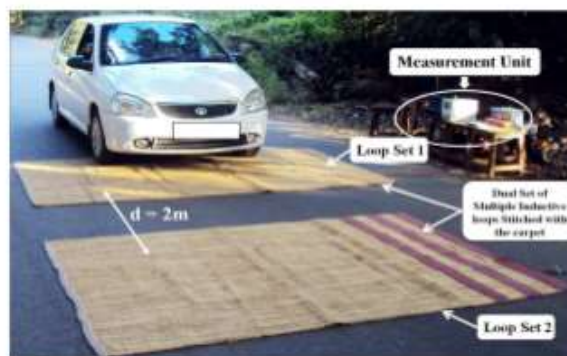

Figure 128: A schematic of the dual multiple loop system for the speed measurement. This test was performed to verify the accuracy of speed measurement using the new loop system.

In the prototype unit, set-1 and 2 have three loops each. Set-1 and set-2 are placed at a distance of 2 m apart. Set-1 contains loops L_1, L_2 and L_3 and set-2 contains loops L_4, L_5 and L_6 respectively. For a vehicle to pass both the sets, it has to move a distance of $(2D + d + l_v)$, where D is the length of the loop, d is distance between set-1 and set-2 and l_v is the length of the vehicle detected. Let us consider that t_{11} is the time at which the vehicle enters set-1 and t_{22} is the time at which the vehicle leaves the set-2. Thus, the speed 's' of the vehicle can be calculated using the equation (7.2),

$$S = \frac{(2D + d + l_v)}{(t_{22} - t_{11})} \qquad (7.2)$$

Figure 129 shows the signature of a motorcycle recorded when it was moving from set-2 to set-1. In this case, when it entered into the loop system it was above L_4 (set- 2) and then over loop L_1 (set-1). In Figure 129, the continuous curve shows the output signal from set-1 whilst the dotted curve indicates the signal from set-2. In a homogeneous traffic, direction of movement of vehicle can be obtained using existing loop system.
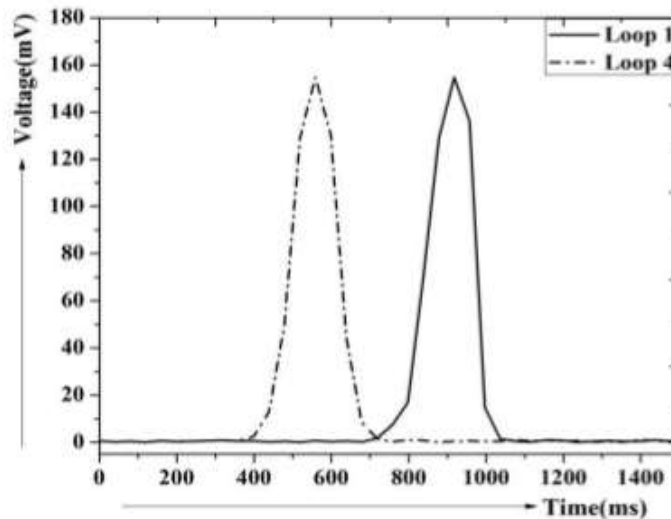

Figure 129: Shows the signature of a motorcycle running from loop L4 to L1 at a speed of 37 km/hr. It is clear that the direction is reversed (opposite to that marked, next to motorcycle in Figure 101).

The same can be easily obtained from the dual multiple loops system in a heterogeneous traffic. Tests were conducted on a single set and a dual set multiple loop detector system to measure the speed of a vehicle. Simultaneously, during the test, the speed of each vehicle was also measured using a Laser gun from TruCAM [38]. The measurement from the laser gun is taken as the reference measurement.

Figure 130 shows signature of a car captured by the dual multiple loop system during the measurement of speed. During the test, the car was made to run, over the dual loop system, at different speeds such as 11 km/hr, 24 km/hr, 30 km/hr and 45 km/hr. Figure 131 shows signatures of a motorcycle recorded while it was running at various speeds like 11 km/hr, 16 km/hr, 25 km/hr and 36 km/hr over the multiple loop detector. The speed measured (for car and motorcycle) using a Laser gun is shown in Figure 132. Accuracy of measurement using the single set and dual sets of multiple loop detectors were calculated, considering the reading from laser gun as the reference, and are given in Table 33 and Table 34 . The maximum deviation, with-respect-to the Laser Gun.
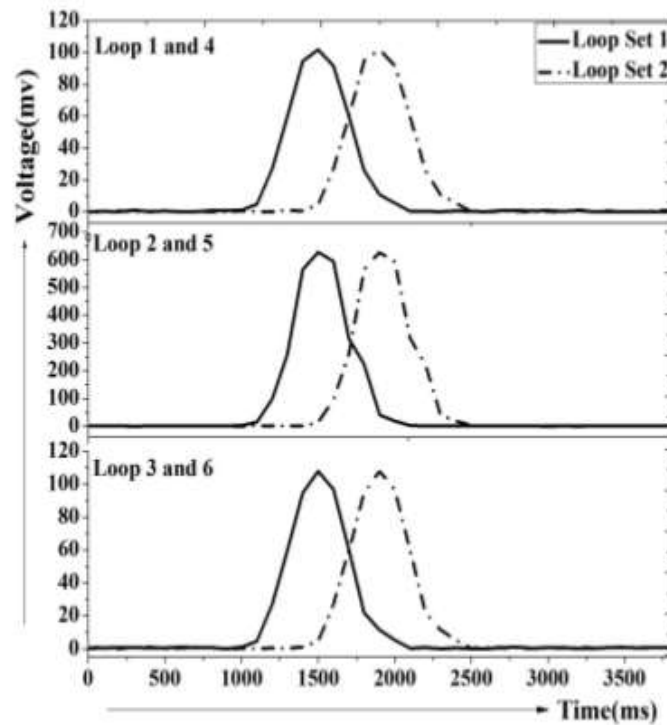

Figure 130: Shows the signature of a car observed in the dual multiple inductive loop system used for measurement of speed.
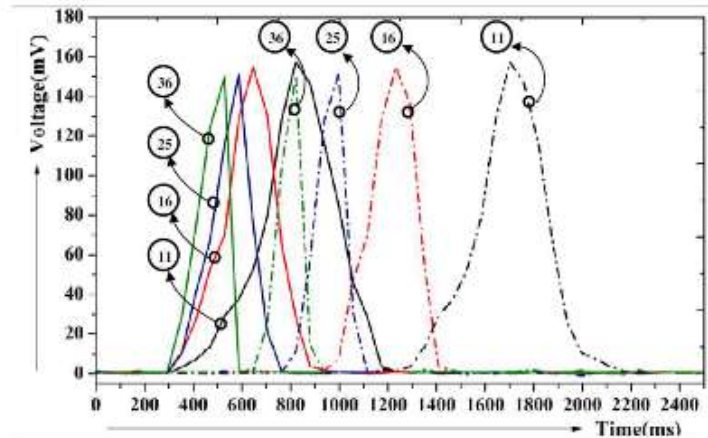
Figure 131: Shows the signature of a motorcycle measured using a multiple inductive loop system. The continuous curve show the response from loop set-1 and dotted curves represents the output from loop set-2 (Figure 101). The speed of the vehicle is indicated (in km/hr) in the graph.

Figure 132: Speed given by the laser gun during the test. This is used as the reference measurement

Table 33: Speed measured for a motorcycle

Speed Measured in km/hr			Error in Speed (km/hr)	
Laser Gun*	Single set of MILD	Dual set of MILD	Single set of MILD	Dual set of MILD
11	10.76	10.79	-0.24	-0.21
16	16.49	15.85	0.49	-0.15
25	25.45	25.04	0.45	0.04
36	35.48	35.26	-0.52	-0.74
MILD - Multiple Inductive Loop Detector				
* Output from the Laser gun is taken as the true reading				

Table 34: Speed measured for a car

Speed Measured in km/hr			Error in Speed (km/hr)	
Laser Gun*	Single set of MILD	Dual set of MILD	Single set of MILD	Dual set of MILD
11	11.17	10.74	0.17	-0.26
16	23.42	23.49	-0.58	-0.51
30	30.97	29.01	0.97	-0.99
45	45.62	46.54	0.62	1.54
MILD - Multiple Inductive Loop Detector				
* Output from the Laser gun is taken as the true reading				

a) Prototype and Experiment - III

This subsection presents details of a heavy-duty adhesive tape based, temporary installation of the multiple loop system in a typical roadway having heterogeneous traffic and the results obtained. Six inductive loops were formed using insulated stranded copper wire of 2.5 mm2 cross-sectional area, which is easily available commercially. This wire is meant for home or office wiring and not designed to withstand high pressures that will be experienced when a heavy vehicle goes over it. We used this, since it is a temporary installation. Similar wires may be used if the loops are placed in the pavement after making suitable saw-cuts. A continuous wire was used to form the entire multiple loop (six loops) so that no joints are required between individual loops. The two ends of the wire from this series connected loop system were brought down to side of the roadway and connected to the measurement system. Suitable marking were made on the road and the loop formed were placed on the roadways as per the markings. Adhesive tape, which is usually used for similar applications, was applied covering the entire loops. A photograph of the set-up is shown in Figure 133. Figure 133 (a) shows the multiple loops installed

on a roadway using adhesive tape while (b) shows the loops, which are under the tape now, formed using the insulated wire. The measurement system is also visible in the top right corner of Figure 133 (a). Few photographs of the traffic during the test are given in Figure 133 (c)-to-(e), indicating the heterogeneous nature of the traffic.

Table 35: Results from the field test

Vehicle type	Count	True count	% Accuracy
Bicycle	21	22	95.5
Motorcycle	241	247	97.6
Scooter	42	43	97.7
Tricycle	3	3	100
Car	73	74	98.6
Auto rickshaw	43	43	100
Mini Bus	6	6	100
Bus	10	10	100
Total	439	448	97.8

The loops connected in series were set to same resonance frequencies as given in subsection 7.1.4. The measurement system employed was same as that developed for performing the tests described in the subsection 7.1.4. A video of the entire experiment was recorded. The video showed the vehicles travelling over the loop system and corresponding display in the computer showing the signature given by each loop and the vehicle detected. The experiment was conducted for a duration about 8 hours. Data recorded during two peak hours was processed and the results were compared with the recorded video. Table 35 shows the count and classification accuracy obtained for each type of vehicles from the test conducted. Results show the capability of the developed system to detect and classify vehicles in a heterogeneous traffic.
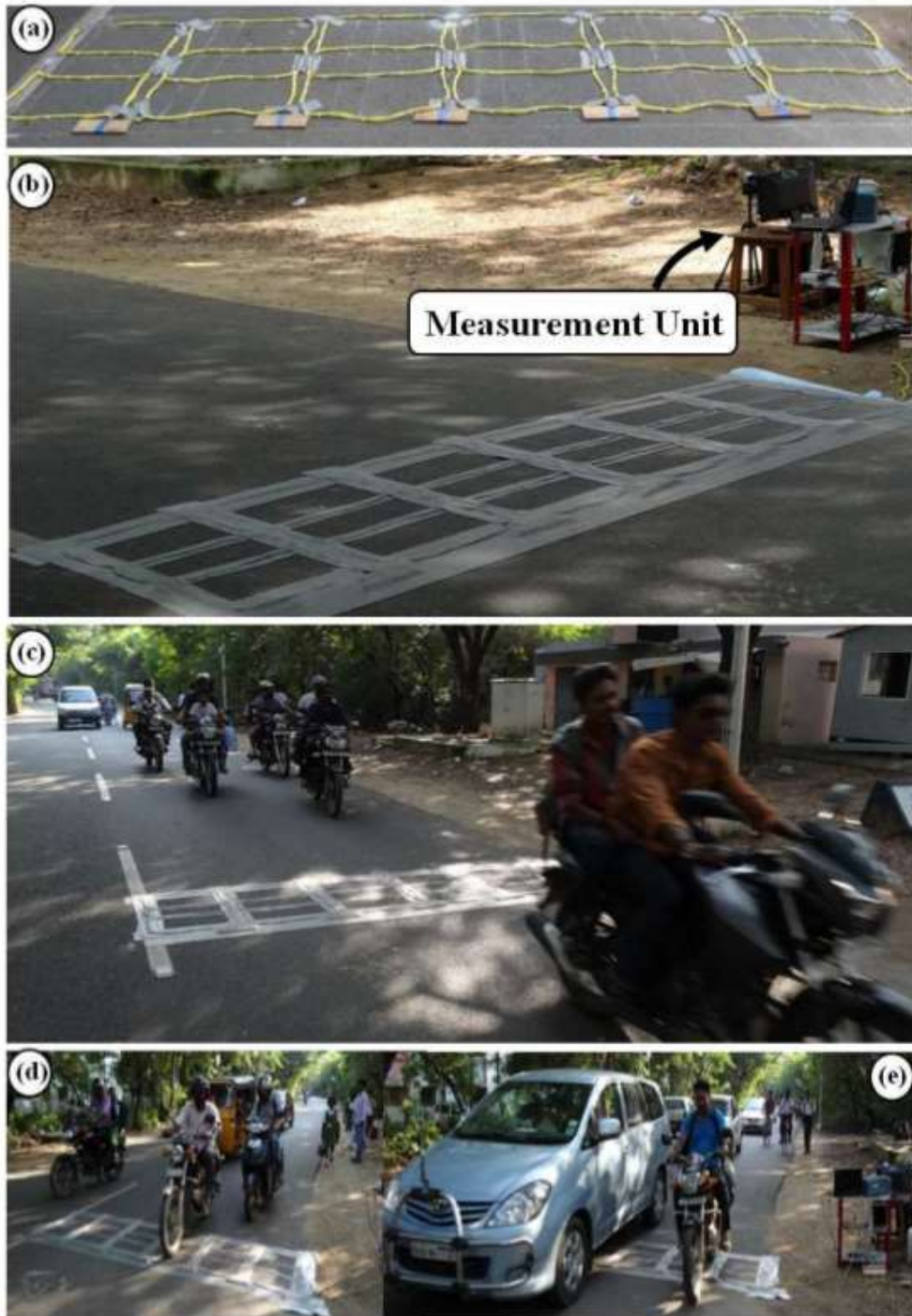
Figure 133: A photograph of the loop installed using heavy-duty adhesive tape. (a) shows the loops formed using the insulated wire, (b) shows the multiple loops installed in the roadway while. The tape is applied over the loops. Measurement system is visible in the top right corner. Photographs of typical traffic observed during the test are given in (c), (d) and (e).

7.1.6 Installation and Maintenance of Multiple Inductive Loop System

Temporary installation of the multiple loop system using a mat/carpet (loops stitched to carpet) and using a heavy-duty adhesive tape was discussed in the previous subsections. Such a scheme is useful for performance evaluation or temporary studies, or when there is an urgent requirement to monitor the heterogeneous traffic for a short duration. Other methods based on road tube and pneumatic counter can also be used for temporary studies, but only in a homogeneous traffic. For these methods, complex sensors structures may be required to detect and classify vehicles in a heterogeneous and lane-less traffic. In order to install the proposed multiple loop system in a concrete or asphalt roadway, like the currently available loop systems, we need to make the necessary saw-cuts, on the roadways, which suit the shape of the loop. As the loop system consists of multiple numbers of loops, the number of saw-cuts required in the pavement will be more than that required for a conventional loop. Once the required saw-cuts are made on the pavement, using typical concrete saw, the loop can be laid in the slots and the slots can be sealed with appropriate loop sealants. As the saw cuts are on the surface layer of the pavement, the strength of the road may not get affected. As far as maintenance is concerned, the new loop system will not face any serious additional challenges compared to standard / conventional inductance-based sensor designs.

a) Loop Placement and Number of Loops

In the proposed scheme, we found that it is very difficult to detect small vehicles like bicycles or motorcycles that go through the gap between the adjacent loops, if the gap of more than 10 cm. Thus, all the small vehicles that go through the gap between the loops (if the gap is large) will be missed. We also need a minimum gap between the adjacent loops, otherwise a vehicle (say, bicycle) going in-between the loops will give large output signals in two loops and this will introduce errors in the classification process. Thus, a 10 cm gap is preferred between adjacent loops. The width of individual loop was finalized considering the minimum space that will be occupied by the smallest expected vehicle (bicycle). A person riding a bicycle will occupy at least 1/2 a meter width of the road. Thus, if we keep a loop with approximately 1/2 a meter width, it can be assured that two such vehicles (bicycles) cannot share same loop at same time. If two vehicles covers same loop, we will get unpredictable signatures. Also, if two large vehicles (or a small and a large) go in parallel, a minimum of 1/2 a meter lateral gap is observed in a heterogeneous traffic (where many a time, the traffic rules concerning minimum lateral gap between vehicles moving in parallel are not followed). Considering these facts we set the width of each loop as 55 cm and the gap as 10 cm. As mentioned above, in order to make sure that even the smallest vehicle is detected accurately, the entire road width needs to be covered with such loops. Thus, width of the road was divided by width of the loop plus 10 cm (gap between loops) and loops were laid. The loops were electrically

connected in series as explained in section 7.1.3. The modified multiple loop system with new loop configuration gave better performance in terms of complexity, reliability and accuracy. The installation is also easier in this scheme.. From the field test results, we can conclude that the prototype system has the ability to classify each of the vehicle type, count the number of vehicles and the find the speed and direction of movement of the vehicles successfully. A new scheme that helps to convert the conventional loop to a multiple loop system for heterogeneous traffic is presented in the next chapter.

7.1.7 Mutually Coupled Multiple Inductive Loop System

a) Introduction

A new loop sensor system that uses a conventional loop as an outer loop and number of special loop is presented in this section. The inner loops are identical as in the scheme presented in the previous sections. But they are neither connected with a cable to measurement system nor connected in series, instead they are magnetically linked to the outer loop (conventional loop). Measurements are made directly from the outer loop. A simplified diagram of the proposed method is illustrated in Figure 134. This scheme is very simple and effective and can be employed to convert an existing, conventional, single loop system to a multiple loop system by incorporating the inner loops. Once converted, it can be used in a heterogeneous traffic. A prototype of the proposed system has been built and the practicality has been tested. A suitable measurement scheme based on a synchronous detection is employed in the prototype. A special excitation that ensures parallel resonance of the whole inductive system is employed, which keeps the power consumption minimum. The new system correctly sensed the vehicles, categorized and counted them in an undisciplined traffic. The proposed system has been, also extended to detect the direction of travel and speed of the vehicle and tested. Results obtained from the prototype were found to be accurate showing the system to be ready for field implementation for real time traffic monitoring and ITS applications under heterogeneous and lane less traffic.

b) Mutually Coupled Multiple Inductive Loop System

A diagram of the proposed mutually coupled inductive loop system is shown in Figure 135. It has an outer loop and many inner loops indicated as 1, 2,.., n as in Figure 135. The outer loop, as in a conventional system, covers the full width of a lane/road. The inner loop is the special loop is shown in the right side of the Figure 135. The inner and outer loops are magnetically coupled and no electrical connections exist between inner loop and outer loop. Similarly, there are no electrical connections between the inner loops and they are also connected only magnetically. All inner loops are identical. These factors help to simplify the manufacturing and installation process of the multiple loop detector.
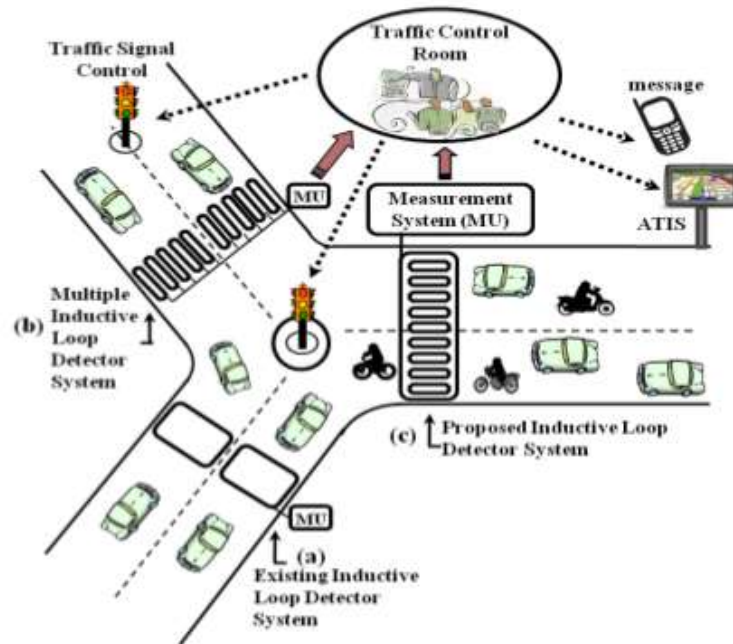
Figure 134: Illustration of a (a) conventional, (b) multiple loop and (c) new mutually coupled inductive loop detector systems. (a) is designed only for homogeneous and lane-based traffic while (b) and (c) are suitable for detection of parameters even in an undisciplined traffic. ATIS is advanced traveler information system
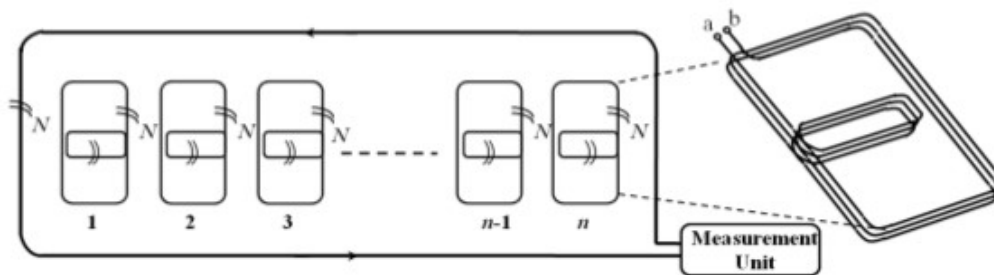

Figure 135: Mutually coupled inductive loop detector with the multiple inner loop (1, 2, ... n) and a single outer loop. All the inner loops are identical and a pictorial view of the loop employed (for inner alone) is shown on the right side

An electrical equivalent circuit of the inductive system is given in Figure 136. The outer loop has a self inductance of L while there exists mutual inductance of M_1, M_2, ... M_n between outer loop and inner loop 1, 2, ..., n respectively. Inner loop also has self inductance. This is indicated using L_1, L_2, ... L_n for loop 1, 2, ..., n respectively. Capacitors of C_1, C_2, ... C_n are respectively connected across the terminals (between

'a' and 'b' in Figure 135) of inner loop 1, 2, ..., n. This will introduce a resonance condition in each inner loop. The mutual inductance's M_1, M_2, ... M_n are stable (negligible change when a conductive object approaches the inner loop vicinity) due to the fact that at least two sides of each inner loop are kept very close to the outer loop as indicated in Figure 135. When a vehicle move over the loop system the self inductance's L_1, L_2, ... L_n of the inner loop changes. Number of inner loops (out of 1 to n) that shows a change in inductance depends on the width of the vehicle. Let us assume now that the width of the inner loop is approximately a meter. In such a case, when a small vehicle like bicycle moves over the detector, it will occupy only one of the inner loops and the self inductance of that inner loop alone will change. In the case of a large vehicle like bus that occupies more than one inner loop crosses, the self inductance's of all the corresponding loops will change. The rest of this section discusses how the change in self inductance of inner loop can be observed from the outer loop.
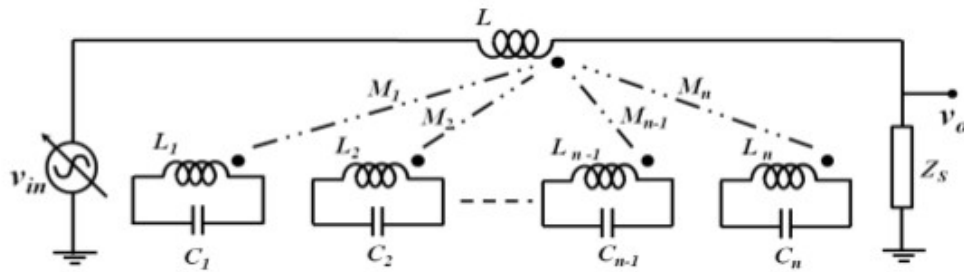

Figure 136: Simplified electrical equivalent circuit of the proposed mutually-coupled inductive loop system

Consider that the outer loop is excited from an AC source V_{arb} and the current flowing through L is observed as a voltage across a resistance R_s connected in series with L. Equivalent circuit of the outer loop L and one of the inner loops is shown in Figure 137(a). For ease of explanation and analysis, a T-network of the same system is given in Figure 137(b). This system will have a parallel resonance at frequency f_{p1}. An AC analysis is performed using SPICE simulation tool LT spice for such a system with parameters L = 130 μH, M_1 = 60 μH and L_1 = 100 μH and the output obtained is given in Figure 138. Figure 138 also shows the voltages obtained for L_1 = 101 μH, 102 μH, 103 μH, etc., while keeping L and M_1 unchanged. It can be seen from Figure 138 that there is a parallel resonance at f_{p1}. Thus, the current flowing through L will be at minimum for f_{p1}. The voltage across C_1 is also shown in Figure 138. This shows a series resonance, say, at f_{s1}. When there is a change in L_1 (whenever there is a vehicle in the vicinity of the loop-1) f_{p1} and f_{s1} will shift. It can be seen that the quality factor is quite good for the parallel resonance. Also, the power drawn by the loop system will be at minimum when in parallel resonance. Due to these facts, it was decided to perform the measurement at the parallel resonance frequency f_{p1}.

Similarly, there will be parallel resonances at f_{p2}, ..., f_{pn} corresponding to each inner loop 2, 3, ..., n. Thus, if we can generate a signal V_{arb} which has the frequency components f_{p1}, f_{p2}, ..., f_{pn} alone, then the power drawn from the source will be minimum. The current flowing through the outer loop measured across R_s (voltage V_0) will contain these frequency components. If one of the inductance's (among L_1, L_2, ... L_n) changes, e.g., L_1, then f_{p1} changes to, say, $f_{0p\,1}$ and hence the magnitude of signal at f_{p1} seen at V_0 will increase. If a vehicle is present above any of the inner loop, the corresponding self inductance and parallel resonance frequency will change resulting in an increase in output voltage V_0 at those frequencies [39]. The details of the scheme to measure amplitude of signal V_0 accurately at all parallel resonance frequencies f_{p1}, f_{p2}, ..., f_{pn} are explained below.
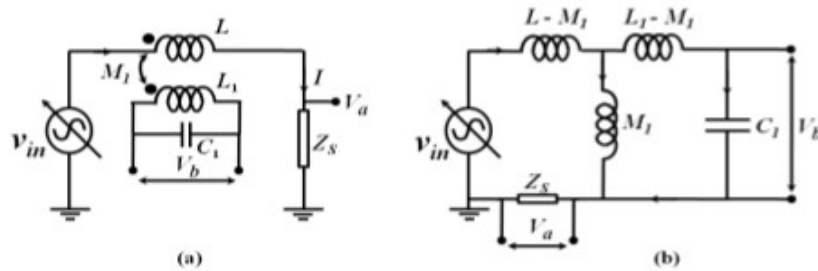

Figure137: (a) Equivalent circuit of the mutually coupled outer loop and an inner loop. (b) A T-Network representation of (a).
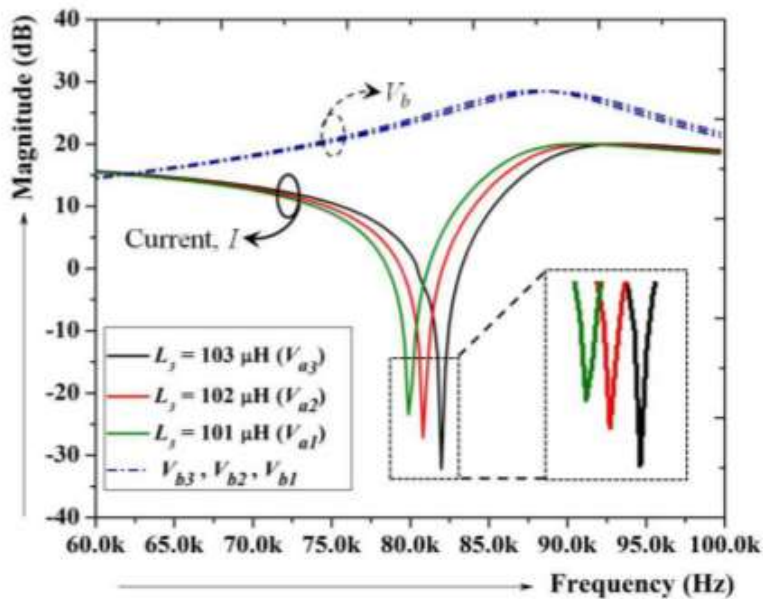

Figure138: Results from the AC analysis performed using SPICE package on the mutually coupled outer loop and inner loop indicated in Figure 111 The parallel

resonance and its shift with respect to change in self inductance are clearly visible

c) Measurement Scheme

The measurement scheme employs synchronous detection method [40]. A functional block diagram of the measurement unit is shown in Figure 139. As discussed in the previous section, the outer loop with self inductance L is excited from an AC source V_{arb}. Consider that the single source V_{arb} contains frequency components at f_{p1}, f_{p2}, ... and f_{pn} i.e,

$$V_{arb} = V_m\left(\sin 2\pi f_{p1}t + \sin 2\pi f_{p2}t +, \ldots.. + \sin 2\pi f_{pm}t\right) \qquad (7.3)$$

As we are using synchronous demodulation, V_{arb} can be a signal that contains all the frequencies starting from f_{p1} to f_{pn} but it is better to keep as in equation (7.3) so that the power consumption will be low. V_{arb} as in equation (7.3) can be realized using various means such as using a programmable arbitrary function generator or a computer controlled Digital to Analog Converter (DAC). The voltage across R_s is converted to digital domain using an Analog to Digital Converter (ADC) and the data is given to a computer where the synchronous demodulation is performed as shown in Figure 139. The reference (V_r) sine and cosine signals, required for synchronous detection, for each frequency f_{p1}, f_{p2}, ... and f_{pn} are generated in the computer. The block diagram for the demodulation of one of the frequency component (say f_{p1}) alone is given in Figure 139. The magnitude and phase of the signal component at f_{p1} can be obtained by this method as indicated in Figure 139. The same is accomplished for other frequencies, from the same ADC output data, by choosing appropriate frequency (f_{p2} to f_{pn}) for the reference sine and cosine waves. When there is a change in self-inductance in an inner loop, as discussed in the previous section due to the presence of a vehicle, the magnitude (V_{01}) and phase (Φ) at the corresponding parallel resonance frequency f_p will change (say from f_p to f_{0p}). This can be observed as a change in the synchronous demodulator output V_0 and Φ. Next section discusses the details of the prototype loop system, experimental set-up and results obtained for various vehicles.
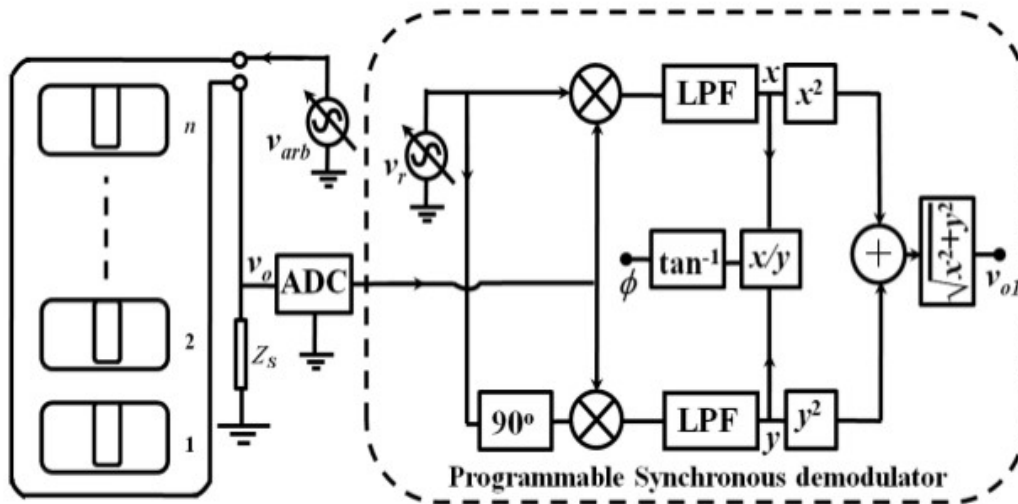
Figure 139: The measurement scheme employed for the magnetically coupled inductive loops. This is a simplified diagram. The outer loop is excited from Varb and the response current is digitized using an ADC. The programmable synchronous demodulator is implemented in a computer in a LabVIEW environment. Vr is a sinusoidal source at fp1. V01 is the output corresponding to magnitude of signal current in the outer loop at fp1. The programmable demodulator unit (with corresponding Vr) is replicated in the LabVIEW for measuring responses for other loops 2, 3, ..., n (all such units uses the same data from the ADC).

d) Experimental Set-up and Results

A prototype of the magnetically coupled inductive loop detector system with identical inner loops and a single outer loop was developed. The outer and inner loops were wound and stitched to a carpet for preliminary tests. Each inner loop has 5 turns and has a self inductance ($L_1 \approx \_L_2 \approx L_3 \approx L_n$) of 100 μH. The outer loop also has 5 turns 47 and self-inductance (L) of 150 μH. The developed prototype system has three inner loops. A capacitor was connected across the terminal of each inner loop. The capacitor values were chosen such that each inner loop has its-own resonance frequency. The capacitor values used were $C_1 = 41nF$, $C_2 = 68nF$, $C_3 = 105nF$ and the parallel resonant frequencies obtained were $f_{p1} = 55$ kHz, $f_{p2} = 64$ kHz and $f_{p3} = 83$ kHz, respectively for inner loops 1, 2 and 3. Few kHz of gap was maintained between the resonance frequencies. This was to reduce the effects due to cross-sensitivity between the inner loops. An arbitrary function generator from Tektronix was programmed to generate the excitation signal V_{arb} which contains the frequencies $f_{p1} = 55$ kHz, $f_{p2} = 64$ kHz and $f_{p3} = 83$ kHz. The output V_0 from the outer loop was acquired using a 16 bit data acquisition system from National instruments (USB 6216) [30] at a sampling rate of 400 kSa/s.

As we explained in subsection 7.1.7, V_0 contains all the individual frequency components of the excitation signal whose magnitudes (at each resonant frequency) are modulated due to the change in the self inductance of corresponding inner loop. The change in the magnitude/phase for each frequency component in the output signal V_0 can be detected using the measurement scheme discussed in the previous section. The programmable synchronous demodulator indicated in Figure 139 was implemented in a Labview environment (virtual instrument) in a computer. This virtual instrument controls the data acquisition and computes the magnitude and phase of the output signal at frequencies f_{p1}, f_{p2} and f_{p3} using synchronous detection method. Then, based on the change in amplitude observed corresponding to individual inner loops (at the synchronous detector output) and the signature due to the variation in output (as a function of time), a suitable threshold based algorithm was used to detect the type of vehicle (classification) and number of the vehicles (count) in each type.

e) Proximity Test

In order to experimentally verify the shift in the parallel resonance frequency in the presence of a conductive/metallic object, the following test was conducted. The frequency of the input excitation to the outer loop of the prototype varied from 40 kHz to100 kHz with a step size of 100 Hz and recorded the magnitude of the output voltage V_0. The test was conducted for two cases, (a) vacant condition and (b) after placing a metallic object of dimensions 90 cm x 40 cm and a thickness of 1.5 mm at a height of 20 cm from the plane of the loop. The object was kept above loop number 2. The magnitude response was recorded for both the cases (a) and (b). It was observed that the resonant frequency f_{p2} alone shifted from 65 kHz to 67 kHz in the presence of a metallic object. This data is given in Figure 140. The test with metallic object was repeated by keeping the object at a height of 10 cm, from the plane of the loop, and observed that the resonant frequency shifted from 65 kHz to 69 kHz. Thus, we clearly observed a shift in the resonant frequency when a metallic object was placed above one of the inductive loops (inner loop-2 in this test case). We observed no change in resonant frequencies for the inner loops where no metallic objects were present. These observations show that we can detect metallic object or vehicle moving above the magnetically coupled inductive loop and identify how many loops are covered by a vehicle.
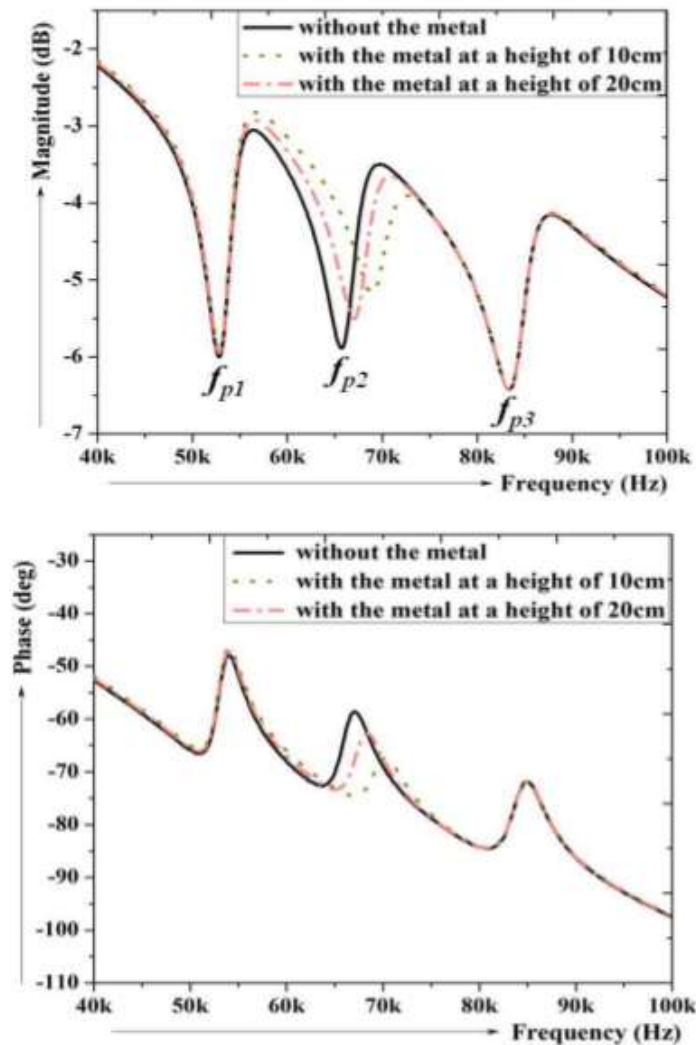
Figure 140: The (a) magnitude and (b) phase plots of the prototype loop detector with and without the presence of a metallic object above inner loop-2. The test was repeated by keeping the object at two different heights. A shift in the 2nd parallel resonance frequency (fp2) is visible. Other parallel resonance frequencies did not change as no metallic object was present above those inner loops.

f) Field Test with Three Inner Loops

After the proximity test, the developed system was installed in a roadway and recorded the output for various types of vehicles such as bus, motor cycle, car, bicycle, etc. A snap-shot of the experimental set-up is shown in Figure 141. As soon as it was installed, the system was calibrated by sweeping the excitation frequency from

40 kHz to 100 kHz with a step size of 100 Hz and detected all parallel resonance frequencies. A signal (which consists of all these frequencies) was then generated using an arbitrary function generator and excited (V_{arb}) the outer loop. This process can be done in a periodical way to calibrate the system for best performance. After the calibration, output signal was recorded for few hours. Figure 142 shows recorded output data observed for a bus. The bus covers all the three inner loops and the resulting change in output can be observed for each corresponding resonant frequency. The wheels of the bus went over loops-1 and 3 while the middle portion was above loop-2. Recorded data from the system for a typical car is shown in Figure 143. If we compare the signatures obtained for a bus and a car, it can be seen that both the vehicles cover three loops but the signatures (shapes) are easily distinguishable. Two spikes that can be seen in the waveforms in Figure 142 are due to the front and rear axles/wheels of the bus and these reading are highly repeatable. The signatures are similar to the ones we observed in the previous schemes. The chassis and body of a car is more continuous than a chassis and body of a bus seen from bottom as far as the metallic parts seen by the loops are concerned. Also, the chassis of car is more close to the plane of the loop system compared to that of a bus. This is the reason for a smooth change in output for a car as in Figure 143. Figure 144 shows the output recorded when there was a parallel movement of various types of vehicles such as bicycle, motorcycle, scooter, etc. During the test, the prototype system accurately detected all the vehicles that passed above the loop system.
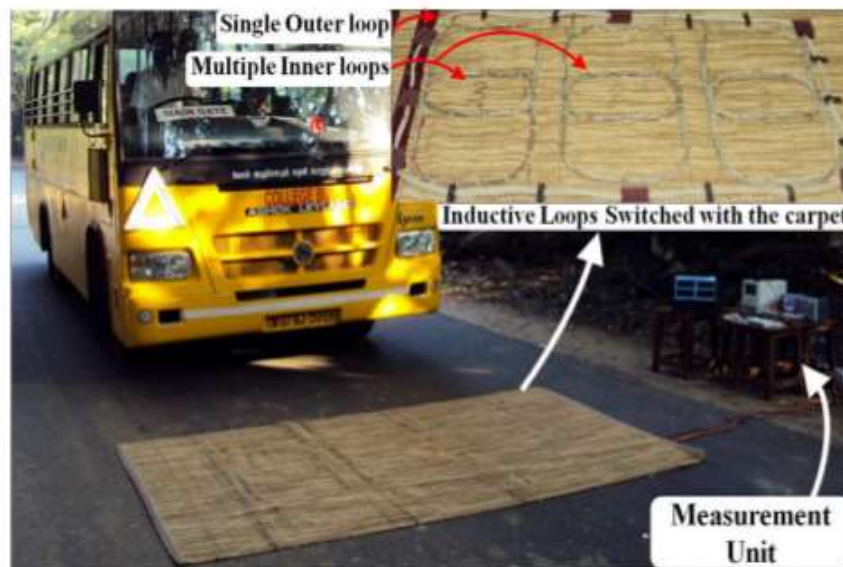

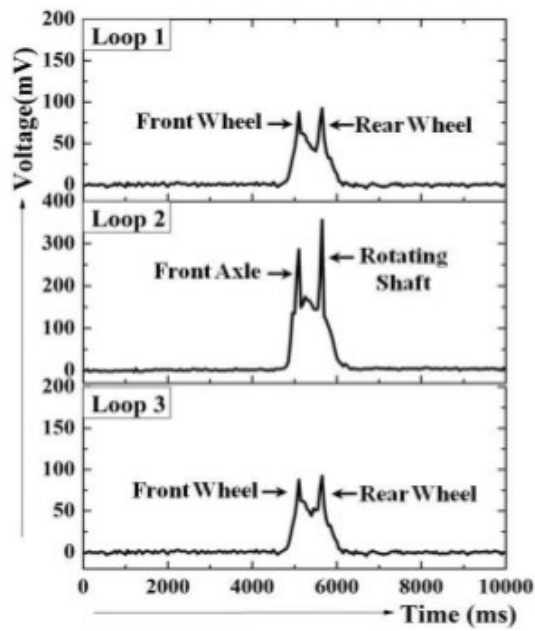**Figure 141**: A photograph of the experimental set up (first stage).

Figure 142: Output signal (signature) observed for a bus from the magnetically coupled inductive loop vehicle detector.
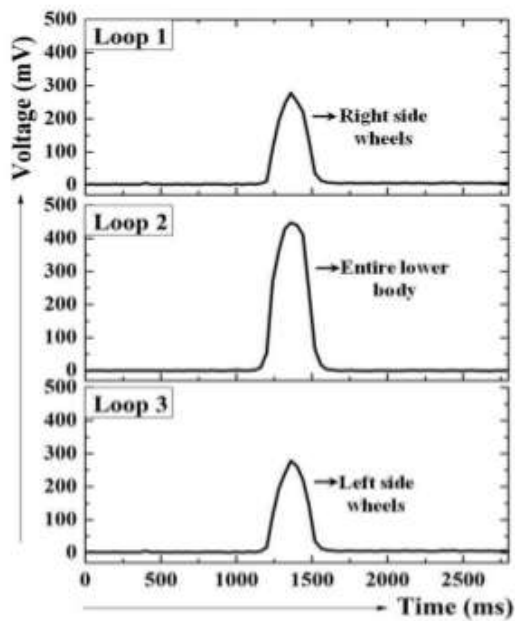

Figure 143: Output observed from the developed detector system for a typical car.
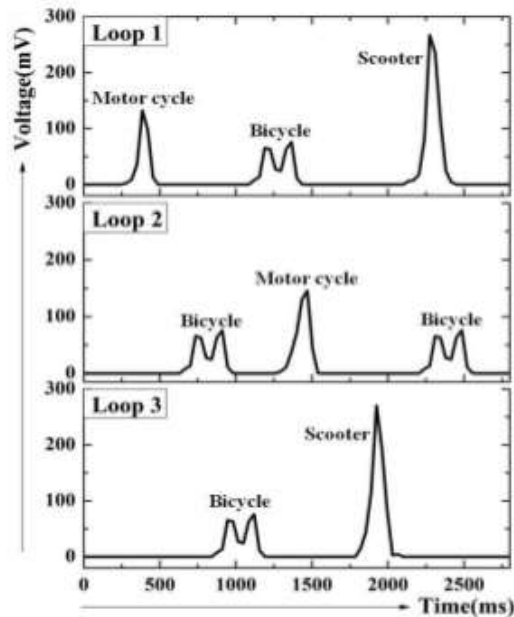
Figure 144: Output data recorded (from all the 3 loops simultaneously) when there was a parallel movements of vehicles.

g) Additional Information from the Outer Loop

In the experimental results discussed above, the multiple inner loops inside the single outer loop were in resonance but not the outer loop. This sub-section discusses the possibility of using the outer loop as an additional sensing element. This has been tested experimentally. In order to do this, the outer loop was resonated by connecting a capacitor $C_{OL} = 47$ nF across the outer loop, which has an inductance of 150 μH. The resonant frequency was 57 kHz. The excitation was also modified to include a frequency component at the resonance frequency of outer loop. Figure 145 shows the results obtained in this condition, when a bus passed through the sensing system. Figure 146 shows the signatures obtained for a car. It can be observed from Figure 147 that the outer loop is not very sensitive to small vehicles as expected. The outer loop provided unique signatures for each large vehicle like car, bus, etc. and gave negligible output for small vehicles like motor cycle, bicycle, etc. Thus, this additional information from the outer loop, along with output from the multiple inner loops, will improve the classification accuracy.

h) Extended Prototype with Six Inner Loops and a Comparative Study with Conventional ILD

The prototype with three inner loops covers only one lane and more inner loops are required to cover the full road width. Three additional inner loops and an outer loop (for the new inner loops) were constructed to cover the entire road width, where we conducted the field tests. As mentioned in subsection 7.1.7 (g), measurements corresponding to each outer loop (in this case it is named as outer loop-A and B) is

also recorded. Figure 148 shows a snap-shot of the new experimental set-up. Similar tests as in subsection 7.1.7 (f) were conducted with this set-up to verify its functionality. The signatures were identical to the one showed in Figure 145, Figure 146 and Figure 147 for same type of vehicles. Figure 148 shows the signatures obtained for continuous movement of various vehicles over the extended prototype. Inner loops 1 to 3 are inside outer loop-A while loops 4 to 6 are inside outer loop-B. Results from the outer loops are also shown in Figure 149 (in the first and last rows). From Figure 149, it can be seen that even if a portion of bus goes through set-A and rest of the portion in set-B, the signatures remain identical to that obtained by a 3 loop system described in previous subsection.
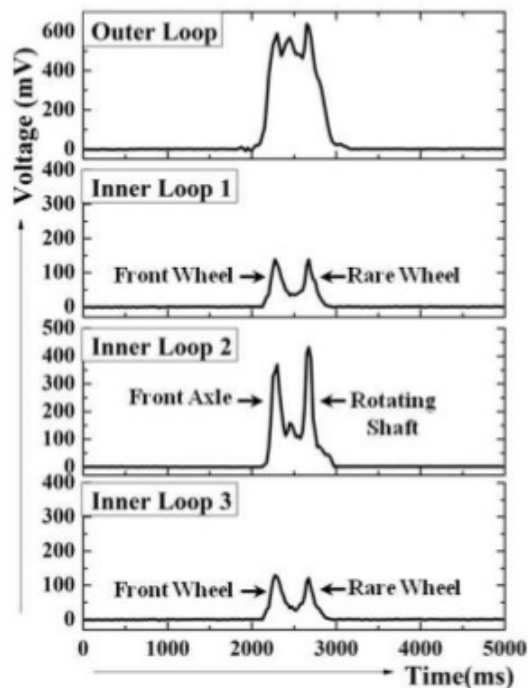
Figure 145: The output observed (for a bus) from the developed detector system when outer loop was also used as a detector element along with multiple inner loops
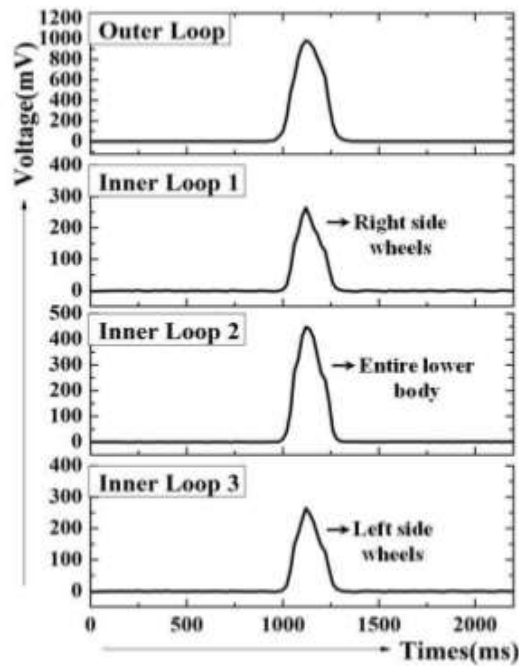
Figure 146: The output observed for a car from the outer as well as inner loops.
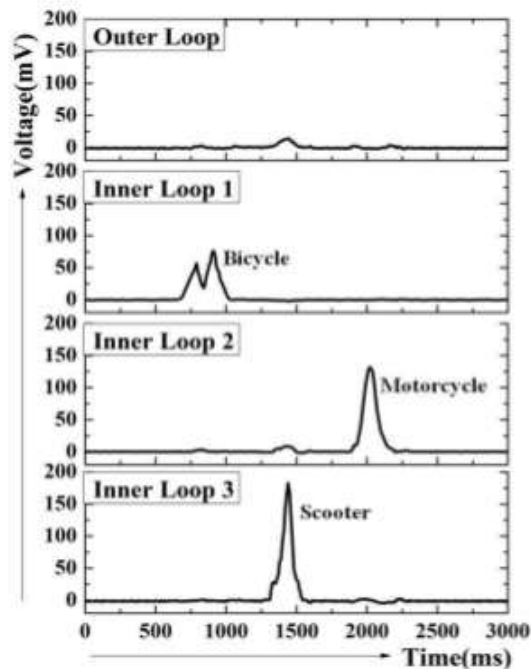
Figure 147: The output observed for small vehicles like motor cycle, bicycle and scooter from the outer as well as inner loops. Signatures observed in the outer loop for these vehicles have negligible amplitude.

Figure 148: Shows the snap-shot of the detector system covering the entire road width. The Inductive Loop Detectors (ILD) stitched to a carpet is shown in inset picture.

Figure 149: Shows the signatures obtained during continuous movement of various types of vehicles from a multiple loop system with six inner loops. Results from the outer loops are also recorded and shown.

The performance of the new system was also compared with the conventional Loop Detector (CLD) having dimension 6ft x 4ft. Figure 150 shows a snap shot of the experimental set-up. As in Figure 150, the standard inductiv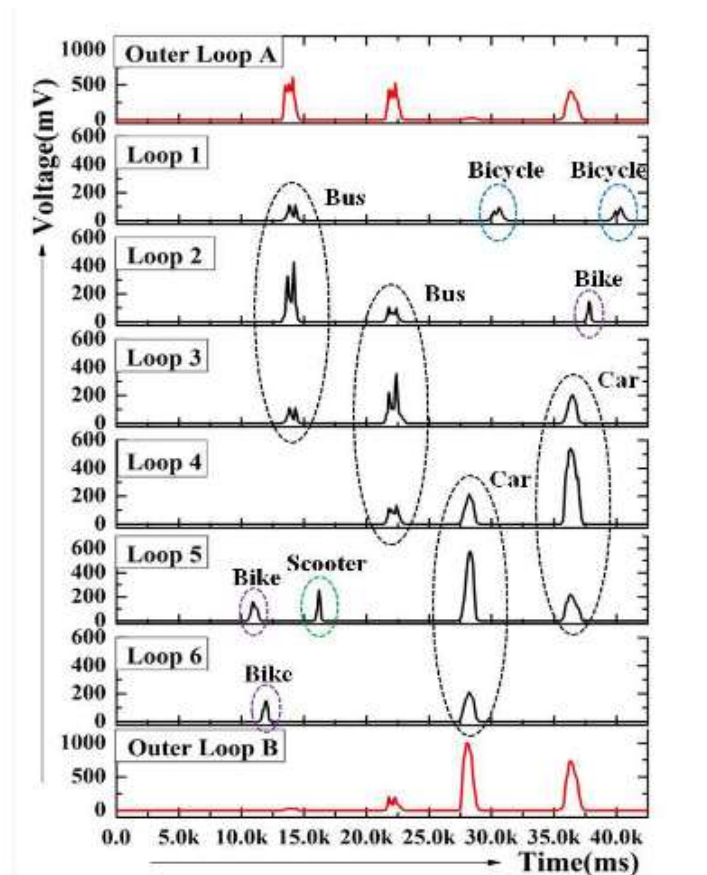e loop and mutually coupled multiple inductive loop were installed in the same roadway. Both the systems were separated by a gap of 1 m. Outputs from both were recorded simultaneously. Table 36 shows the field test results recorded for about two hours. During the test, the multiple inductive loop detectors correctly detected 96.63% of bicycles, 98.18% of motorcycles and 100% of scooters, cars and buses passed through the test area. The overall detection accuracy was 98.54%. The conventional loop detected only 2.52% of bicycles, 9.09% of motorcycles and 34.14% of scooters and the accuracy of detection of cars and buses were 73.5% and 71.6 % respectively, leading to an overall detection accuracy of 30%in a heterogeneous traffic. It can be observed that accuracy of detection of medium and large vehicles are also low for conventional loops, especially when there is parallel movement of vehicles.

Figure 150: Shows the experimental set-up of the comparative study of inductive loop detectors.

Table 36: Shows the field test results performed to compare performances of multiple loop detector (MLD) and conventional loop detector (CLD) in a heterogeneous traffic

Vehicle classes	Actual number	Count from MLD	Count from CLD	%Accuracy of MLD	% Accuracy of CLD
Bicycle (A)	119	115	3	96.63	2.52
Motorcycle (B)	165	162	15	98.19	9.09
Scooter (C)	41	41	14	100	34.14
Car (D)	83	83	61	100	73.49
Bus (E)	74	74	53	100	71.62
Total	482	475	146	98.54	30.29

CLD - Conventional Loop Detector
MLD - Multiple Loop Detector

7.1.8 Travel Direction and New Loop Configuration

The loop system presented above cannot detect travel direction as in a conventional (no-dual loop) loop detector. A modified configuration of the mutually coupled multiple loop system is proposed to solve this problem (similar to conventional dual loop system). The new system not only gives unique signatures as in the above discussed scheme but also provides direction of movement of vehicles. This can be used where direction information is necessary. Figure 151 shows the new configuration of the loops. It uses six identical loops (special loop as in Figure 135 right side) and a large loop in the middle as illustrated in Figure 151. All the six small loops are magnetically coupled to the main large loop. For ease of explanation, we group loops L_1, L_2 and L_3 into set-1 and L_4, L_5 and L_6 into set-2. Loops are made to resonate as in the previous configuration and an excitation pattern having frequency components at every resonant point of the system is generated and loaded in the function generator.
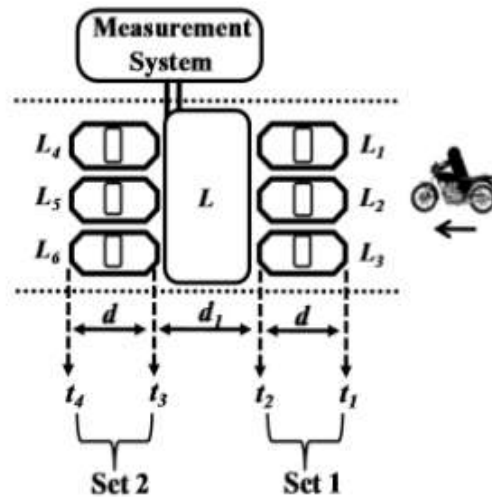
Figure 151: A new configuration of the loop system. The direction of movement of vehicle can be sensed and its speed can be measured with this scheme.

Measurements were taken from the middle large loop. The principle of measurement employed was same as the one illustrated in Figure 139. A photograph of the prototype unit developed is shown in Figure 152. Results obtained from the new system for a bus is shown in Figure 153. As can be seen, loops in set-1 and that in set-2 detected the vehicles correctly. Both the sets provide almost identical signatures. It

is clear that, for the case shown in Figure 153, the bus entered into set-1 first and set-2 later. Thus, from this information, direction of movement of the vehicle can be easily detected.

Figure 152: Photographs of the experimental set-up (left) and the new configuration of the loop system stitched to the carpet (right).

7.1.9 Measurement of Speed and Occupancy with the New Loop Configuration

The new setup can be used for finding speed and occupancy, which are two important traffic parameters. Occupancy is usually expressed as the ratio of time during which a facility is cumulatively occupied to the total observation time. As shown in Figure 152, set-1 and set-2 can be kept at a known distance of 'd_1' and length of each set be 'd'. In the prototype, $d = d_1 = 80$ cm. All the vehicles will be detected twice by the system as in Figure 153. The time t_x between the beginnings of signatures from set-1 and set-2 can be measured as indicated in Figure 154, from which occupancy can be obtained. The speed, S, can be computed using $S = (d+d_1)/t_x$. For this measurement, it is assumed that the vehicles move at a constant speed when it is crossing the distance of $(d + d_1)$ above the loop system.
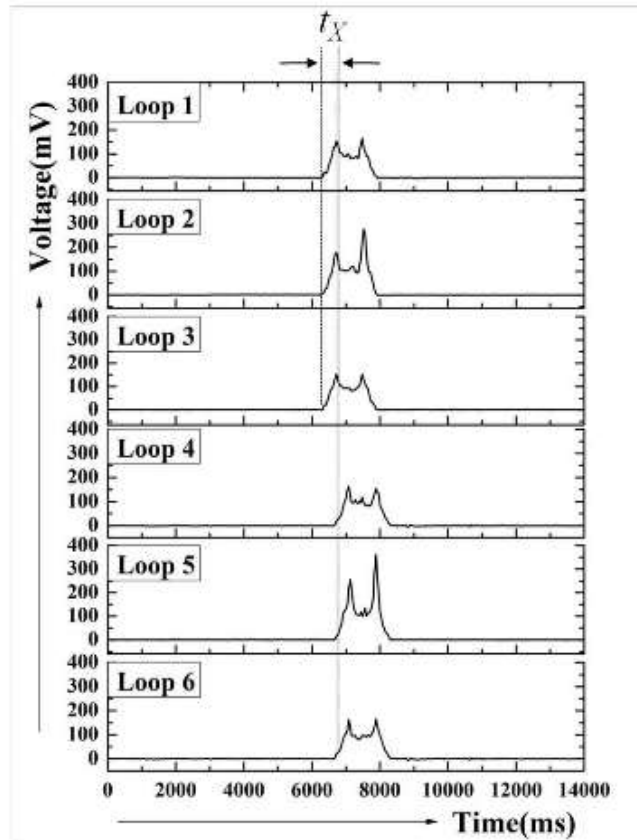
Figure 153: Shows the signature of bus moving from right to left. This is recorded from the set-up shown in Figure 151 and Figure 152. As can be seen the direction of movement can be clearly detected. tX is the time taken by the bus to travel a distance of (d + d1) as indicated in Figure 152.

Figure 154 shows the signatures of a bicycle and motor cycle moving at various speeds. The time tx for each case is indicated in Table 37. Speed measurement, using the loop, was performed for a bicycle, motor cycle and a car. The results were compared with the simultaneous readings from a Laser gun (from TruCAM [38]) and provided in a tabular form in Table 38. As can be seen from Table 38, the scheme can provide speed of the vehicle detected quite accurately.

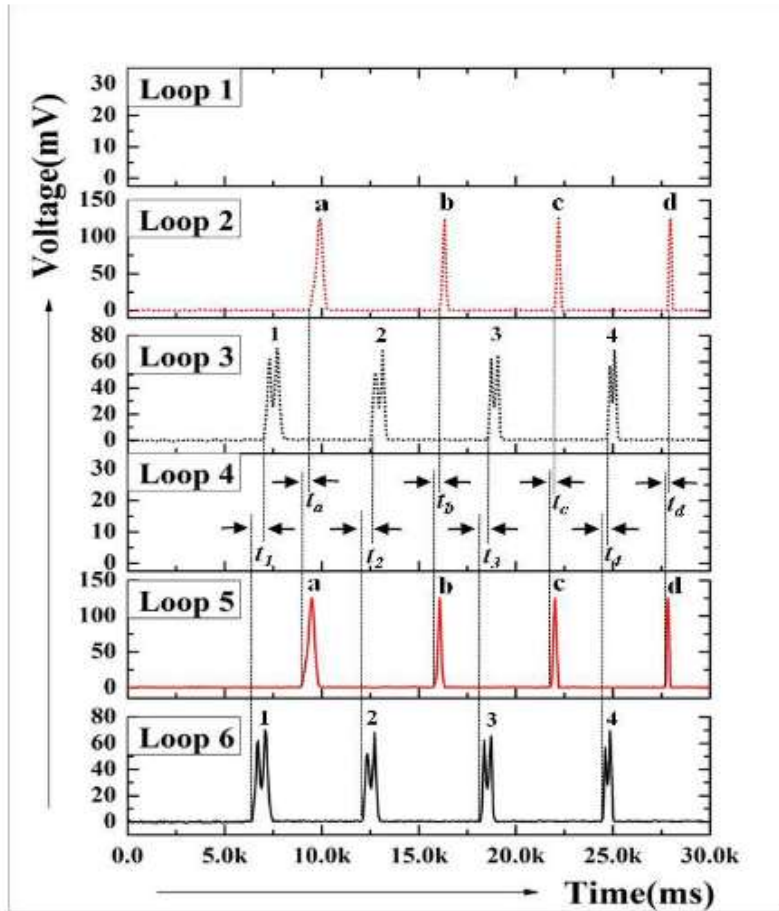**Figure 154**: Shows the signatures of a bicycle and a motor cycle from the dual set of loops shown in Figure 151. Both vehicles are moving from left to right. As can be seen the direction of movement and speed can be detected. These vehicles are moving at different speeds (shown ascending order in the figure, i.e., 4 is the fastest and 1 is the slowest, similarly, vehicle 'd' is the fastest and 'a' is the slowest) and corresponding tX is marked. The values of tX for each case is given in Table 47

Based on these results we can conclude that the mutually coupled inductive loop system can be used for modifying the existing single loop detector system that is suitable for homogeneous and lane based traffic to a multiple loop detector system suitable for heterogeneous and lane less traffic. Additionally the new schematic also helps in finding the travel direction, occupancy and speed of the vehicles. Next chapter presents the possible algorithm for automation of the detection, classification and counting process.

Table 37: Values of tX for each case in Figure 154

Vehicle	time, tx (ms)			
Bicycle	t1=594.03	t2=474	t3=354.02	t4=269.96
Motorcycle	ta=474.02	tb=240.01	tc=174.01	td=114.01

Table 38: Speed measured for various vehicles with the new configuration of coupled loops

Vehicle	Speed measured(km/hr)		% Error
	LG	DSIL	DSIL
Bicycle	10	9.89	1.09
	13	12.39	3.7
	16	15.59	3
	22	21.34	2.4
MotorCycle	13	12.76	1.9
	25	25.19	1.8
	38	37.73	2.3
	47	46.98	0.03
Car	13	12.76	3.9
	25	25.19	3.5
	38	37.73	3.6
	47	46.98	2.1
LG - Laser Gun (give reference measurement)			
DSIL - Dual set of Inductive Loop as in Figure 151			

7.1.10 Automation of Classification Algorithm

a) Introduction

This chapter describes the vehicle classification algorithms for the multiple inductive loop detector (MILD), developed for heterogeneous and lane less traffic. Various classification algorithms have been reported for conventional single and dual loop systems for lane based traffic [41] - [48]. The classifications were based on parameters like length of vehicle, signature, etc. Algorithms were also developed based on trapezium method [41], signal pattern matching [42], [43], self organizing feature map [44], data fusion [45], back propagation neural network [46], [47], discrete Fourier transform and principal component analysis [48]. The classification algorithm employed in this study, uses number of loops a vehicle occupies, the magnitude employed and the shape of the signature to classify vehicles. Details of the method and comparison of results with other methods are explained in the sections below.

b) Algorithm for Vehicle Classification

The multiple inductive loop system developed uses many small loops of identical structure. The inductive loop and the associated signal conditioning circuit is designed in such a way that there will be change in inductance and hence output, only in those loops where the vehicle is present. Figure 155 shows typical signatures obtained for various vehicles from a prototype system developed. Figure 156 shows the snap shot of the experimental setup used to conduct field measurements with a

prototype system developed. This has six inductive loop detectors stitched to a carpet and covering the entire road width. Algorithms can utilize output parameters such as amplitude, shape of the signal and number of loops a vehicle occupies to classify the vehicles as discussed below.
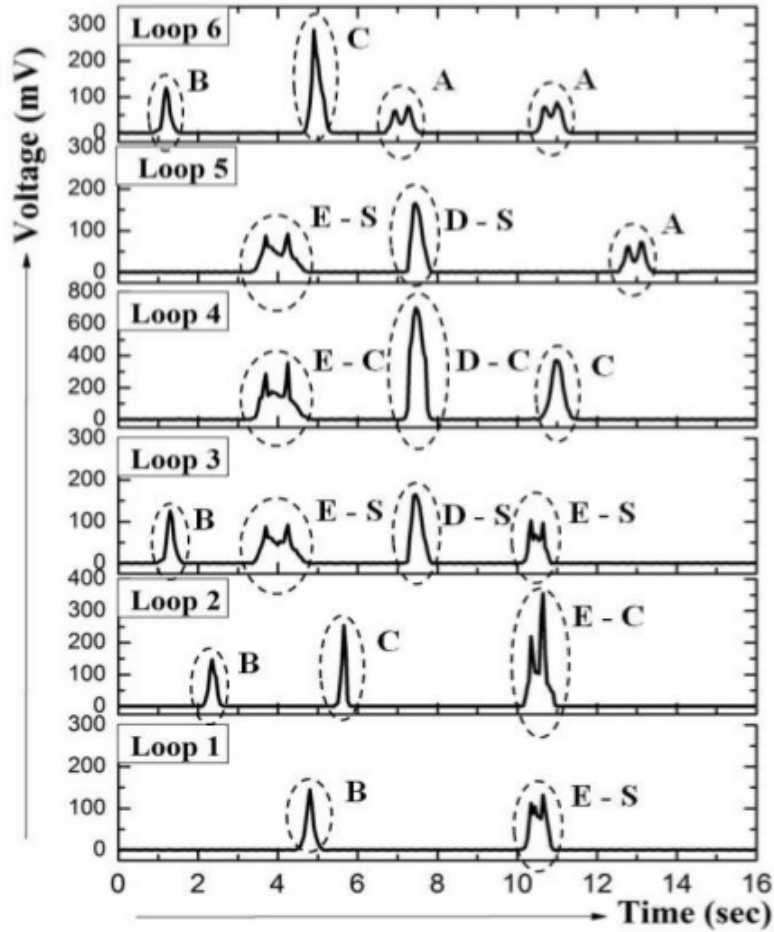

Figure 155: Signature of different classes of vehicles for a particular interval of time. (A) bicycle, (B) motorcycle, (C) scooter, (D-S) car seen by the side loops and (D-C) car middle loop, (E-S) bus detected by the side loops and (E-C) bus middle loop.

Figure 156: Experimental setup used for conducting field studies with six inductive loops stitched to a carpet.

c) Threshold based Algorithm

This algorithm uses various preset threshold levels for detection and classification of vehicles. From the experimental results, the peak of the signature for the smallest vehicle (bicycle) was identified. Averages of this peak $V_{P(BY\ C)}$ from signatures of 20 similar bicycles were taken and 10 percent of this value ($V_{P(BY\ C)}$) is set as the threshold value for the output for all the loops. If output for any loop crosses this value, we know that it is covered by a vehicle. If the peak of this output is within 80 % to 120 % of $V_{P(BY\ C)}$, then it is considered as a bicycle. Similarly, the highest peak for the car was identified. The loop that sees the middle portion of the car gives this value. Again, average of peaks of 20 vehicles was computed from experimental studies. If signal from any loop is between 80 % and 120 % of this set value it is classified as a car. It is again supported by the fact that two side loops will also cross minimum thresholds at the same time. Similarly, a bus will also occupy three loops. Peak values for middle and side loops were computed from experimental data and used later for classification. Other vehicles were also detected and classified based on similar approach.
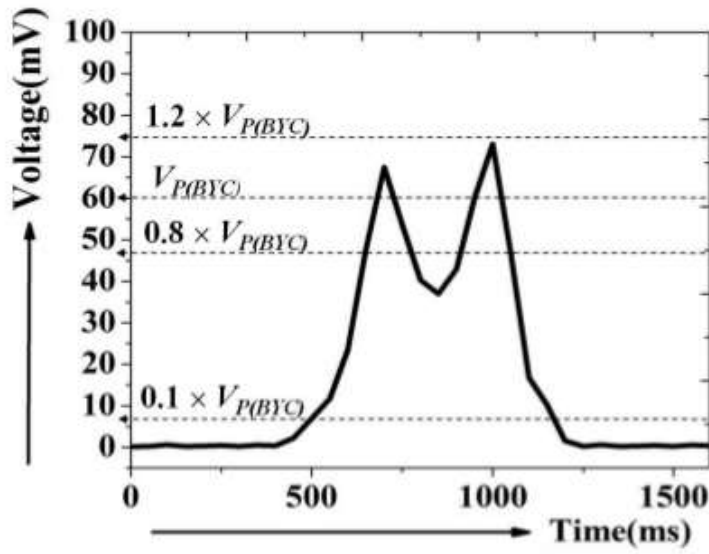
Figure 157: Signature of a bicycle obtained from a single loop

d) Signature based Algorithm

In this method, a threshold is assigned for each of the loop as in the previous method. Whenever a signal goes above a predefined threshold, the data is captured. Here, to classify vehicles using signatures, the numbers of peaks in the signature within the data length captured when it was above the minimum threshold were considered. For a bicycle it produces two peaks from a single loop as shown in Figure 157 and for a bus it produces two peaks from three loops it occupy. The two wheelers produce a single peak and in the case of a car, it gives one peak per loop, for three loops. An experimental study was conducted to validate these techniques (Threshold based and signature based algorithms) and concluded that a machine learning based approach may give higher accuracy for classification, and is detailed below.

e) Random Forest Method

A large number of machine learning methods are available to perform the classification task, such as nearest neighbor classifier, artificial neural networks, support vector machine, and decision tree classifiers. In this study, it was decided to experiment with randomized decision tree classifiers or random forest due to their simplicity of use and ability to provide an insight into how the classification is being performed. Decision tree classifiers divide one large complex question into a series of simple sequential questions, hence forming a hierarchy of questions like in the tree used in computer science. This is illustrated in Figure 158. A node can be seen as a 'question' which has two possible answers, viz. yes or no and hence the name 'binary tree'. In the training phase, a tree is 'grown' using manually labeled training data and with the help of machine learning techniques [49]. In the testing phase, test data is passed through the decision tree by 'answering questions' at each node until it

reaches the bottom-most node. The label decided in the training phase for that particular bottom-most node is assigned to the test data, thus accomplishing the classification task.

Random forest is a collection of many decision trees. Each training data example has number of properties associated with it, called features. In the conventional single decision tree classifier, a node is created by defining the associated 'question' about all the available features, e.g. the question could be whether the features are above certain threshold.
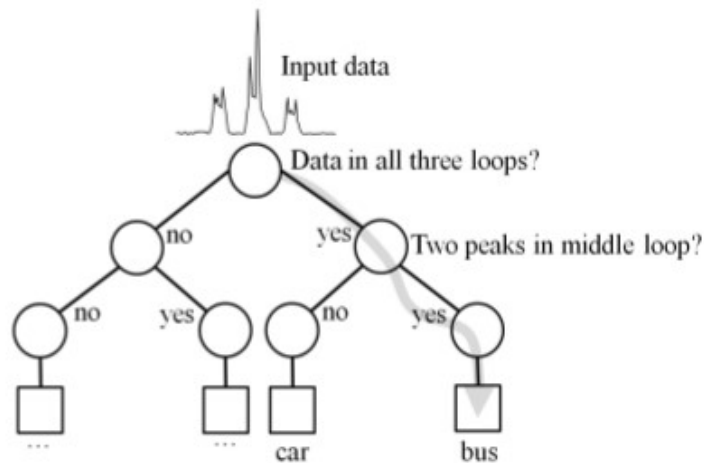

Figure 158: Visual illustration of the concept of binary decision tree.

While creating a node, only a fraction of randomly chosen features are used among the available features and hence the name 'random forest' [50]. In order to obtain good classification accuracy, low bias and low correlation between the constituent trees are essential. To get low bias, trees are grown to maximum depth. To get low correlation, randomisation, by selecting random subset features to split a node and of training samples to build a tree, is applied [51]. In this study an available implementation scheme of the random forest classifier with default parameter settings is used [52].

7.1.11 Experimental Results

a) Threshold based algorithm
An experiment was conducted using the prototype developed and collected signatures for various vehicles passed over the loop system. Data collected for a duration of about 2 hours were processed using threshold based algorithm. The results are given in Table 39. It can be seen from Table 39 that compared to the two

wheelers, the four wheelers were classified with a lower accuracy. The total system accuracy was found to be 88.17 % and this varies by +/- 4%. Figure 159 shows the virtual instrument developed using LabVIEW to identify, count and classify different classes of vehicles using threshold based algorithm.
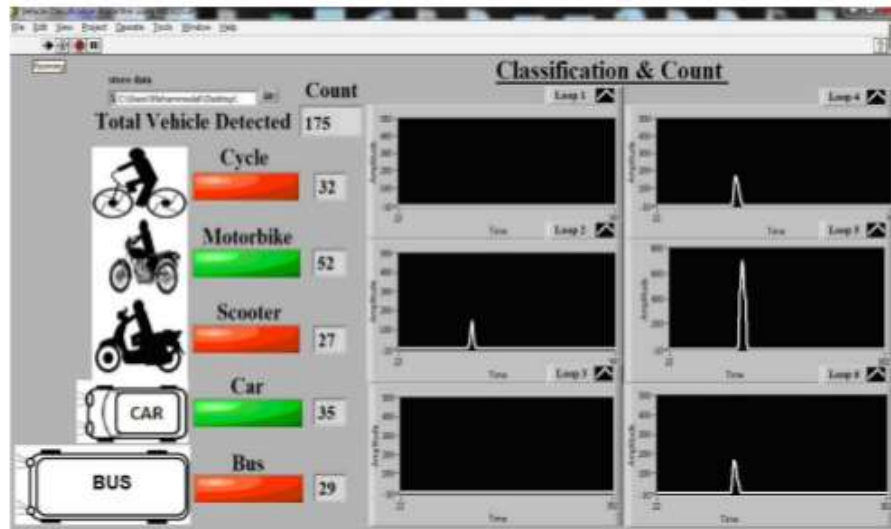
Figure 159: The virtual instrument developed using Labview, to detect, classify and count different classes of vehicles.

Table 39: Results from the threshold based Algorithm

Vehicle classes	Actual number	Count from detector	% Accuracy
Motorized and non motorized two wheelers	240	223	92.9
Car	56	44	78.57
Bus	76	61	80.26
Total	372	328	88.17

b) Signature based Algorithm
When the same data, employed for threshold based algorithm, was tested with signature based algorithm, the accuracy increased to 98 % for motorcycle and scooter, 94 % for car. The accuracy was low for bicycle and bus. Next section discusses the results of RFM.

c) Random Forest Method

The signatures of vehicles from the field study were captured and re-sampled to twenty data points, to capture all the morphological features present in the signature. For each vehicle class, ten signatures were taken for training. Random Forests grows many classification trees. To classify a new object from an input vector, put the input vector down each of the trees in the forest. Each tree gives a classification, and we say the tree 67 "votes" for that class. The forest chooses the classification having the most votes (over all the trees in the forest) [53]. The number of trees used was 100, which is the default setting. The classification, using the RF method, was carried-out in two stages. In the first stage, vehicles were classified within two wheelers and four wheelers. Bicycle (A), motorcycle (B) and scooter (C) data were tested simultaneously using the diagram. As the two wheelers occupy only one of the loops, 20 data points (for each vehicle) were available for analysis.

Table 40 shows the results obtained for the two wheelers tested. Out of the 62 bicycles (A), 60 were counted as (A) and 2 were counted as (B). Out of the 128 motorcycles (B) counted manually, all 128 were counted as (B). Out of the 50 scooters (C) tested, 49 were counted as (C) and 01 was counted as (B). The accuracy in percentage (P) was calculated for each case and were found to be P(A) = 96.7%, P(B) = 100% and P(C) = 98%. Car (D) and bus (E) occupies three loops simultaneously, and hence had sixty data points for analysis. Table 41 shows the performance matrix obtained for the four wheelers tested. Out of the 56 cars (D) tested, all 56 were counted as (D) and out of the 76 buses (E) tested, 76 were counted as (E), giving an accuracy percentage of 100% for (D) and (E).

Table 40: Performance matrix for two wheelers

	A	B	C
A	60	2	-
B	-	128	-
C	-	1	49

Table 41: Performance matrix for four wheelers

	D	E
D	56	-
E	-	76

In the second stage, the data points from each loop were considered separately leading to seven different classes. This is due to the fact that in the case of four wheelers, which occupy multiple loops (three loops) at an instant of time, the signature from the side loops were symmetric and hence treated as one class and the signature of the middle loop as a separate class. Table 42 shows the performance matrix developed using random forest method for the above scenario. The columns of this table represent the class labels and the rows represent classifier label. Table 43

shows the percentage accuracy of classification of the vehicles. As expected, the classification accuracy among the two wheelers was high compared to four wheelers with bicycle (A), motorcycle (B) and scooter (C) giving an accuracy of 96.77 %, 99.2 %, 98 % respectively. D-S and E-S represents the side loops of the car and bus, which has an accuracy of 80.35 % and 96.7 %. (D-C) and (E-C) represents the middle loops of the car and bus which as an accuracy of 100% for both. From the table we can see that 12.5 % of the (D-S) is getting confused with B, 7 % of (D-S) is confused with (D-C), 1.9 % and 1.3 % of (E-S) is confused with (A) and (B) respectively. Since the middle loop of car (D-C) and bus (E-C) have a higher accuracy, the side loops are discarded, but still it is considered as a separate classifier label since we will not know beforehand which of the loops will be of side loops and hence the classification accuracy of car and bus was 100%.

Table 42: Performance matrix for each of the single loop

	A	B	C	D-S	D-C	E-S	E-C
A	**60**	2	-	-	-	-	-
B	-	**127**	-	-	-	1	-
C	-	-	**49**	-	-	-	1
D-S	-	14	-	90	8	-	-
D-C	-	-	-	-	**56**	-	-
E-S	3	2	-	-	-	147	-
E-C	-	-	-	-	-	-	**76**

Table 43: Accuracy percentage of vehicles

Vehicle classes	Actual number	Count from detector	% Accuracy
Bicycle(A)	62	60	96.7
Motorcycle(B)	128	127	99.2
Scooter(C)	50	49	98
Car(D)	56	56	100
Bus(E)	76	76	100
Total	372	368	98.9

From Table 43 it can be seen that the total accuracy percentage for the RF based multiple inductive loop vehicle classification algorithm is around 99%, which is quite good even in comparison with classification accuracy levels for a homogeneous traffic.

CHAPTER 8
QUALITATIVE EVALUATION OF SENSORS

8.0. Introduction

This project is aimed at evaluating the qualitative and quantitative performance of various traffic detection systems under heterogeneous traffic conditions. Sensors were evaluated in a variety of traffic and environmental conditions. Emphasis was placed on urban traffic conditions. These traffic detectors/sensors were deployed in the field and comparison was done with the actual data. The following sections discuss the qualitative evaluations and comparative study of these different data collection devices under heterogeneous traffic conditions. In addition to accuracy, these techniques must be cost effective and field implementable for them to be installed on a wider network in India. The following section discusses such a qualitative comparison of these sensors namely TIRTL (The Infrared Traffic Logger),Traficam Collect-R, Wavetronix Smart Sensor, GRIDSMART and Trazer.

8.1. Qualitative analysis

Table 44 shows the cost analysis of the five detection systems studied.

Table 44: Cost comparison of the detectors

Instrument	Traficon (Hardware +software)	Tirtl (Hardware +software)	Trazer (Only software)	Wavetronics (Hardware and software)	Gridsmart (Camera + Processor)
Detector Cost	Less than 2 lakhs	Above 10 lakhs	5-10 lakhs	4-5 lakhs	4-5 lakhs

Table 45 compares the five devices in terms of their ability for counting vehicles, detecting vehicle speed, occupancy, headway gap and classification, the number of lanes that can be detected, night time function and the effect of climatic conditions on sensor's performance.

Table 45: Comparison of detector characteristics

Traffic Parameter	Instrument: Traficam Collect-R	Instrument: TIRTL	Instrument: Wavetronix	Software: Trazer	Software: GRIDSMART
Count	√	√	√	√	√
Vehicle Speed	√	√	√	√	√
Occupancy	√	√	√	√	
Headway gap	√	√	√		
Classified data	√ (classify upto **three** classes based on the **length** of the vehicle)	√ (classification based on data base of inter axle distances)	√ (classify upto **four** classes based on the **length** of the vehicle)	√ (TW, Auto, LMV and HMV)	√ (Gives the **length** of the vehicle)
No: of lanes	4	18(9+9)	10 (5 + 5)	3	Intersection
Night time performance	X	√	√	X	X
Effect of Climatic conditions	Reduced accuracy during rain and cloudy conditions	No visible effect	No visible effect	Reduced accuracy during rain and cloudy conditions	Reduced accuracy during rain and cloudy conditions

8.2. Memory Backup Storage

Table 46 lists the backup memory capacity of the five detectors

Table 46: Comparison of backup storage memory

Instrument	Trafficam Collect R	TIRTL	Wavetronix	Trazer	Gridsmart
Backup memory	2 weeks data including vehicle classification at an integration interval of 5 min	1 GB	20 sec to 17 days/1 hour interval 20months	Depending on the processor memory backup	36 GB

8.3. Nature of Process

All five perform under both online and offline conditions.

8.4. Power Consumption/Communication

Table 47 lists the details of power consumption and remote data communication of the various detectors considered.

Table 47: Comparison of power and communication requirements of the devices

Communication	Trafficam Collect R	TIRTL	Wavetronix	Trazer	Gridsmart
Power and Consumption	+5V dc (600mA) to +26V dc (200mA)	0.64-2.5W @10-16V DC	9-28VDC	230VAC	230VAC
Communication Modem	External Modem RS 232 or USB cable	Internal modem RS-232C or RS485	External modem RS-232 or RS485	High bandwidth video communication	External Modem (RS 485)
Communication Service	Ordinary SIM with data plan	Static IP SIM	Ordinary SIM with data plan		Regular data SIM, high speed connection required, if video transfer

8.5. Other features of the five detectors

Table 48 compares the efficiency of the five detector system based on the initial results under heterogeneous traffic conditions.

Table 48: Comparison of efficiency of the detection systems evaluated in this project

Systems	Count	Classification	Speed	Comments
Collect R	🔴	🔴	🔴	
TIRTL	🟢	🟢	🟢	
Wavetronix	🟡	🔴	🟡	
Trazer	🟡	🟡	🔴	
Gridsmart	🔴			

Rating: 🟢 Excellent, 🟡 Very Good, 🔴 Good

Table 49 compares the difficulty in the installation of the five devices.

Table 49: Comparison of difficulty in installation of the devices

Systems	Difficulty in Installation	Assistance from company/ Ease of debugging errors	Ease of data extraction	Comments
Traffic Collect R	Medium	🟡	🟡	Lane based sensor. Camera should cover all lanes for a 20 m distance
TIRTL	Medium to difficult	🟢	🟡	TIRTL beam level should be at 100 - 200 mm from the lowest point (wheel base height of vehicles) and should be greater than 50 mm from the highest point on the roadway (to avoid obstruction of beam). These requirements lead to TIRTL having poor

				performance or not usable in locations with high camber. Will not communicate if there is median or any obstruction between the edges.
Wavetronix	Medium	🔴	🟠	The devise should be installed such that the radar beams should not get refracted by any obstructions on the road side
Trazer	Medium	🟢	🟢	View required is top front and hence require overhead masts for camera fixing. Only the software is provided by the manufacturers
Gridsmart	Medium	🟠	🟠	Camera should be mounted at least 30 feet above the roadway, no more than 75 feet from the centre of the intersection and no more than 150 feet from the front of the furthest stop line.

Ratings: 🟢 Excellent, 🟠 Very Good, 🔴 Good

CHAPTER 9
CONCLUSIONS

Based on a comprehensive review of existing knowledgebase and commercial viability, the following technologies were identified as potential sensors that can be adapted to suit Indian traffic conditions:

- Video based sensors
- Radar based sensors
- Infrared based sensors
- Inductive loop detector

Video based sensors have the potential to work under varying traffic conditions and are evaluated in this study. Collect-R, a commercially available integrated system that processes videos at site, was evaluated. Trazer, a real-time video processing systems suited for heterogeneous traffic conditions have been analyzed for mid-block locations. GRIDSMART from GRIDSMART technologies was evaluated for data collection at intersections. Attempts are also underway for in-house development of an image processing solution. The TIRTL (Transportable Infra-Red Traffic logger), an IR detector manufactured by CEOS Pty Ltd, Australia, was tested for its capacity to classify vehicles, detect the lane in which the vehicle is passing, speed and volume. Smartsensor, a commercially available radar based sensor of Wavetronix, was also evaluated.

Presently available Inductive loop detectors are better suited for lane-based organized traffic and hence cannot be used under traffic conditions with poor lane discipline. Hence, inductive loop detectors were considered developmental work in this project.

This report summarizes results that have been obtained during preliminary testing of the selected data acquisition devices. These results pave the way for more extensive testing that will aid in the development of indigenous data acquisition technologies for future intelligent transport systems in India.

References

1. "India Automotive 2020: The Next Giant from Asia," J.D. Power and Associates.[2011]
2. http://www.citymayors.com/gratis/indian_cities.html
3. Census of India, Provisional Population Totals, Figures at a glance, 2011
4. India to Outpace China's Growth by 2013-15, "Living in a bubble", Global Economic Forum, Chetan Ahya, Morgan Stanley, 2010
5. Chennai Metropolitan Development Authority; Draft Master Plan – II for Chennai Metropolitan Area, Govt. of Tamilnadu, India, 2008.
6. Air pollution in most Indian cities rising, The Indian Express, July 28, 2010
7. World Bank India, Development Dialogue; Spending on Infrastructure Drives Growth, World Bank India Newsletter, New Delhi, India, 2009.
8. ITS Synthesis Report, Centre of Excellence in Urban Transport, IIT(M), 2010
9. http://seattletransitblog.com/2009/04/11/what-is-active-traffic-management/
10. http://www.garagecraft.net/aviservice.html
11. Travel data time Handbook (4-27)
12. P.G. Kaminski; Global Positioning System Standard Positioning Service Signal Specification. Department of Defence, USA, 1995.
13. http://www.allaboutsymbian.com/features/item/The_future_of_GPS equipped_smartphones.php
14. https://www.diamondtraffic.com/node/125
15. Traffic Detector Handbook Third Edition Volume-1
16. http://www.siemens.com/press/en/presspicture/?press=/en/presspicture/ picturespecials/ mobility.php
17. http://www.topfreebiz.com/product/1308106/Ultrasonic-Detector.htm
18. V. Muralidaharan, P. Ravikuma, Area Traffic Control System Implementation at Pune, A case Study.[Jan 2007]
19. http://www.intranse.in/its1/sites/default/files/D1-S2-02_Mumbai%20Area%20Traffic%20Control%20Project_0.pdf
20. Jalihal, S, Reddy, T.S., Nataraju, J. "Evaluation of automatic traffic counters under mixed traffic conditions", IE(1) Journal, vol 86, Nov. 2005 pp 96-102
21. www.wavetronix.com
22. R. L. Anderson. "Electromagnetic Loop Vehicle Detectors", IEEE Trans. Vehicular Technology, vol.vt-19, pp. 23-30, February 1970.
23. M. J. Prucha and M. View, ''Inductive loop vehicle presence detector", U.S. Patent 3576525, Apr. 27, 1971.
24. "Traffic Detector Handbook,"U.S. Department of transportation, Federal highway Administration, vol. 3, no. FHWA-HRT-06-108, pp. 1.1 – 4.61, Oct-2006.
25. R. L. Anderson, "Electromagnetic Loop Vehicle Detectors", IEEE Trans. Vehicular Technology, vol.vt- 19, pp. 23 – 30, Feb -1970.
26. W. H. Lin, J. Dahlgren, H. Huo, "Enhancement of Vehicle Speed Estimation with Single Loop Detectors," In Transportation Research Record: Journal of the Transportation Research Board, vol. 1870, pp. 147 – 152, July 2004.

27. Y. K. Ki, D. K. Baik, "Vehicle-Classification Algorithm for Single-Loop Detectors Using Neural Networks," IEEE Trans. Vehicular Technology, vol- 55, pp. 1704 – 1711, Nov. 2006.

28. Y. Oh, C. Lee, "The Decision of the Optimal Shape of Inductive Loop Detector for Real-Time Signal Control," Journal of Transportation Research Society of Korea, vol- 13, no. 3, pp. 67 – 86, 1995.

29. S. S. M. Ali, B. George, L. Vanajakshi, V. Jayashankar and V. J. Kumar, "A Multiple Loop Vehicle Detection System for Heterogeneous and Lane-less Traffic,"IEEE Trans. on Inst. and Meas., vol. 61, no. 5, pp. 1353 – 1360, May 2012.

30. 16 Bit, 400 kS/s Isolated M series MIO DAQ, Bus powered, [Online]. Available: http://sine.ni.com/nips/cds/print/p/lang/en/nid/207099:

31. S. S. M. Ali, B. George, L. Vanajakshi, "A Simple Multiple Loop Sensor Configuration for Vehicle Detection in an Undisciplined Traffic," Proc.of 5th IEEE Conf. ICST, Palmerston North, New Zealand, pp. 644 – 649, Dec. 2011.

32. T. Cherrett, H. Bell, and M. McDonald, "Traffic Measurement Parameters from Single Inductive Loop Detectors," Transportation Research Record 1719, pp. 112 – 120, 2000.

33. A. Pushkar, F. L. Hall, and J. A. Acha-Daza, "Estimation of Speeds from Single Loop Freeway Flow and Occupancy Data Using Cusp Catastrophe Theory Model," Transportation Research Record 1457, pp. 149 – 157, 1994.

34. J. Zhanfeng, C. Chen, B. Coifman and P. Varaiya, "The PeMS algorithms for accurate, real-time estimates of g-factors and speeds from single-loop estimates of g-factors and speeds from single-loop detectors," in Proc. IEEE ITSC, pp. 536 – 541, 2001.

35. C. Sun and S. G. Ritchie, "Individual vehicle speed estimation using single loop inductive waveforms," J. Transp. Eng., ASCE,vol. 125, no. 6, pp. 531 - 538, Nov./Dec. 1999.

36. Y. K. Ki, D. K. Baik, "Model for Accurate Speed Measurement Using Double- Loop Detectors," IEEE Trans. on vehicular technology, vol- 55, pp. 1094 – 1101, July 2006.

37. J. Ametha, S. Tumer, S. Darbha, "Formulation of a new methodology to identify erroneous paired loop detectors," Proc. IEEE ITSC, Oakland (CA), USA, pp. 591 – 596, 2001.

38. Vehicle Speed Measurement Device using Laser, [Online]. Available: http://www:lasertech:com/TruSpeed **-** Laser - Speed - Gun.aspx

39. S. S. M. Ali, B. George, L. Vanajakshi, "A Magnetically Coupled Inductive Loop Sensing System for Less-lane Disciplined Traffic," Proc. of IEEE I2MTC -12, Graz, Austria, pp. 827 – 832, May 2012.

40. T. Bretterklieber, H. Zangl, M. Motz, D. Hammerschmidt and T.Werth, "Versatile Sensor Front End for Low-Depth Modulation Capacitive Sensors," Proc. of IEEE I2MTC 2008, British Columbia, Canada, pp. 830 - 835, May 2008.

41. M. Pursula, I. Kosonen, "Microprocessor and PC-based vehicle classification equipments using induction loops," Proc. IEEE 2nd Int. Conf. Road Traffic Monit., pp. 24 – 28, 1989.

42. J. Gajda, R. Sroka, M. Stencel and T. Zeqlen, "Measurement of the road traffic parameters using a single inductive loop detector," Proc. of 9th International

Symposium, IMEKO TC-4, Glasgow-Scotland, pp. 221 – 224, 1997.

43. J. Gajda, R. Sroka,"Vehicle classification by parametric identification of the measured signals," Proc. of XVI IMEKO World Congress, Vienna, vol - 09 , pp. 199 – 204, 2000.

44. C. Sun, "An investigation in the use of inductive loop signatures for vehicle classification, "Inst. Transp. Stud., Univ. California, Berkeley, CA, California PATH Res. Rep., UCB-ITS-PRR-2000 4 March 2000.

45. R. Sroka,"Data fusion methods based on fuzzy measures in vehicle classification process," in Proc. 21st IEEE IMTC, vol - 03, pp. 2234 – 2239, May 18 - 20, 2004.

46. G. H. Zhang, Y. H. Wang, and H. Wei,"Artificial neural network method for length-based vehicle classification using single loop outputs," Traffic Urban Data, Transp. Res. Rec, no. 1945, pp. 100 – 108, 2006.

47. Y. K. Ki, D. K. Baik, "Vehicle-Classification Algorithm for Single-Loop Detectors Using Neural Networks," IEEE Trans. Vehicular Technology, Vol. 55, pp. 1704 – 1711, Nov. 2006.

48. S. Meta, M. G. Cinsdikici, "Vehicle-Classification Algorithm Based on Component Analysis for Single-Loop Inductive Detector," IEEE Trans. on vehicular Technology, vol- 59, pp. 2795 – 2805, July 2010.

49. C. M. Bishop,"Pattern Recognition and Machine Learning," Springer Science+ Business Media LLC, pp. 663, 2006.

50. L. Breiman,"Random Forest," Machine Learning, vol - 45, pp. 5 - 32, 2001.

51. A. Verikas, A. Gelzinis, M. Bacauskiene,"Mining data with random forests: a survey and results of new tests," Pattern Recognition, vol. 44, pp. 330-349, 2011.

52. Random Forest implementation for Matlab, [Online]. Available: http : //code.google.com/p/randomforest-matlab/

53. L. Breiman,"Consistency For a Simple Model of Random Forests," Technical Report 670, UC Berkeley, 2004. URL http://www.stat.berkeley.edu/breiman.

54. R. J. Koerner and C. Park,"Inductive loop vehicle detector", U.S. Patent 3989932, Nov. 2, 1976.

55. H. M. Patrick, J. L. Raymond "Vehicle presence loop detector", U.S patent 4472706, 1984.

56. M. A. G. Clark, "Induction loop vehicle detector ", U.S patent 4568937, 1986

57. S. H. Lee, Y. Oh, S. Lee, " New Loop Detector Installation Guidelines for Real – Time Adaptive Signal Control System", Journal of the Eastern Asia Society for Transportation Studies, vol. 6, pp. 2337 – 2348, 2005.